The Dissertation Committee for Christine Ky Linh Dao Certifies that this is the approved version of the following dissertation:

The underlying mechanisms of UCP3-dependent thermogenesis in skeletal muscle

Committee:

Edward M. Mills, Supervisor

Casey W. Wright

Somshuvra Mukhopadhyay

John L. Ivy

Shawn B. Bratton

The underlying mechanisms of UCP3-dependent thermogenesis in skeletal muscle

by

Christine Ky Linh Dao, B.A.

Dissertation

Presented to the Faculty of the Graduate School of

The University of Texas at Austin

in Partial Fulfillment

of the Requirements

for the Degree of

Doctor of Philosophy

The University of Texas at Austin
December 2015

Dedication

To my parents, Son and Huong Dao, who have always supported me in every way possible.

Acknowledgements

First and foremost, I would like to thank my mentor, Dr. Ted Mills, for the enormous support and guidance he has provided me with during my time in his laboratory. He has always encouraged me to be creative and to take initiative when it comes to facing new challenges, and I hope to continue building on his teachings in the next step of my career.

I am also grateful to have been able to work with such a diverse group of people in the Mills lab. Thank you to all the past and present lab members for their help, and more importantly their friendship. I would especially like to acknowledge Gloria Fang. I am so grateful to have been able to work with and learn from such an amazingly intelligent and caring individual. Your drive and passion for helping others has always inspired me, and I can't imagine this experience without you. I hope you know how remarkable you are, and I can't wait to see what amazing things you will do in the future.

To my parents and family, who have always believed in me and supported me during this long journey. I am extremely blessed to have such a wonderful family that I look up to, and motivates me to be the best person I can be. Lastly, I would like to thank my best friend and future husband, Dan Blair. Although there were times when I was unsure of myself, you always reminded me to "bet" on myself and continue pushing forward. I couldn't have asked for a better teammate and I can't wait to start this next chapter in my life with you by my side.

The underlying mechanisms of UCP3-dependent thermogenesis in skeletal muscle

Christine Ky Linh Dao, Ph.D.

The University of Texas at Austin, 2015

Supervisor: Edward M. Mills

Mitochondrial uncoupling proteins (UCPs) are anion / solute transporters that dissipate the proton gradient used to drive ATP generation. By allowing protons to flow down their electrochemical gradient, UCP activation releases the energy generated from mitochondrial substrate oxidation as heat. This thermogenic process is important in normal thermoregulation (i.e. non-shivering thermogenesis), and also serves as an attractive target in the treatment of obesity by lowering metabolic efficiency.

The skeletal muscle (SKM) enriched UCP homologue, UCP3, is associated with increased energy expenditure, fatty acid metabolism, and insulin sensitivity. Unlike the cold-induced prototypical pathway of UCP1-mediated non-shivering thermogenesis in brown adipose tissue (BAT), the mechanisms underlying the thermogenic actions of UCP3 in SKM are not well characterized. Although global UCP3 knockout mice exhibit normal thermoregulatory responses to cold under fed conditions, they exhibit an attenuated hyperthermic response when administered amphetamine-type drugs. In our initial investigation, we show that selective overexpression of UCP3 in SKM by the human α-skeletal actin promoter restored methamphetamine (Meth)-induced

hyperthermia in the UCP3$^{-/-}$ background (TgSKM UCP3$^{-/-}$), but not in the UCP1/UCP3 double knockout background (TgSKM UCP1$^{-/-}$+UCP3$^{-/-}$). Taken together, these findings further bolster the role of UCP3 as a thermogenic mediator in SKM, and suggest a novel mechanism of crosstalk between BAT UCP1 and SKM UCP3 in Meth-induced hyperthermia.

In the second aspect of my project, we characterized the underlying mechanisms of UCP3-dependent thermogenesis within SKM by utilizing an immunoprecipitation-based mass spectrometry approach to identify interacting partners of UCP3. These analyses corroborated previous work performed by our lab, and demonstrated that UCP3 interacts with a subset of fatty acid metabolizing enzymes. Interestingly, one such enzyme, enoyl-CoA hydratase-1 (ECH1), is involved in the metabolism of oleic acid, a known ligand activator of UCP3. This work reveals that ECH1:UCP3 complex formation enhances uncoupled-respiration and fatty acid metabolism, and that genetic mouse models in vivo show that UCP3 and ECH1 participate in a common pathway of thermogenesis. These findings support a new model by which UCP3-dependent thermogenesis in SKM is mediated in part through its cooperation with ECH1, and suggest new approaches for treatment of obesity and related metabolic diseases.

Table of Contents

List of Tables

List of Figures

List of Illustrations

List of Abbreviations

Acadm	Medium chain specific acyl-CoA dehydrogenase
Acat 1	Acetyl-CoA acetyltransferase
ATP	Adenosine triphosphate
BAT	Brown adipose tissue
β-oxidation	Beta-oxidation
BKCD	Branched-chain ketoacid dehydrogenase complex
BMI	Body mass index
BMR	Basal metabolic rate
CACT	Carnitine-acylcarnitine translocase
CPT1	Carnitine palmitoyltransferase 1
CPT2	Carnitine palmitoyltransferase 2
DECR	2,4-dienoyl-CoA reductase
ECH1	$\Delta^{3,}$, $\Delta^{2,4}$-dienoyl-CoA isomerase/enoyl-CoA hydratase-1
ECHs1	Short enoyl-CoA hydratase 1
ECI	Δ^{3}, Δ^{2}-enoyl-CoA isomerase
e-	Electrons
ETC	Electron transport chain
ETF	Electron transferring flavoprotein dehydrogenase
F_1/F_0-ATPase	F_1/F_0-ATP synthase, complex V

FABP	Fatty acid-binding proteins
FABPpm	Plasmalemmal fatty acid-binding protein
FADH2	Flavin adenine dinucleotide
FAT/CD36	Fatty acid translocase
G3PDH	Glycerol-3-phosphate dehydrogenase
G6P	Glucose-6-phosphate
GLUT	Glucose transport protein
GLUT1	Glucose transporter-1
GLUT4	Glucose transporter-4
GLUTs	Glucose transporters
H+	Protons
Hadhb	Subunits of trifunctional enzyme
HK	Hexokinase
HRT	Heart
HSL	Hormone sensitive lipase
LDH	Lactate dehydrogenase
MDH2	Malonate Dehydrogenase 2
MDMA	3,4-methylenedioxymethamphetamine
Meth	Methamphetamine
NADH	Nicotinamide adenine dinucleotide
PDH	Pyruvate dehydrogenase

PPARα	Peroxisome proliferator-activated receptor-α
ROS	Reactive oxygen species
SKM	Skeletal muscle
SNS	Sympathetic nervous system
TCA	Tricarboxylic acid
UCP	Uncoupling proteins
ΔΨ	Membrane potential

[1]Chapter 1: Introduction

1.1 Background: Cellular bioenergetics and thermogenesis in the treatment of obesity

Obesity is a complex disease that develops when energy intake exceeds energy expenditure. This energy imbalance leads to an excess accumulation of body fat or adiposity, which is associated with many devastating medical complications including type 2 diabetes mellitus, metabolic syndrome, cardiovascular disease, Alzheimer's, and even some type of cancers (Haslam & W. P. T. James 2005). According to the CDC, more than 34.9% of US adults are classified as obese with a body mass index (BMI) >30 (Ogden et al. 2014).

Current therapies primarily focus on reducing caloric intake to oppose the energy imbalance that causes obesity. Apart from maintaining a healthy diet and increasing physical activity, the available clinical approaches to treat obesity are risky and/or relatively ineffective in terms of long-term weight loss (Melnikova & Wages 2006). This includes invasive bariatric surgical procedures, and a select few FDA approved drugs that are associated with devastating side effects for the patient. Therefore, it is essential to

[1] Portions of this chapter are adopted from:

Dao, C.K., Nowinski, S.M. & Mills, E.M., 2014. The heat is on: Molecular mechanisms of drug-induced hyperthermia. *Temperature*, 1(3), pp.183–191.

Author contributions: C.K.D. performed research and wrote the manuscript. S.M.N and E.M.M edited the manuscript.

develop new obesity therapies that can lower toxicity in patients and also have a more substantial effect on weight loss in the long-term.

An attractive alternative approach to treat obesity is through targeting cellular bioenergetics to increase energy expenditure. On a molecular level, cellular bioenergetics, in large part, occurs in the mitochondria where the oxidation of nutrients through the tricarboxylic acid (TCA) cycle and electron transport chain (ETC) is coupled to ATP production (i.e. oxidative phosphorylation). More specifically, intermediates from the TCA cycle contribute electrons to the ETC, which causes complexes of the ETC to pump protons from the mitochondrial matrix into the intermembrane space. This generates an electrochemical gradient that is used to drive ATP synthesis by allowing protons to flow back down the gradient through F_1/F_0-ATP synthase (F_1/F_0-ATPase).

Although oxidative phosphorylation is a tightly coupled process, chemical energy conversion is an inefficient process by nature, where some energy is inherently lost as heat. Indeed, in mammalian systems there are many examples of specific physiologically uncoupled or "futile cycling" processes that are energy consuming and thermogenic. The idea of utilizing these thermogenic processes to lower metabolic efficiency and increase energy expenditure as a means to combat obesity, originates from research regarding inducible proton leak mediated by uncoupling protein 1 (UCP1) in brown adipose tissue (BAT) (Feldmann et al. 2009). UCP1 is expressed on the inner mitochondrial membrane and has the ability to uncouple oxidative phosphorylation by allowing protons to leak back into the mitochondrial matrix. As protons flow down their concentration gradient and circumvent F_1/F_0-ATP synthase, the energy used to fuel ATP generation is released

in the form of heat. This mechanism is the basis of a process known as adaptive non-shivering thermogenesis that occurs generally in BAT of rodents and newborn babies, where heat is generated in response to cold in order to maintain core body temperature (Cannon et al. 1982; Cannon & Nedergaard 2004).

The use of uncoupling to increase energy expenditure and achieve weight loss has already been demonstrated with the clinical use of the non-selective uncoupler of oxidative phosphorylation known as 2,4-dinotrophenol, starting back in the 1930's. Although effective in weight loss, the drug has a narrow therapeutic window and can have toxic side effects including hyperthermia, tachycardia, diaphoresis, tachypnea, and even death (Grundlingh et al. 2011).

Uncoupling-dependent non-shivering thermogenesis in the treatment of obesity and –related metabolic diseases has gained attention over the past decade with the discovery that adult humans possess greater amounts of BAT depots than originally postulated (Nedergaard et al. 2007). Importantly, it has also been shown that in addition to BAT, non-shivering thermogenesis can also occur in skeletal muscle tissues (SKM). However, our understanding of the mechanisms that regulate the complex interplay between mitochondrial uncoupling and energy balance are still unclear. Regardless, these new findings highlight the potential opportunities in targeting cellular bioenergetics through uncoupling in BAT and SKM. Our work provides valuable insight into the mechanisms that regulate non-shivering thermogenesis that will likely be relevant in developing novel strategies to combat the energetic imbalance seen with obesity by lowering metabolic efficiency.

1.2 Bioenergetics and metabolism

Normal energy metabolism is driven by the oxidation of three principle substrates derived from nutrients- glucose, fatty acids, and amino acids. These substrates can be

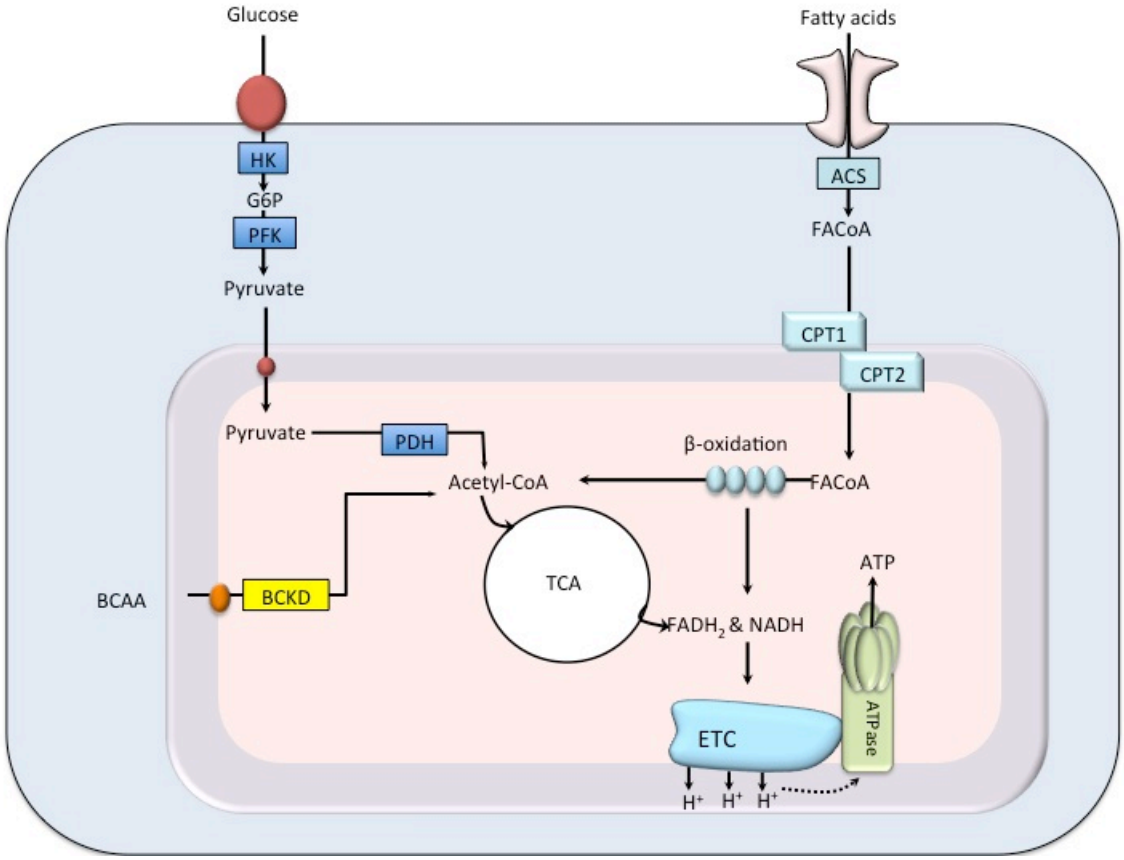

Illustration 1.1 Normal cellular bioenergetics

The catabolism of glucose, fatty acids, and branched chain amino acids (BCAA) all generate acetyl-CoA, which fuels the tricarboxylic acid cycle (TCA). The TCA cycle produces the reducing equivalents, NADH and $FADH_2$, which provide electrons to the electron transport chain (ETC). As the electrons flow through the complexes, protons are pumped in to the intermembrane space of the mitochondria. The resulting proton gradient is coupled to F_1/F_0 ATP synthase (ATPase) to generate the high-energy substrate, ATP, which can be used for cellular work.

taken up exogenously from diet, or can be released from intracellular stores that involve catabolic processes such as glycolysis, lipolysis, and proteolysis (amino acid catabolism). Distinct metabolic pathways in the mitochondria metabolize the different fuel substrates, however these processes all converge with the formation of acetyl-CoA, a key substrate that is fed into the TCA cycle (Illustration 1.1). Each turn of the TCA cycle generates reduced coenzyme equivalents (NADH and $FADH_2$) that deliver electrons to the ETC and fuels ATP generation through oxidative phosphorylation. Ultimately, all cells rely heavily on these metabolic processes to meet their energetic needs.

1.2.1 Glucose metabolism

Carbohydrates and sugars, such as glucose, serve as an important energy fuel source for cells. In healthy individuals, whole body glucose homeostasis is maintained through 4 key metabolic processes: glycolysis, glycogen synthesis, glycogenolysis, and gluconeogenesis. It is important to note that depending on the tissue type, the interplay between these metabolic processes in maintaining glucose homeostasis can vary. For example, in a fasted state the rates of glycolysis in the liver decreases and the glucose stored in the liver via gluconeogenesis and glycogen synthesis is released into the bloodstream to be delivered to brain and SKM (Guo et al. 2012). Here, we will focus mainly on glucose metabolism in SKM, as it is a principle tissue-site of glucose uptake, and accounts for up to 70-80% of glucose disposal in humans administered a hyperinsulinemic-euglycemic clamp test (DeFronzo et al. 1981; Shulman et al. 1990).

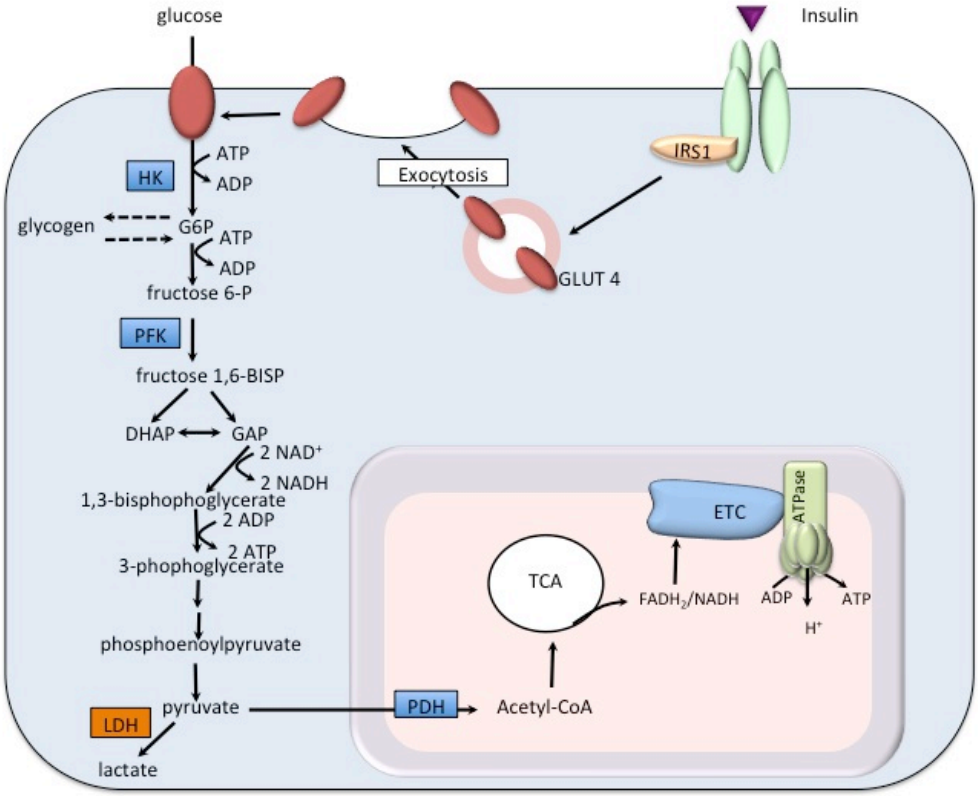

Illustration 1.2 Insulin-stimulated glucose uptake and metabolism in SKM

Insulin binds to the insulin receptor and initiates a signaling cascade that stimulates GLUT4 translocation to the cell membrane through exocytosis. Glucose is taken up into the cell through the GLUT4 transporter and can either be stored as glycogen or be further degraded through glycolysis. The 10 enzymatic reactions of glycolysis result in the net generation of 2 molecules of pyruvate, ATP, and the reducing equivalent NADH. In anaerobic conditions, pyruvate can be converted to lactate by lactate dehydrogenase (LDH). In aerobic conditions, the mitochondrial pyruvate dehydrogenase complex (PDH) catalyzes oxidative decarboxylation of pyruvate to acetyl-CoA, which is subsequently fed into the TCA cycle to generate the reducing equivalents ($NADH_2$ and FADH) which fuel ATP generation through the electron transport chain.

Glucose uptake into SKM is facilitated by specific members of the glucose transporter family (GLUTS), GLUT1 and GLUT4. While GLUT1 mediates constitutive and basal glucose uptake in cells, GLUT4- dependent glucose transport is stimulated by insulin (Larance et al. 2008). In an absorptive state right after a meal, the spike in plasma glucose concentration stimulates insulin release from the pancreatic β-cells, which leads to an increase in SKM glucose uptake and inhibition of fatty acid oxidation (Randle et al. 1963). Insulin stimulates translocation of the GLUT4 receptor to the plasma membrane through exocytosis (Rea & D. E. James 1997). Glucose is transported into the cell via GLUT4, and is then phosphorylated by hexokinase (HK) to produce glucose-6-phosphate (G6P). At this point in the glycolytic pathway, G6P can either be stored as glycogen or undergo further degradation through a series of glycolytic reactions in the cytoplasm that results in the generation of two molecules of pyruvate and a net of two molecules of ATP (Illustration 1.2). It has been reported that about 30-40% of glucose is oxidized while approximately 15% is stored as glycogen following an oral glucose tolerance test (Kelley et al. 1988).

The metabolic fate of pyruvate generated from glycolysis varies with anaerobic and aerobic conditions. For example, in fast twitch-glycolytic muscle fibers that have a low oxidative capacity and contain low levels of the oxygen binding protein, myogoblin, pyruvate can be rapidly metabolized by lactate dehydrogenase (LDH) to generate and release lactate into circulation (Kruszynska et al. 2001). However, in highly oxidative muscle fibers, pyruvate is taken up into mitochondria, and is subsequently metabolized

by pyruvate dehydrogenase (PDH) to generate acetyl- CoA, a principal substrate that feeds into the TCA cycle.

1.2.2 Fatty acid oxidation

Fatty acids serve as another important metabolic fuel source, especially for tissues with high energetic requirements including heart, liver, BAT, and SKM. Fatty acid metabolism becomes particularly important in certain physiological contexts such as fasting (i.e. hypoglycemia), hyperthermia/heat-related illness, and metabolic stress.

Fatty acids can be released into circulation through hydrolysis/lipolysis of triglyceride stores by hormone-sensitive lipase (HSL). Once liberated, fatty acids are bound to albumin for transport in the blood stream to surrounding tissues, and into cells through membrane-associated proteins, including fatty acid translocase (FAT/CD36) or plasmalemmal fatty acid-binding protein (FABPpm) (van der Vusse et al. 2002). Once inside the cell, the fatty acids are bound to cytoplasmic fatty acid-binding proteins (FABPs), and then further modified by fatty acyl Coenzyme A synthetases (FACs) for uptake into certain intracellular organelles. Before fatty acids can be taken up they must be conjugated to a molecule of coenzyme A, forming fatty acyl-CoA. Most fatty acyl-CoAs are then transported into either peroxisomes or mitochondria through two distinct uptake mechanisms mediated through ATP-binding cassette transporters or carnitine transporters, respectively. Both peroxisomes and mitochondria possess the machinery to perform fatty acid oxidation aka β-oxidation, however it has been reported that a majority of β-oxidation occurs in the mitochondria (Kunau et al. 1995).

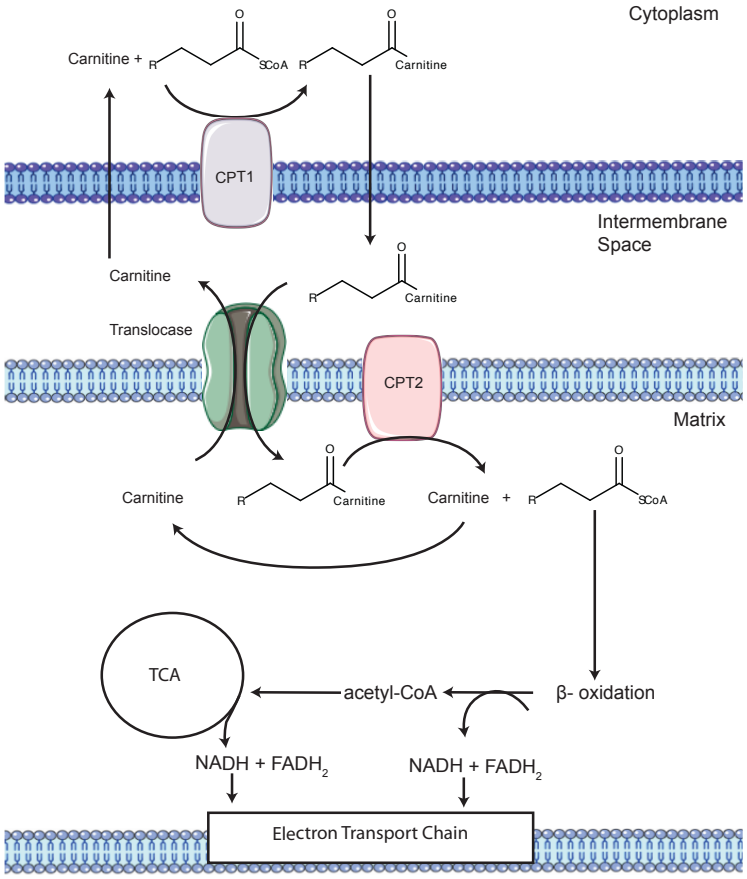

Illustration 1.3 Carnitine transport cycle in mitochondria

When fatty acid metabolism is favored (e.g. fasting) fatty acyl-CoA molecules are transported in the mitochondrial matrix via the carnitine transport cycle. This specific carrier system consists of three enzymes- carnitine palmitoyltransferase I (CPTI) , carnitine-acylcarnitine translocase (CACT), and carnitine palmitoyltransferase I (CPTII). CPTI, located on the outer mitochondrial membrane, catalyzes the rate-limiting step of this transport system and replaces the coenzymeA moiety (SCOA) with carnitine. In the final step, the fatty acyl-carnitine is converted back into fatty acyl-CoA by CPTII, which is located on the inner face of the inner mitochondrial membrane. The resulting fatty acyl-CoA enters the β-oxidation spiral and generates one molecule of acetyl-CoA that is subsequently fed into the TCA cycle. The reduced cofactors produced from the TCA cycle and the β-oxidation fuel ATP generation through the electron transport chain.

While, mitochondrial β-oxidation is closely associated with energy production through oxidative phosphorylation, peroxisomal β-oxidation is thought to be more involved in the degradation of complex fatty acid species, such as branched chain fatty acids or very long chain fatty acids(Kunau et al. 1995). Therefore, initial processing of complex fatty acids through peroxisome β-oxidation gives rise to medium chain fatty acids that can then be transported to mitochondria for complete oxidation (Borgne & Demarquoy 2012).

Unlike peroxisomal uptake of fatty acids mediated through an ATP-binding cassette transporters (van Roermund et al. 2011), the transport of the fatty acyl-CoA metabolites into mitochondria requires the carnitine shuttle system. The outer mitochondrial membrane is impermeable to fatty acyl-CoA esters. The first reaction of the shuttle system (rate-limiting step) is catalyzed by carnitine palmitoyltransferase 1 (CPT1), on the outer mitochondrial membrane (Kopec & Fritz 1971). Before the fatty acyl-CoA is allowed to transverse the membrane, CPT1 converts fatty acyl-CoA into acylcarnitine. Once in the intermembrane space, the acyl-carnitine is shuttled by carnitine-acylcarnitine translocase (CACT) into the mitochondrial matrix where the carnitine moiety is replaced with CoA by CPT2. The resulting mitochondrial acyl-CoA molecule undergoes a series of enzymatic reactions, collectively known as β-oxidation, resulting in the formation of acetyl-CoA that can be fed into the TCA cycle (Illustration 1.3).

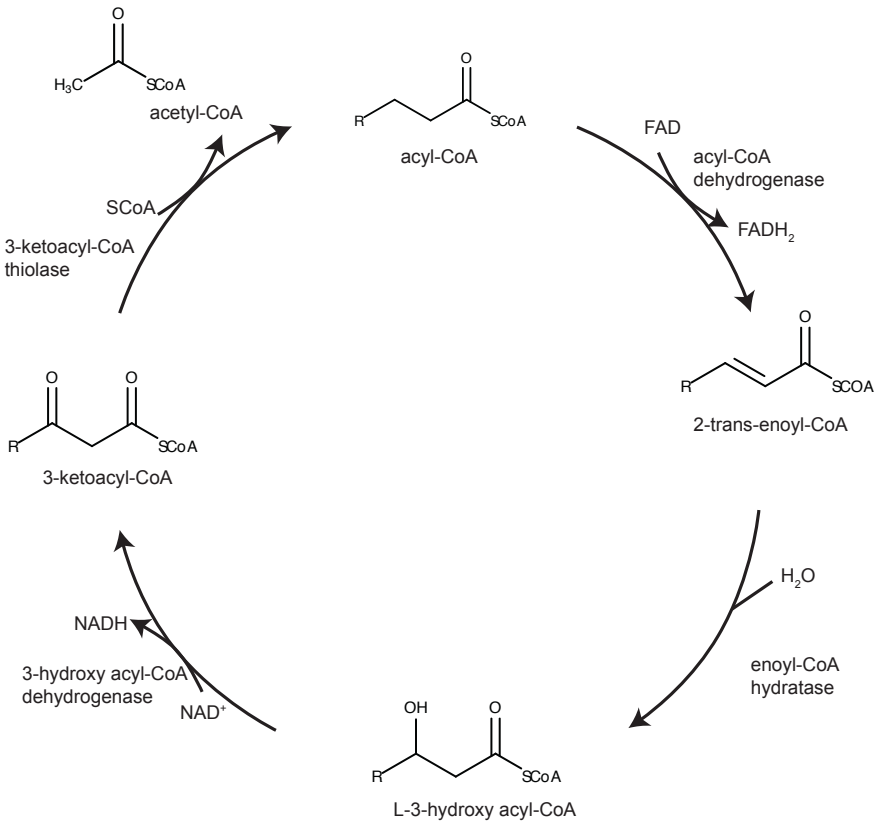

Illustration 1.4 The β-oxidation spiral

The catabolism of fatty acyl-CoA molecules through β-oxidation leads to the generation of acetyl-CoA, NADH, and $FADH_{2}$. There are 4 enzymes involved in β-oxidation: acyl-CoA dehydrogenase, enoyl-CoA hydratase, hydroxy acyl-CoA dehydrogenase, and ketoacyl-CoA thiolase. In the final step of β-oxidation, ketoacyl-CoA thiolase links a coenzymeA moiety to the third carbon in the fattty acid chain, resulting in the formation of one molecule of fatty acyl-CoA and acetyl-CoA. The resulting fatty acyl-CoA (now two carbons shorter) then re-enters the β-oxidation cycle for further degradation.

1.2.2.1 Mitochondrial β-oxidation of saturated fatty acids

β-oxidation involves a series of 4 enzymatic reactions that act in a repetitive cycle catalyzed by acyl-CoA dehydrogenase, enoyl-CoA hydratase, hydroxyacyl-CoA dehydrogenase, and ketoacyl-CoA thiolase. It is important to note that multiple forms of these enzymes with the same mechanistic properties exist, but differ based on their localization and specificity for substrates of different fatty acid chain lengths (Kunau et al. 1995). Although the functional and physiological organization of these enzymes in the mitochondria remains unclear, it has been proposed that these β-oxidation enzymes organize as large multienzyme complexes to channel substrates from one enzyme to another. Existing as an organized enzyme complex, rather than free floating enzymes, would provide a clear kinetic advantage and would explain the observed struggle in detecting intermediates of β-oxidation(Liang et al. 2001; Sumegi et al. 1991).

With each turn of the β-oxidation cycle one molecule of NADH, $FADH_2$, and acetyl-CoA is generated, and the fatty acyl-CoA chain is shortened by two carbons (Illustration 1.4). This cycle continues until the fatty acid chain is completely degraded to acetyl-CoA. The fatty acid chains containing an odd-number of carbons are degraded to the three-carbon molecule propionyl-CoA, which can then be converted to succinyl-CoA and fed directly into the TCA cycle (Schulz 2002).

1.2.2.2 Unsaturated fatty acid metabolism

The presence of *cis* double bonds along the carbon chain of (poly)unsaturated fatty acids prevents the complete degradation of these species through normal β-

oxidation. Indeed, unsaturated fatty acid metabolism requires a set of auxiliary enzymes to act on these pre-existing double bonds before they can enter the β-oxidation spiral (Stoffel & Caesar 1965). Depending on the placement of the double bond(s) along the fatty acid chain, either in an odd-numbered or even-numbered position(s), unsaturated fatty acids can be metabolized by different pathways (Illustration 1.5).

Even-numbered double bonds can be metabolized by the collective actions of two enzymes, the NADPH-dependent 2,4-dienoyl-CoA reductase (DECR) and Δ^3,Δ^2-enoyl-CoA isomerase (ECI) enzymes before entering the β-oxidation spiral. In contrast, the degradation of unsaturated fatty acids with double bonds in odd-numbered positions (e.g. oleic and linoleic acid) is more complex and can be potentially metabolized by either the classic isomerase-dependent or reductase-dependent pathway. Kinetic studies to characterize the relative contribution of these two pathways in oleic acid metabolism r and revealed that the isomerase dependent pathway accounted for more than 80% of the total flux (Shoukry & Schulz 1998). Despite the relatively small contribution of the reductase-dependent pathway, it is still regarded as an essential component in the degradation of unsaturated fatty acids with double bonds in odd-numbered positions. It has been proposed that the absence of the reductase-dependent pathway would lead to the accumulation of the 3-trans, 5-cis-dienoyl-CoA intermediate (Schulz & Kunau 1987) that is exclusively metabolized by the enzyme, $\Delta^{3,5}$, $\Delta^{2,4}$-dienoyl-CoA isomerase/enoyl-CoA hydratase-1 (ECH1) (Filppula 1998; Luo et al. 1994).

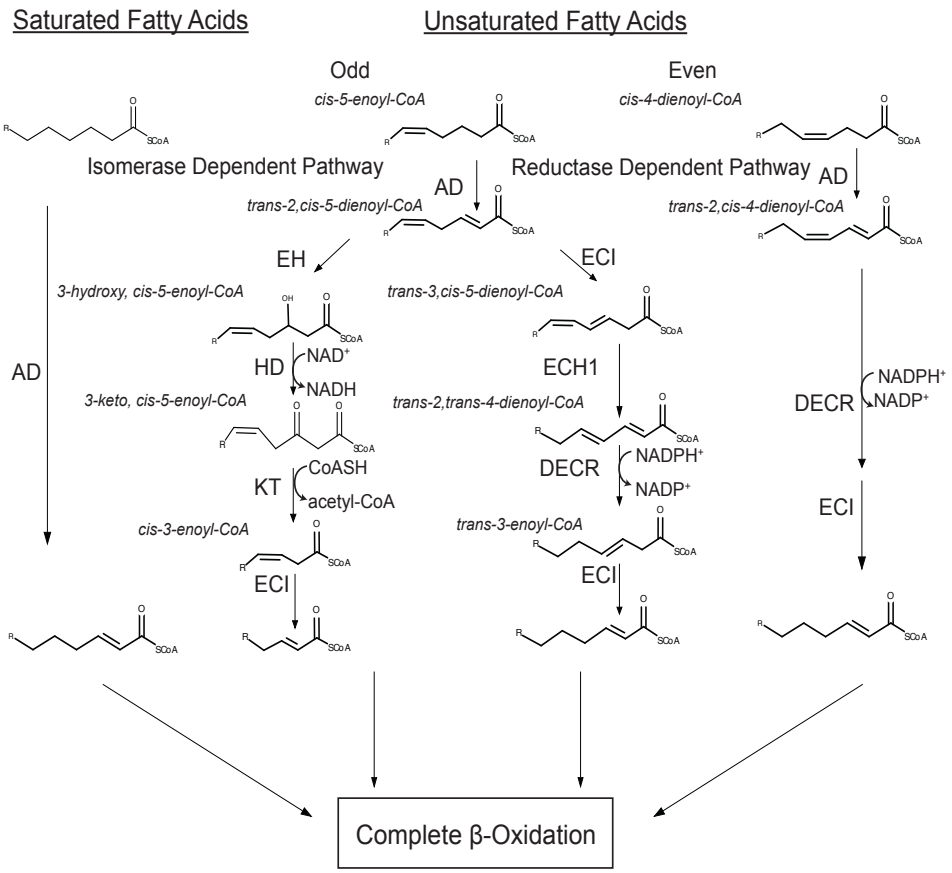

Illustration 1.5 Degradation of different types of unsaturated fatty acids

Saturated fatty acids can be completely degraded through traditional β-oxidation. Unsaturated fatty acids with double bonds on even numbered carbons along the fatty acid chain (e.g. linoleic acid) must be converted to a trans-2, enoyl-CoA ester by acyl-CoA dehydrogenase (AD), dienoyl-CoA reductase (DECR) and enoyl-CoA isomerase (ECI) before being degraded through β-oxidation. Unsaturated fatty acids with double bonds on odd numbered carbons (e.g. oleic acid) are converted to the trans-2,cis-4-dienoyl-CoA ester by AD before being metabolized to the trans-2-enoyl-CoA intermediate either through the isomerase dependent pathway or the reductase dependent pathway. Enoyl-CoA hydratase (EH); hyoxyacyl-CoA dehydrogenase (HD); Keto-thiolase (KT); Enoyl-CoA Isomerase (ECI); Enoyl-CoA hydratase 1 (ECH1)

1.2.3 Oxidative phosphorylation

The degradation of glucose, amino acids, and fatty acids (i.e. unsaturated and saturated) all lead to the formation of acetyl-CoA, a principle substrate in the TCA cycle. When acetyl-CoA enters the TCA cycle it is combined with oxaloacetate to form citrate, which then undergoes a series of oxidizing reactions that ultimately lead to the regeneration of oxaloacetate to restart the cycle. Each turn of the cycle generates two molecules of CO_2 and one molecule of GTP, as well as the reduced cofactors, NADH and $FADH_2$ that subsequently contribute their electrons to the ETC.

The ETC is located on the inner mitochondrial membrane and consists of protein complexes that serve as electron donors and acceptors. NADH delivers electrons to complex I (NADH dehydrogenase) while $FADH_2$ donates electrons to complex II (succinate dehydrogenase) of the ETC. The electrons can flow from either complex I or II to the Q cycle (coenzyme Q), which then delivers electrons to complex III (cytochrome c oxidoreductase). Interestingly, electrons can also be fed directly into the Q cycle via FAD-linked proteins including electron transferring flavoprotein dehydrogenase (ETF) and glycerol-3-phosphate dehydrogenase (G3PDH) (Fisher-Wellman & Neufer 2012). Electrons from the Q cycle then flow from complex III to complex VI (cytochrome c oxidase) via cytochrome c (cyt c). In the final step of the ETC, molecular oxygen is reduced to H_2O (oxygen consumption). As electrons flow through the ETC, the complexes use the energy released from each redox reaction to pump protons (H^+) from the matrix into the intermembrane space. This establishes an electrochemical gradient that provides the proton motive force to drive ATP production

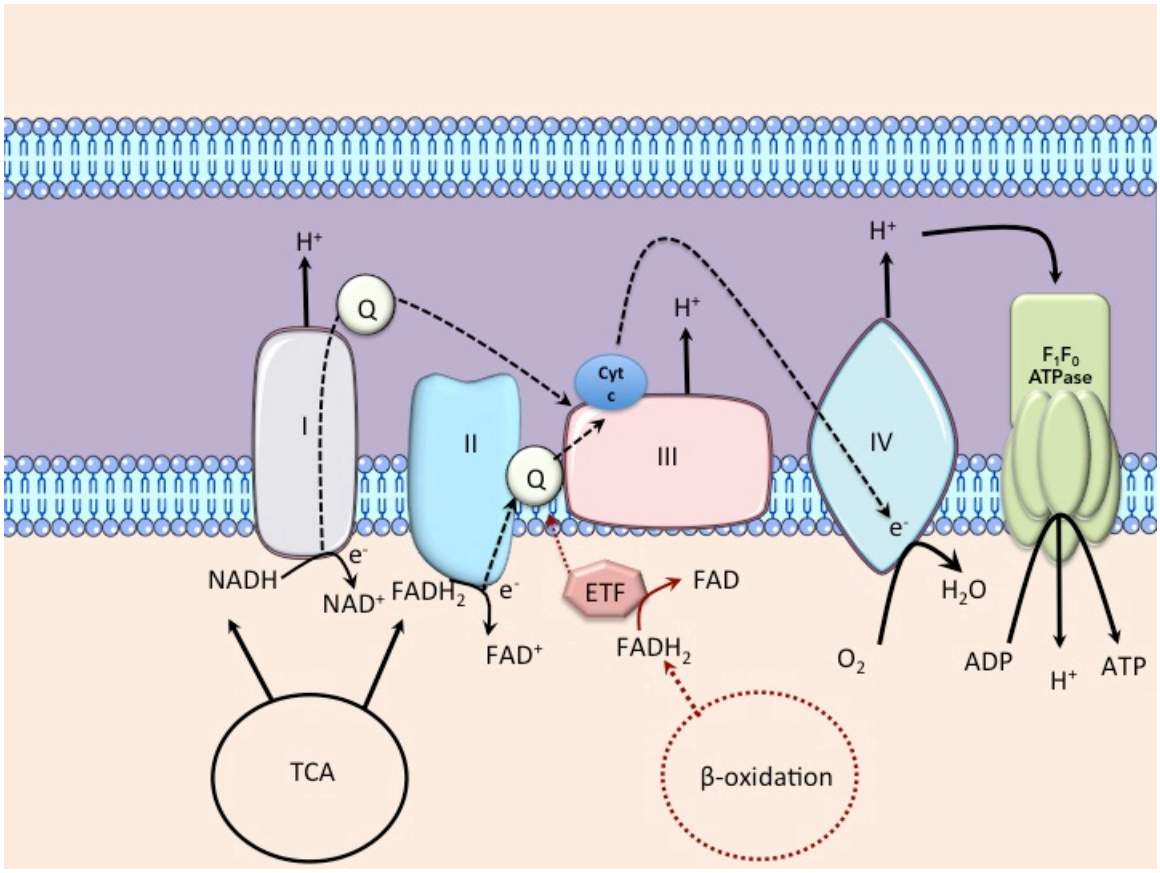

Illustration 1.6 The electron transport chain and oxidative phosphorylation

The TCA cycle generates the reducing equivalents, NADH and $FADH_2$ which provide electrons (e^-) to complex I and II located on the inner mitochondrial membrane, respectively. Within the electron transport chain (ETC), e^- flow through complex I and II to the ubiquinone cycle (Q). $FADH_2$ generated from the degradation of fatty acids through β-oxidation can be directly fed into the Q cycle via electron transferring flavoprotein dehydrogenase (ETF). From the Q cycle, e^- are passed to complex III, cytochrome C (Cyt C), complex IV, and the final acceptor, molecular oxygen (O_2) to form water. As e^- flow through the complexes, protons are pumped into the intermembrane space by complexes I, III, and IV, resulting in an electrochemical gradient. The proton motive force generated by the electrochemical gradient is used to drive the rotary motion of F_1/F_0ATP synthase (F_1/F_0ATPase).

and generate ATP through F_1/F_0 ATPase (complex V of the ETC), a process known as oxidative phosphorylation. For the most part, the ETC is coupled to oxidative phosphorylation and the only way for flux through ETC to continue is if energy from the electrochemical gradient is dissipated. In other words, if the rate of proton re-entry into the matrix slows down, this change will be accompanied by a corresponding alteration in electron flow, O_2 consumption, and ATP generation. Therefore, assessing the ratio between the respiration rates before and after ADP addition, i.e. respiratory control ratio, is considered an excellent measure of mitochondrial dysfunction in isolated mitochondria (Brand & Nicholls 2011). Another excellent measure of mitochondrial dysfunction is the excess generation of reactive oxygen species (ROS), which is also implicated in the etiology of diseases including diabetes, cancer, and inflammatory disorders (Sena & Chandel 2012). ROS generation is a natural byproduct of mitochondrial metabolism that occurs as membrane potential ($\Delta\Psi$) builds across the inner mitochondrial membrane, thus creating a 'back pressure' that opposes proton pumping in the intermembrane space and slows electron flow through the ETC. This negative pressure can cause electrons to slip from the complexes and react with molecular oxygen to form superoxide and other ROS species. ROS generation can play a diverse role in normal cellular physiology function as key signaling molecules, however excess ROS production can lead to oxidative stress and damage. Given this dichotomy, in healthy cells mitochondrial ROS generation is regulated through antioxidant systems that mitigate ROS production (Sheu et al. 2006) to maintain energy and redox balance.

1.3 Basal metabolic rate and thermogenesis

The majority of the energy obtained from nutrient uptake is used to meet the energetic demands of an organism, or is converted to thermal energy. By nature, cellular metabolism has low thermodynamic efficiency where energy can be lost as heat (Silva 2011). Obligatory thermogenesis or basal metabolic rate (BMR) is the rate of energy utilized to perform basic life functions in a resting state at thermoneutrality. It can also be viewed as the constitutive heat production of an organism and major determinant in "setting" core body temperature i.e. basal thermogenesis.

Unlike poikilotherms, homeotherms have the ability to maintain core body temperature within a narrow range. For example, in response to severe cold temperatures where obligatory thermogenesis is unable to defend core body temperature, the body can activate mechanisms of heat production and conservation (i.e. cutaneous vasoconstriction and piloerection). The physiological heat-generating processes involved in maintaining core body temperature (shivering and non-shivering thermogenesis) are collectively referred to as facultative thermogenesis (Silva 2006).

1.3.1 Thermoregulation

At thermoneutrality, the temperature at which animals are not required to generate "extra" body heat to maintain normal body temperature, basal core temperature is maintained by heat generated from the combined inefficiency of all cellular and bodily metabolic reactions (i.e. obligatory thermogenesis, BMR). By contrast, in response to diverse stimuli including chronic cold exposure, endotherms have the ability to rapidly

generate heat in order to maintain core body temperature through adaptive facultative thermogenesis. The hypothalamus is commonly referred to as the master controller of thermoregulation (Charkoudian 2003) and coordinates the central and peripheral neurochemical mechanisms that regulate thermogenesis and heat dissipation. In response to elevated temperatures, the hypothalamus can activate heat dissipating mechanisms through sympathetic signaling to increase cutaneous vasodilation and sweating (in humans) (Nielsen 1998). Similarly, when mammals are faced with acute cold exposure, hypothalamic activation of the SNS initially inhibits heat dissipation through cutaneous vasoconstriction, and stimulates shivering thermogenesis in skeletal muscle (SKM) where muscle activity is increased to generate heat (De Witte 2002). However, shivering thermogenesis is energetically inefficient and impractical to sustain for longer periods of time. Therefore, endotherms have evolved other mechanisms of heat generation that are recruited to withstand chronic cold exposure without shivering (Silva 2006), i.e. non-shivering thermogenesis (Table 1.1). These thermogenic processes can also be induced by certain pharmacological agents (Rusyniak & Sprague 2006).

1.3.1.1 Fever versus toxicant-induced hyperthermia

A variety of pharmacological and toxicological agents can trigger a thermogenic response by altering hypothalamic and sympathetic nervous system (SNS) regulation of body temperature (i.e. toxicant-induced hyperthermia). The most well characterized toxicant-induced hyperthermic syndromes include neuroleptic malignant syndrome, serotonin syndrome, anticholinergic poisoning, sympathomimetic syndrome, and

Category	Component	Site	Main Mediators	Description of Thermogenic Systems
Obligatory Thermogenesis	Standard Metabolic Rate	All Tissues	Thyroid Hormone, Leptin, Insulin, Glucagon *Drugs: Levothyroxine*	Heat produced from all metabolic reactions necessary to maintain basic organ function
Facultative Thermogenesis	Shivering Thermogenesis	SKM	CNS	Heat produced from muscle movement in response to cold
	Non-Shivering Thermogenesis	BAT	SNS, Thyroid Hormone *Drugs: Sympathomimetics, Serotoninergic Agents*	Heat produced in response to cold, food, and certain pharmacological agents UCP1 and UCP3(?)
		SKM	SNS, Thyroid Hormone, Catecholamines *Drugs: Sympathomimetics, Serotoninergic Agents, Inhalational Anesthetics*	Heat produced in response to cold, food(?), and certain pharmacological agents UCP3 and Ca^{2+} cycling
	Movement-Related Heat Production	SKM	CNS	Heat produced from exercise or other voluntary muscle movement

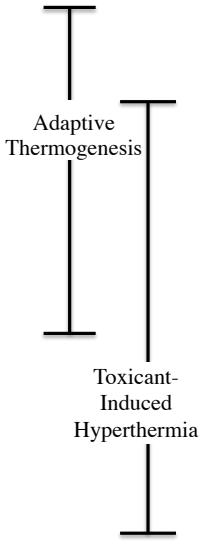

Table 1.1 Categories of thermogenesis

The energy obtained from nutrient intake is used for key metabolic processes or lost in the generation. Different categories of thermogenesis are classified based on their function/component and sites of heat production. Obligatory thermogenesis contributes to an organism's standard metabolic rate and refers to the heat generated from all processes required to maintain a basal state. Facultative thermogenesis refers to regulated-heat production in response to environmental changes or diet. Cold temperatures can activate systems of shivering and non-shivering thermogenesis as part of an adaptive response to maintain core body temperature. Pharmacological agents that interfere with mechanisms of normal thermoregulation can activate different components of facultative thermogenesis and lead to toxicant-induced hyperthermia.

hyperthermia. These conditions are associated with devastating medical complications including hyperkalemia, renal failure, metabolic acidosis, liver failure, rhabdomyolysis (Chan et al. 1997; Olson & Benowitz 1984), and even death.

It is important to distinguish between fever and drug-induced hyperthermia. Even though both conditions result in elevated core body temperatures, the underlying mechanisms are distinct. Fever is a regulated process that presents as a physiological response to infection when the hypothalamus increases the body's "set point" (Stitt 1979). In drug-induced hyperthermia, hypothalamic control is compromised and the body is pushed into a hypermetabolic state where excessive heat production cannot be mitigated by normal autoregulatory mechanisms of temperature control (Chan et al. 1997). Therefore, the use of antipyretics including acetaminophen and salicylates are ineffective in treating drug-induced hyperthermia where the implicating mechanisms stem from hypothalamic dysregulation (Stitt 1979; Chan et al. 1997). The only available treatments of drug-induced hyperthermia focus on alleviating the severity and duration of the hyperthermia through supportive care methods including rehydration and external cooling (Chan et al. 1997; Musselman & Saely 2013).

1.3.2 Facultative thermogenesis

Facultative thermogenesis occurs primarily in BAT and SKM, and can be classified into two categories, shivering and non-shivering thermogenesis. The initial response to cold temperatures is to increase muscle activity through shivering

thermogenesis in order to generate heat. However, prolonged exposure to cold temperatures requires the activation of adaptive non-shivering thermogenesis. SNS activation of BAT mitochondrial uncoupling protein 1 (UCP1) is the prototypical mechanism of nonshivering thermo. UCP1 (originally identified as thermogenin) was initially characterized as a thermogenic regulator back in the 1980's (Lin & Klingenberg 1980) and belongs to a family of highly conserved mitochondrial solute carriers that have the ability to increase mitochondrial respiration and uncouple oxidative phosphorylation from ATP production. By allowing protons to leak back into the matrix and circumvent the F_1/F_0-ATPase complex of the ETC, UCP1 converts the energy stored in the electrochemical gradient to thermal energy (released as heat).

UCP-mediated proton leak is a biochemical futile cycle where two metabolic processes are "uncoupled, and thus energy consuming. From an evolutionary standpoint, the existence of these uncoupled/futile cycling systems can be kinetically advantageous in severe situations that require rapid energy release (Rolfe & Brown 1997). Sarcoplasmic reticulum calcium extrusion and ATP dependent calcium uptake in SKM is another futile cycle that is implicated in adaptive non-shivering thermogenesis (Bal et al. 2012) as well as drug-induced hyperthermia (Rusyniak & Sprague 2006; Dao et al. 2014). Other examples of futile cycles include the actin-myosin cycling in SKM contraction, leakage of the sodium-potassium ATPase pump, and triglyceride/fatty acid cycling (Rolfe & Brown 1997) (She et al. 2007).

Although, research towards the clinical uses of BAT has been reinvigorated with the discovery that adult humans have more BAT than originally postulated (Nedergaard

et al. 2007; Cypess et al. 2009), the extent to which BAT contributes to non-shivering thermogenesis in adult humans remains unclear (Heaton 1972). Compared to rodents and newborns, adult humans possess minimal amounts of BAT. Therefore it is likely that alternative mechanisms of non-shivering thermogenesis, independent of BAT, have evolved. Indeed, animals that lack BAT (amphibians, reptiles, and birds) still exhibit SNS-dependent thermogenesis (Hissa et al. 1975; Harri & Hedenstam 1972; Barre & Rouanet 1983).

Skeletal muscle (SKM) is an attractive site of non-shivering thermogenesis due to its sheer size and the fact that it is a highly metabolic tissue in the body. As mentioned earlier, SKM is also the primary site of shivering thermogenesis, another subcategory of facultative thermogenesis. However, the mechanisms involved in muscle non-shivering thermogenesis are far less well characterized compared to BAT. Several studies have implied that thermogenic systems similarly designed to SNS regulation of UCP1-mediated proton leak in BAT may also exist in SKM (Silva 2011; Block & Franzini-Armstrong 1988; Bal et al. 2012). This idea is supported by studies that show NE administration can increase metabolism and thermogenesis in isolated muscle systems (Mejsnar & Jansky 1971). In addition to this, work elegantly done by Astrup and colleagues has demonstrated that ephedrine-induced thermogenesis is mainly derived from SKM in adult humans (Astrup et al. 1985; Astrup et al. 1984). Furthermore, most if not all types of drug-induced hyperthermic conditions are associated with SKM damage (Rusyniak & Sprague 2006). For example, malignant hyperthermia (MH) involves a well-defined mechanism of drug-induced hyperthermia in susceptible populations that

carry mutations in the SKM ryanodine receptor calcium channel (RYR1). In response to inhalational anesthetics, these mutations can alter Ca^{2+} leakage in SKM and lead to uncontrolled hyperthermia by allowing Ca^{2+} to pass down its concentration gradient, thus uncoupling the sarcoplasmic/endoplasmic reticulum Ca^{2+}-ATPase pump (SERCA) from ATP hydrolysis (Bal et al. 2012). Although it is not established whether RYR1 is a direct regulator of non-shivering thermogenesis under normal, physiological circumstances, it is likely that SKM intra-myocyte calcium handling, in general, plays an important role in adaptive non-shivering thermogenesis. This idea is corroborated with recent studies showing that mice lacking sarcolipin, a negative regulator of SERCA were unable to defend core body temperature in cold environments (Bal et al. 2012).

1.4 Metabolic derangements in obesity-induced insulin resistance

Recent research regarding the governing mechanisms of obesity-induced insulin resistance focuses heavily on the interplay between mitochondrial bioenergetics and fatty acid metabolism. Although there is a clear association between ectopic fat accumulation and the development of insulin resistance in SKM, the underlying mechanisms at a molecular level remain a matter of controversy. The two prominent theories that have emerged to explain obesity-induced insulin resistance in SKM both center on mitochondrial dysfunction. The first theory is based on a series of clinical studies that showed fatty acid metabolism and overall SKM mitochondrial oxidative capacity was severely diminished in severely obese or insulin resistant settings (Morino et al. 2006; Petersen et al. 2003; Petersen et al. 2004; J. Y. Kim et al. 2000). These observations led

to a proposed model of fatty acid-induced insulin resistance where deficiencies in mitochondrial oxidative function and fatty acid metabolism lead to the accumulation of diacylglycerol and other toxic lipid intermediates that antagonize insulin signaling (Roden et al. 1996). This model is attractive in that it implies that increasing mitochondrial fatty acid oxidation would improve insulin sensitivity.

In recent years another model of obesity-induced insulin resistance has gained momentum and centers on the principles of mitochondrial bioenergetics to explain that the observed mitochondrial deficiencies seen with insulin resistance are actually a consequence of fuel supply exceeding energy demand. This model is based on the premise that oxidative phosphorylation is governed by energy demand/expenditure, and is thus rarely operating at maximal capacity. Therefore, enhancing fatty acid oxidation alone without a corresponding increase in energy expenditure/demand will impinge persistent pressure on mitochondrial respiration and function, thus leading to an impairment of insulin signaling pathways. This model is supported by the observation that despite an up-regulation of key fatty acid metabolizing enzymes in response to high fat diet, fatty acid intermediates still accumulate due to the energetic imbalance where supply exceeds energy expenditure (Koves et al. 2008; Turner et al. 2007). Furthermore, studies in different animal and human models of obesity-induced insulin resistance have shown that administration of pharmacological drugs that inhibit CPT1, a master regulator of mitochondrial β-oxidation, can improve glucose homeostasis (Deems et al. 1998; Barnett et al. 1992).

Another relevant topic regarding the underlying mechanisms of mitochondrial overload in obesity-induced insulin resistance is the generation of reactive oxygen species. ROS generation can greatly antagonize mitochondrial function and induce oxidative stress, but can also serve as potent activators of several stress-responsive kinases that impair insulin signaling in SKM, including c-jun amino-terminal kinases (JNK), IκB kinase catalytic subunit β (IKK-β), and protein kinase C (PKC) (S. Chakraborti & T. Chakraborti 1998). In understanding how excess metabolic fuel can have detrimental effects on mitochondrial respiration it is important to remember that proton conductance governs electron flow which is determined by the demand of the reducing equivalents (NADH and $FADH_2$) that are generated through substrate uptake and subsequent metabolism. Therefore, the accumulation of excess reducing equivalents due to chronic over nutrition will impose additional pressure at the entry point of the electron transport chain into complex I (NADH) and/or the ubiquinone cycle ($FADH_2$). Furthermore, it has also been shown that the relative proportion of electrons that feed into complex I, or the ubiquinone cycle can also affect redox balance. For example, the oxidation of saturated fatty acid palmitate feeds electrons directly into the ubiquinone cycle via ETF, and is associated with higher rates of H_2O_2 generation (St-Pierre et al. 2002; Seifert et al. 2010). Regardless, the chronic pressure on the electron transport chain alters mitchondrial redox balance and creates a microenvironment that is highly susceptible to the generation of reactive oxygen species (Fisher-Wellman & Neufer 2012). This model is supported by studies that show genetic and pharmacologic

interventions that mitigate mitochondria oxidative stress can improve insulin signaling and glucose homeostasis (Henriksen 2006; Houstis et al. 2006).

Although chronic overnutrition can trigger a complex series of metabolic events that contribute to obesity-induced insulin resistances, a clear approach to target all these metabolic derangements is to increase energy expenditure/demand. As mentioned earlier in the preceding sections, increasing the rate of substrate oxidation alone, more specifically β-oxidation, without a corresponding elevation in energy demand can further exacerbate the problem of mitochondrial overload on the electron transport chain. However, if the flux through β-oxidation increases as a consequence of added demand, this metabolic shift complies with the principles of mitochondrial bioenergetics that are governed by energy demand/expenditure. Thus, our current understanding of mitochondrial bioenergetics and obesity-induced insulin resistance suggests the key to developing treatments with long-term efficacy involve new strategies that attack the root cause of the problem and promote energy inefficiency.

1.5 The mitochondrial uncoupling protein family

Research regarding the clinical use of uncoupling proteins (UCPs) in the treatment of obesity and -related metabolic disorders have been prominent since their initial characterization in the late 1970s (Brand & Esteves 2005). Mitochondrial UCPs are nuclear encoded members of the mitochondrial solute carrier (SLC) family that have the ability to lower mitochondrial membrane potential through proton leak. Five UCP homologues (UCP1-5) have been identified in mammals with UCP1 being considered the

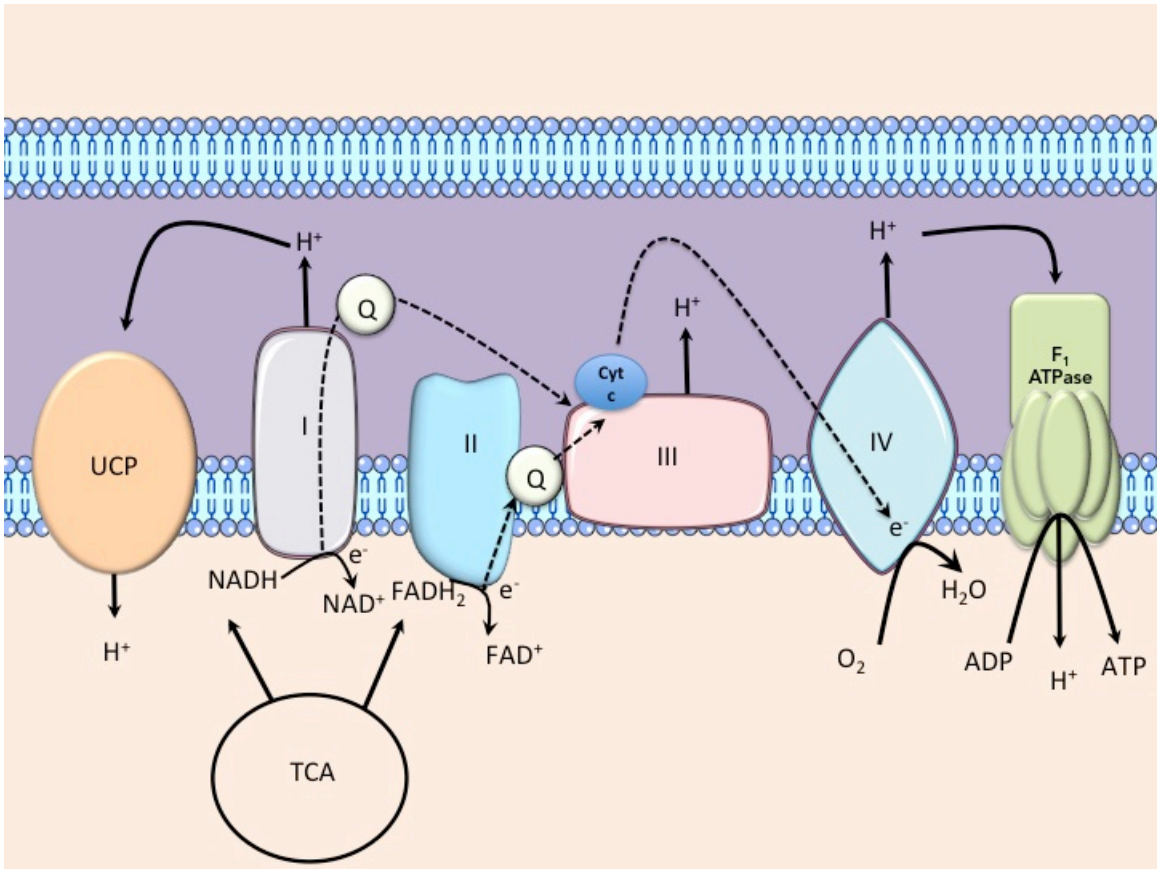

Illustration 1.7 Futile proton cycling through mitochondrial uncoupling proteins
Mitochondrial Uncoupling Proteins (UCPs) are members of the mitochondrial solute carrier family (SLC) family that have the ability to uncouple the electron transport chain from ATP production. By allowing protons to flow down (H^+) gradient and circumvent F_1/F_0ATP synthase (F_1/F_0ATPase), UCPs promote inefficient energy utilization and increase mitochondrial respiration. Therefore, cells have to increase flux through the catabolic pathways that feed into the TCA cycle in order to replenish the reducing equivalents NADH and $FADH_2$ that fuel the electron transport chain.

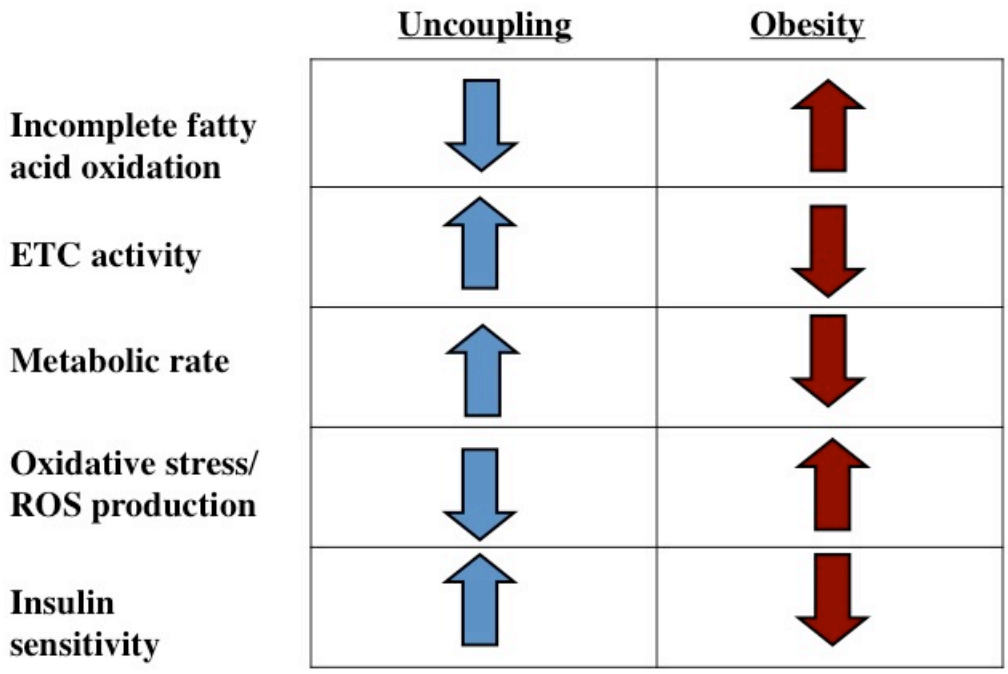

Table 1.2 Uncoupling proteins counteract the metabolic derangements seen with obesity-related complications

The metabolic effects of mitochondrial uncoupling on fatty acid oxidation, reactive oxygen species (ROS) production, energy metabolism directly oppose the metabolic phenotypes seen with obesity-related pathologies. Through uncoupling of the electron transport chain and ATP generation, these proteins can drive substrate oxidation and relieve pressure on the electron transport chain to lower ROS production by counteracting the energy surplus seen in obese states.

"canonical" UCP member. While UCP1 is exclusively expressed in BAT, the tissue distribution of the other UCP homologues is more diverse. Compared to UCP4 and UCP5, UCP2 and UCP3 share high sequence homology with UCP1 (Krauss et al. 2005). Interestingly, all members of the UCP family have been described in diverse roles related to metabolism, however their physiological relevance is still under investigation (Krauss et al. 2005).

The effects of UCP activity on mitochondrial bioenergetics directly opposes the energetic and physiological abnormalities seen in obesity and –related metabolic disorders (Table 1.2). True to their name, UCPs have the ability to uncouple nutrient oxidation from ATP synthesis by dissipating the proton gradient. UCP-regulated proton leak decreases the efficiency of oxidative phosphorylation, which results in a compensatory increase in substrate oxidation and flux through the ETC by mitochondria in order to maintain membrane potential and ATP production. In conjunction with increasing flux and lowering the proton motive force, UCPs can relieve the reducing pressure on the ETC from nutrient overload and mitigate ROS production (Esteves & Brand 2005).

1.5.1 The canonical uncoupling protein

UCP1, also referred to as thermogenin, constitutes a significant portion (~10%) of the mitochondrial membrane protein in BAT (Rousset et al. 2004). In the canonical adaptive response to cold, the hypothalamus activates the SNS, triggering the release of

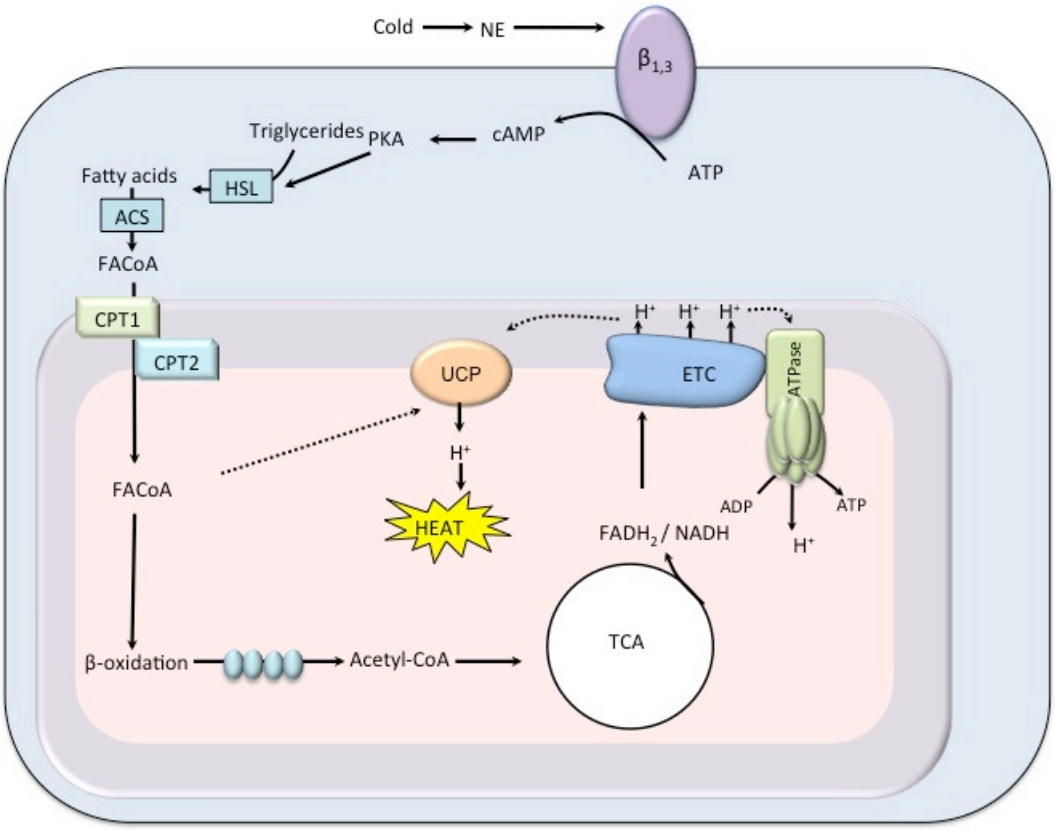

Illustration 1.8 Cold-induced non-shivering thermogenesis in BAT

Adaptive non-shivering thermogenesis is an evolutionary process that occurs through UCP1 expression in brown adipose tissue of small rodents and newborn babies. In response to cold, rodents and newborns are able to maintain their body temperature when norepinephrine (NE) is released to activate the cyclicAMP-protein kinase A-hormone sensitive lipase (cAMP-PKA-HSL) pathway which leads to the lipolysis of triglycerides and the release of fatty acids. This event is critical in thermogenic function as the fatty acids play an important role in activating UCP1 and serve as a combustive fuel source for mitochondria.

norepinephrine (NE) from sympathetic neurons that densely innervate BAT tissue depots (R. E. Smith & Horwitz 1969). NE binds to β_3-adrenoreceptors (β_3AR) on brown adipocytes, initiating a signaling cascade that leads to the generation of free fatty acids from cytoplasmic multilocular lipid droplets via the cyclic AMP-protein kinase A-hormone sensitive lipase signaling pathway (cAMP-PKA-HSL) (Nicholls & Locke 1984a; Jezek & Freisleben 1994). Free fatty acids are then transported into BAT mitochondria via the carnitine shuttle system, where they are used as fuel substrates for β-oxidation, and activate UCP1-mediated thermogenesis (Cannon & Nedergaard 2004).

An interesting characteristic of UCP1-dependent non-shivering thermogenesis in response to cold is its regulation through fatty acids, as well as its inhibition by purine nucleotides (ATP or GDP). The physiological importance of fatty acids in stimulating non-shivering thermogenesis is reinforced by

studies demonstrating that thermogenesis is severely impaired in mice with genetic defects in enzymes that affect fatty acid metabolism and transport (Guerra et al. 1998). Likewise, studies that show fatty acids alone can simulate NE-induced thermogenesis in the presence of UCP1 (Nahrendorf et al. 2000), and that BAT thermogenesis can be blocked through inhibition of lipolysis (Fredriksson et al. 2001), further supports the role of lipolysis in β_3AR –stimulation of UCP1-dependent thermogenesis. With regard to the direct molecular mechanisms underlying fatty activation of UCP1-mediated proton leak, recent work utilizing a patch clamp method to measure UCP1 currents has demonstrated that UCP1 doesn't possess constitutive activity (most likely inhibited by purine

nucleotides) until activated by long chain fatty acids. Once activated, UCP1 acts as long chain fatty acid anion / H^+ symporter to mediate proton leak across the inner mitochondrial membrane (Fedorenko et al. 2012). Thus, UCP1 activation by fatty acids is an essential component of adaptive non-shivering thermogenesis.

Based on our understanding of the thermogenic capabilities of UCP1 on metabolic inefficiency and obesity, one would expect that the absence of UCP1 would result in reduced capacity to burn fat and energy. However, it was surprising and somewhat counterintuitive that UCP1 knockout mice were protected from diet-induced obesity in a manner that was highly dependent on environmental temperature (Enerback et al. 1997). These mice were only susceptible to diet-induced obesity when housed at thermoneutrality, the state at which the body does not need to make additional heat to maintain core body temperature, and thus does not require UCP1 activity (X. Liu et al. 2003). These findings further bolster the association between adaptive non-shivering thermogenesis and weight regulation, and more importantly, suggest that in the absence of UCP1, alternative pathways of non-shivering thermogenesis exist to maintain core body temperature.

1.5.2 Characterization of UCP3

The UCP1 homolog, UCP3, shares more than 50% amino acid homology with UCP1 and has been shown to regulate proton flux (Jaburek et al. 1999; Boss et al. 2000). Compared to UCP1, UCP3 is more broadly expressed and can be found in various tissues including heart, SKM, BAT (Vidal-Puig et al. 1997), and as we recently demonstrated,

skin (Lago et al. 2012). Given its diverse tissue expression in highly metabolic tissues, it has been postulated that UCP3 may play a more extensive role in whole body energy balance.

In the UCP field, a great deal of controversy exists regarding UCP3 as a physiological thermogenic regulator. Soon after its identification in 1997, UCP3 knockout mice were generated and shown to have no thermogenic phenotype when exposed to cold (Gong et al. 1997). However, the mere lack of a cold-phenotype in the UCP3 knockout mice could be due to the existence of compensatory processes that enable these mice to fulfill their heat requirements in response to cold, and thus does not necessarily rule out the involvement of UCP3 in alternative mechanisms of non-shivering thermogenesis.

There are several lines of evidence to support the thermogenic capacity of UCP3 in response to certain pharmacological agents and hormonal stimuli, particularly in SKM. Thyroid hormone, a key endocrine regulator of thermogenesis and energy balance (Silva 1995), is closely tied to UCP3 activation by numerous studies demonstrating that changes in thyroid status can alter UCP3 gene expression (Gong et al. 1999;Larkin et al. 1997). Consistent with these findings, studies utilizing a $\beta_1/\beta_2/\beta_3$-adrenoreceptor knockout (β-less) mouse model that possesses a severely cold-intolerant phenotype, showed that administration of 3,5,3' triiodothyronine (T3), an active form of thyroid hormone, significantly increased UCP3 expression in SKM and also rescued cold-induced thermogenesis in these mice (Flandin et al. 2009).

UCP3 has also been shown to be a key molecular mediator in toxicant-induced hyperthermia. Amphetamine type drugs, also known as sympathomimetics such as methamphetamine and 3,4-methlenedioxymethamphetamine (MDMA, Ecstasy), can trigger life-threatening hyperthermia. Interestingly, mice lacking UCP3 exhibit severely blunted hyperthermic responses to MDMA and are protected from the lethal effects of the drug (Mills et al. 2003). Moreover, in terms of the underlying mechanism of UCP3 activation in sympathomimetic induced hyperthermia, it has been shown that Meth administration leads to the phosphorylation of UCP3 and subsequent increase in proton leak (Kellya et al. 2012).

1.5.2.1 Physiological relevance of UCP3

Despite the controversy surrounding the thermogenic capacity of UCP3, it remains an attractive target in the treatment of obesity and related metabolic diseases. Another prominent area of UCP3 research is devoted to its role in modulating mitochondrial ROS production. Researchers believe that the excess generation of ROS from the chronic pressure exerted on the ETC due to overnutrition could explain how an obese state can lead to the development of insulin resistance. This proposed mechanism centers on the premise that chronic oversupply of mitochondrial oxidative substrates such as lipids, sugars, and amino acids likely facilitate a metabolic environment that is favorable to the generation of ROS (Morino et al. 2006; Muoio & Newgard 2008). Interestingly, mice under-expressing UCP3 showed evidence of significantly higher levels of oxidative damage (Brand et al. 2002). Furthermore, numerous studies have

shown that UCP3 in SKM can lower mitochondrial ROS generation (MacLellan, Gerrits, Gowing, P. J. S. Smith, Wheeler & Harper 2005a) and protect against oxidative stress in SKM (Barreiro et al. 2009). These studies, taken together with the fact that superoxide activates UCP3 (Echtay et al. 2002) has led to a proposed feedback mechanism in which elevated levels of ROS production activate UCP3 to mitigate the generation of these free radicals and protect against oxidative stress.

In addition to its potential role in the protection against oxidative stress and non-shivering thermogenesis, it has also been proposed that UCP3 plays an important role in facilitating complete fatty acid oxidation and transport (Himms-Hagen & Harper 2001; Brand & Esteves 2005). Mice that overexpress UCP3 in SKM have higher levels of fatty acid oxidation (Bézaire et al. 2005; MacLellan, Gerrits, Gowing, P. J. S. Smith, Wheeler & Harper 2005a) and show reduced circulating levels of biomarkers for incomplete β-oxidation (Aguer et al. 2013). The evidence supporting the involvement of UCP3 in facilitating efficient and complete fatty acid oxidation suggests a protective role for this protein in obesity-induced insulin resistance. Indeed, studies in UCP3 heterozygous mice with reduced levels of UCP3 protein expression in SKM exhibited impaired rates of fatty acid oxidation, along with a clear deterioration in insulin signaling when fed high fat diets (Senese et al. 2010). Taken together, these studies emphasize the importance of characterizing the underlying mechanisms that link fatty acid metabolism to UCP3 given the current obesity epidemic in the US.

1.6 Dissertation objectives

In the search to develop new therapeutics to treat obesity, the generation of various novel transgenic animal models has allowed researchers to identify specific molecular targets that can alter body weight and promote insulin sensitivity. A common underlying mechanism in many of these obesity-resistant animal models is elevated energy expenditure (Reitman 2002). Aside from physical activity, an increase in energy expenditure/demand can only occur through thermogenic processes (i.e. uncoupling and futile cycling) that promote energy inefficiency.

The most well described mechanism of thermogenesis is inducible mitochondrial proton leak via uncoupling proteins. UCPs belong to a conserved class of mitochondrial anion / solute carrier superfamily of proteins that are expressed in the inner mitochondrial membrane and have the unique ability to uncouple substrate oxidation from ATP generation by allowing protons to leak back into the matrix and circumvent ATP synthase. By promoting metabolic inefficiency and increasing energy expenditure, mitochondrial uncoupling can drive substrate oxidation to relieve the persistent pressure on the ETC from nutrient overload, and also lower mitochondrial ROS production.

UCP1, the canonical uncoupling protein expressed almost exclusively in BAT, is recognized as the master regulator of adaptive non-shivering thermogenesis. Indeed, UCP1 knockout mice are extremely sensitive to cold temperatures (Golozoubova et al. 2001), and are also susceptible to diet-induced obesity when housed at thermoneutrality (Feldmann et al. 2009). However, when it comes to the other UCP homologues, including UCP3, the molecular mechanisms underlying its thermogenic actions are unclear. Even

though UCP3 knockout mice exhibit normal thermoregulatory responses to cold and do not possess a clear metabolic phenotype (Vidal-Puig et al. 2000), UCP3 overexpression in SKM is positively associated with improved glucose homeostasis(Choi et al. 2007; Huppertz et al. 2001), increased fatty acid oxidation (MacLellan, Gerrits, Gowing, P. J. S. Smith, Wheeler & Harper 2005a; Aguer et al. 2013; Bézaire et al. 2005), and enhanced energy expenditure in SKM(Clapham et al. 2000).

Given that mitochondrial uncoupling can counteract the metabolic derangements seen with obesity-induced insulin resistance, we set out to characterize the mechanisms by which UCP3 controls thermogenesis, fatty acid oxidation, and SKM metabolism. We hypothesized that SKM is the primary site of UCP3-dependent thermogenesis, and that it is interacting with key metabolic proteins involved in maintaining energy balance during nutrient overload. To test this hypothesis, we focused on the following aims: (1) defining the role of SKM UCP3 in regulating sympathomimetic-induced thermogenesis (2) identifying key UCP3-protein interactions in SKM (3) characterizing the interaction between UCP3 and the auxiliary unsaturated fatty acid metabolizing enzyme, ECH1. Collectively, this investigation highlights the importance of UCP3 in regulating thermogenesis and energy balance in SKM. Furthermore, the work shown here establishes a novel mechanism by which complex formation between UCP3 and ECH1 coordinates an increase in fatty acid metabolism and energy demand to protect against metabolic stress.

Chapter 2: Materials and Methods

2.1 Chemicals and reagents

Unless otherwise noted, all reagents were purchased from Sigma (St. Louis, MO).

2.2 Plasmid DNA constructs

Full-length UCP3, UCP1 and ECH1 genes were amplified from mouse heart cDNA library and cloned into pcDNA3.1 (Invitrogen, Carlsbad, CA) with either the C-terminal V5 or Myc tag, respectively.

2.2.1 Quickchange site-directed mutagenesis

Site-directed mutagenesis of plasmids to generate the C-terminal Myc tagged ECH1 catalytic mutants and the C-terminal V5 tagged UCP3 truncation mutants was carried out with Platinum pFX DNA polymerase from (Life Technologies, Grand Island, NY), following the manufacturer's protocols for site-directed mutagenesis. The primers used to generate the Myc tagged- ECH1 catalytic mutants were previously published in Zhang *et al*.

2.3 Cell culture

HEK293T and C2C12 cells were obtained from the American Type Culture Collection (ATCC, Manassas, VA). HEK293T cells were cultured at 37°C with 5% CO_2

in Dulbecco's Modified Eagle Medium (Cellgro, Manassas, VA) containing 10% Fetal Bovine Serum1% and 100X PenG- Streptomycin (Invitrogen, Carlsbad, CA). C2C12s were cultured in similar conditions, with the exception of being grown in high glucose (45000mg/L), Dulbecco's Modified Eagle Medium from Sigma (St. Louis, MO).

2.3.1 Transient transfection of cells

HEK293Ts were plated one day prior to transfection and were transfected with either calcium phosphate or TransIT-LT1 (Mirus, Madison, WI) following the manufacturer's instructions. To improve transfection efficiency of C2C12s, a cell line that is generally difficult to transfect, cells were transfected with Lipofectamine 2000 at a 2:1 ratio (Invitrogen, Carlsbad, CA) immediately after plating cells, according to Mercer *et al*.

2.3.2 Generation of stable C2C12 cell lines

The Precision LentiORF lentiviral packaging system was obtained from Thermo Fisher Scientific (Waltham, MA). Full-length ECH1 was cloned into the pLOC lentiviral plasmid following the manufacturer's instructions.

HEK293T packaging cells were transfected with the pLOC lentiviral plasmid and two viral packaging plasmids pMDG2 and psPAX2, using a standard calcium phosphate transfection method to produce the lentiviral particles. The HEK293T cells were incubated with the transfection complexes in normal growth media supplemented with 25μM choloroquinone for 8 hours. Forty hours after transfection, the virus containing media was harvested. To concentrate the lentiviral particles, the Lenti-X Concentrator

reagent (Clonetech, Mountainview, CA) was used according to the manufacturer's protocols.

For lentiviral transduction, C2C12 myocytes were seeded in 6 well plates at 50,000 cells/wells one day prior to infection. The cells were then incubated with the concentrated lentiviral particles in full growth media supplemented with polybrene (8μg/mL), overnight. Following infection, stable cell colonies were selected with 25μg/mL of blasticidin. Positive colonies were then confirmed through immunoblotting and densitometry.

2.4 Animals

C57BL/6J wild-type mice were obtained from Jackson Laboratories (Bar Harbor, ME). The UCP3 knockout mice ($UCP3^{-/-}$) in the C57BL/6J background were a gift from Dr. Marc Reitman, formerly of the National Institutes of Health. The UCP1 knockout mice ($UCP1^{-/-}$) were a gift from Dr. Leslie Kozak of the Pennington Biomedical Research Institute. The UCP3 $^{-/-}$ mice were crossed with the $UCP1^{-/-}$ mice to generate our UCP1 and UCP3 double knockout line ($UCP1^{-/-}$ + $UCP3^{-/-}$). The transgenic mice overexpressing human UCP3 in SKM generated from human alpha1-actin promoter targeting construct (TgSKM UCP3 $^{+/+}$) were a gift from Dr. Mary-Ellen Harper of the University of Ottawa. The TgSKM UCP3 $^{+/+}$ were then crossed with the UCP3 -/- and DKO lines to generate a transgenic mouse overexpressing human UCP3 in SKM in the $UCP3^{-/-}$ and DKO background (TgSKM UCP3 $^{-/-}$ and TgSKM $UCP1^{-/-}$ + $UCP3^{-/-}$,

respectively). It is important to note that all TgSKM-UCP3 strains were kept as hemizygous breeder colonies.

Unless otherwise noted, all experiments were performed in male mice between the ages of 6-8.5 weeks. All animal husbandry and procedures were carried out in accordance to the Association for Assessment and Accreditation of Laboratory Animal Care (AAALAC) and approved by the Institutional Animal Care and Use Committee at The University of Texas at Austin (IACUC).

2.4.1 Generation of ECH1 $^{-/-}$ mouse model

The custom designed CompoZr® Zinc Finger Nuclease Plasmid targeted to exon 3 of the mouse ECH1 gene on chromosome 7 was obtained from Sigma. In-vitro transcription of the ZFN mRNA was performed following the manufacturer's instructions. mRNA was transfected in cultured cells to validate activity using a Cel-I enzymatic mutation detection assay. The ZFN mRNA (10ng/μl) was then microinjected into 330 mouse BDF1 embryos and implanted into pseudopregnant female mice recipients.

Genotyping of founders (F_0) was done using genomic PCR with the primers following primers provided by Sigma, forward 5'-CGCGATGACAGTTTCCAGTA-3' reverse 5'-CAAACAAAAACCCACTGAGGA-3'. In order to perform DNA sequence analysis, amplified bands of the ZFN target site were cloned in to the pGEM-T Easy Vector system (Promega, Madison, WI) and sequenced by the University of Texas at Austin's DNA Sequencing Facility. Two founders (line 3 and 11) were then selected for

backcrossing and then mated with the wild-type C57BL/6J mice. Speed congenics was performed to select the heterozygous males from each generation for breeding, and to ensure that >99% of the BDF1 background was replaced with the C57BL/6J background. Line 11 was backcrossed a total of 6 generations before proceeding with experiments.

2.4.2 Diet induced obesity studies

At the age of three weeks, mice (n=8) were placed on high fat chow (60% fat kCal, TD.06414) or control chow (10% fat kCal, TD.0.8806)) for 6 weeks. All diets were provided from Teklad Laboratories (Chicago, IL). At the end of the 6 week treatment period mice were sac'd and mitochondria was extracted from SKM and BAT using the previously described procedure.

2.4.3 Intraperitoneal temperature probe placement

Male mice between 6-7 weeks of age, weighing between 20-25 grams were used for all experiments. All surgical tools and operating areas were prepared under sterile technique procedures. The right dorsal flank of each mouse was shaved and cleaned with sterile povidine solution. The mice were then anaesthetized with isoflurane via nose cone and administered a preoperative subcutanous injection of 5mg/kg carprofen. A transverse oblique incision was made dorsally above the iliac crest, followed by another incision through the peritoneal wall. The wireless temperature probe by Starr Life Sciences Corp (Oakmont, PA) was then inserted into the peritoneal cavity. The incision on the peritoneal wall was closed with nonabsorbable Vicryl sutures. Lastly, the skin was closed using sterile skin clips. The following day, mice were given a postoperative

subcutaneous injection of carprofen. The mice were closely monitored for any signs of distress or infection after surgeries.

2.4.4 Thermogenic drug administration

Following the intraperitoneal temperature probe placement surgery, mice were given a one week recovery period prior to experiments. All injections were performed in a temperature-controlled chamber at 25°C. Mice were weighed and placed in individually housed cages with 50g of fresh bedding. Baseline temperatures were recorded and mice were then administered a subcutaneous injection, at the nape of the neck, of either methamphetamine (20mg/kg) or norepinephrine (1mg/kg) dissolved in sterile saline. Core body temperatures were monitored and recorded every minute using the VitalView Software (Starr Life Sciences, Oakmont, PA).

2.4.5 Fasting and cold-exposure studies

Male mice between the ages of 7.5-8.5 weeks old were fasted for 18hrs in individually housed cages with fresh bedding. The body weight of each mouse was recorded before and after fasting treatment. Any mouse under 21g was excluded from the study.

Cold tolerance was then tested by placing mice in a temperature-controlled room at 4°C for 3-6 hours, or until body temperature dropped below 25°C. Core body temperatures was recorded prior to cold-exposure and every hour during treatment with a rectal temperature probe (Physitemp, Clifton, NJ) .

2.5 Isolation of mitochondria from cell and animal tissues

C2C12 cells were homogenized with a 27.5 gauge needle in CP-1 buffer supplemented with protease and phosphatase inhibitors. Homogenates were then centrifuged at 500g for 10 minutes at 4˚C twice, making sure to discard pellets and re-aliquot supernatant in to new tubes in between spins. After second spin, the supernatant was collected and spun at 10,500 g for 10 minutes at 4˚C to pellet mitochondria.

Brown adipose tissue, SKM, and heart tissue samples were isolated from mice and finely minced in either CP-1 buffer or 100mM KCl, 500mM Tris-HCl, 2mM EGTA, 1mM ATP, 5mM $MgCl_2$, 0.5% BSA, pH 7.4 supplemented with protease and phosphatase inhibitors. Tissues were then homogenized with a Teflon pestle drill press in smooth glass homogenizers. Homogenates were then centrifuged at 800g for 10 minutes at 4˚C twice, making sure to discard pellets and re-aliquot supernatant in to new tubes in between spins. After the second spin, homogenates were applied to a 70μm cell strainer and then centrifuged at 10,500g for 10 minutes at 4˚C to pellet mitochondria.

2.6 Immunoprecipitation and mass spectrometric analysis

Mitochondria were isolated from SKM of wild-type C57BL/6J mice and UCP3 -/- following the previously described method of mitochondrial isolation from animal tissues. Mitochondrial pellets were resuspended in immunoprecipitation buffer (50mM Tris-HCL 300mM NaCl, 1% Triton X-100 supplemented with 200 μM PMSF, 1μg/ml Leupeptin, 1μg/ml Pepstatin A, 100 U/ml Aprotonin, 200 μM Sodium Orthovanadate, and 100 mM Sodium Fluoride) and lysed with a bead mill homogenizer for 10 minutes at

4˚C. Mitochondrial protein was quantified using a bicinchoninic acid assay (Pierce Biotechnology, Rockford, IL).

Immunoprecipitation samples were prepped in 600µl immunoprecipitation buffer and incubated with rabbit polyclonal α-UCP3 (custom antibody generated by Washington Biotechnology, Columbia, MD) at 1:50 dilution for ~16 hours at 4˚C with rotation. Prior to adding Protein G Sepharose beads (Pierce Biotechnology, Rockford, IL) to samples, the beads were blocked in 5% BSA in PBS at 4˚C for 16 hours with rotation. Protein G Sepharose beads (1:50 dilution) were added to each immunoprecipitation sample and rotated at 4˚C for 5 hours. Beads were washed 8 times before protein elution. Samples were then prepared for SDS polyacrylamide gel electrophoresis (PAGE) using a BioRad precast gel (BioRad, Hercules, CA).

The coomassie stained protein complex band was cut out of gel and submitted to the ICMB Proteomics Facility at the University of Texas at Austin. Results were analyzed via the Scaffold 3 software (Proteome Software, Portland, OR).

2.7 Immunoblotting

Lysates were prepared in RIPA buffer (50mM Tris-HCl, 1% NP40, 0.5% Sodium Deoxycholate, 0.1% Sodium Dodecyl Sulfate (SDS), 150mM Sodium Chloride (NaCl), 2mM EDTA, pH 8.0) supplemented with protease and phosphatase inhibitor cocktails (Roche, Nutley, NJ). A bicinchoninic acid assay (Pierce Biotechnology, Rockford, IL) was used to quantitate proteins.

Nitrocellulose membranes were probed with the following primary antibodies;

rabbit polyclonal α-V5 (Abcam, Cambridge, MA), mouse monoclonal α-V5 (Life Technologies, Grand Island, NY), α-mouse monoclonal α-myc (Cell Signaling, Danvers, MA), rabbit polyclonal α-ECH1 (custom antibody generated by Washington Biotechnology, Columbia, MD), rabbit polyclonal α-ECH1/ECH1 (Abcam, Cambridge, MA), rabbit polyclonal α-UCP3 (custom antibody generated by Washington Biotechnology, Columbia, MD), and rabbit polyclonal anti-UCP3 (Abcam, Cambridge, MA). Following incubation with primary antibodies, the nitrocellulose membranes were probed with α-rabbit-HRP or α-mouse-HRP (GE Healthcare, Piscataway, NJ). Membranes were developed using Super Signal West Pico chemiluminescent (Pierce Biotechnology, Rockford, IL).

2.8 Co-immunoprecipitation

Immunoprecipitation samples (IP) were prepared using 250-500μg of protein and adjusted to 300μl with the previously described immunoprecipitation buffer. Samples were then incubated with either 1μg of primary antibody or IgG (for controls) at 4˚C for 16 hours with rotation. Protein G Sepharose beads were blocked in 5% BSA in PBS overnight as previously described. Thirty microliters of Protein G Sepharose beads were then added to each immunoprecipitation sample and rotated at 4˚C for 5 hours. Samples were washed 8 times with wash buffer, after then prepared for SDS polyacrylamide gel electrophoresis (PAGE).

2.9 Quantitative RT-PCR

Total RNA was extracted from C2C12 cells and mouse tissues using the TRIzol® reagent (Invitrogen, Carlsbad, CA) according to manufacturer's instructions. RNA was then reverse transcribed using the TaqMan® Reverse Transciption Kit (Life Technologies, Grand Island, NY) and quantative RT-PCR was performed with the SYBR Green dye using a real-time PCR system (Bio-Rad, Hercules, CA). The following primers used for amplification are listed in appendices. Experiments were repeated in triplicates and data represent fold change relative to levels of GAPDH.

2.10 Immunocytochemistry

Twenty-four hours after transfection C2C12s were fixed and permeabilized in 2.5% paraformaldehyde and 0.1 % TritonX-100 at RT for 20 minutes. The cells were then incubated with either anti-Myc or the peroxisomal marker anti-catalase (Abcam, Cambridge, MA), followed by secondary anti-mouse Alexa 568 or anti-rabbit Alexa 488. All fluorescent images were acquired with a Nikon Eclipse Ti-S microscope, 60x Nikon Plan Apo VC Oil objective with numerical aperture 1.40. Images were captured with Photometrics Coolsnap EZ camera and processed using Nikon NIS Elements BR 3.0 software.

2.11 Myocyte oxygen consumption

Respiration rates in SKM myocytes were quantified using a fiber-optic fluorescence oxygen monitoring system (Instech Laboratories, Plymouth Meeting, PA).

Three million cells were added to the 1mL chamber containing Dulbecco's Modified Eagle Medium from Sigma (St. Louis, MO). Basal and oligomycin-induced uncoupled respiration rates were determined from linear regions of the slope observed after each treatment.

2.12 Fatty acid oxidation

C2C12 stable cell lines were grown in a 24-well plate were transiently transfected and assayed for oleate oxidation using the method of Mao et al. (39). Briefly, myocytes were serum starved for 2 hours in substrate-limited media. They were then incubated in 1μC/ml ^{14}C-oleic acid (American Radiolabeled Chemicals, St. Louis, MO), lysed with 70% percholoric acid, and collected radioactivity was measured using a scintillation counter.

2.13 Statistics

Analysis of variance comparisons between genotypes were analyzed by a student's t-test or single factor ANOVA followed by Tukey's post hoc test, with a $p<0.05$ set *a priori* as statistically significant.

Chapter 3: SKM UCP3 in sympathomimetic-induced hyperthermia

3.1 Introduction

As discussed earlier, there are various pharmacological and toxicological agents that can alter the normal mechanisms of thermoregulation and trigger different metabolic pathways of heat-generation, thus resulting in life-threatening hyperthermia. Although the thermogenic capacity of UCP3 in SKM has been greatly debated since its discovery, there have been several lines of evidence to support its role as a thermogenic effector in response to certain pharmacological agents known as sympathomimetics, which include methamphetamine (Meth) and 3,4-methylenedioxymethamphetamine (MDMA) (Sprague, Mallett, et al. 2004). Foremost, the strongest evidence shows that UCP3 knockout mice have severely blunted (80-100%) thermogenic responses to MDMA *in vivo* (Mills et al. 2003).

Despite the mounting evidence implicating UCP3 function in sympathomimetic-induced hyperthermia, the mechanisms that regulate SKM UCP3-dependent thermogenesis in this model remain unclear. SNS activation of BAT UCP1 through fatty acids is the most well characterized mechanism of non-shivering thermogenesis. Given the close association between fatty acids and UCP3 activity it is possible that UCP3 activity in SKM is regulated in a similar fashion through NE stimulation of fatty acids released from white adipose tissue. However, Meth administration can also have complex effects on thermogenesis that are independent of the SNS. Indeed, there is also

a significant amount of evidence to demonstrate that thyroid hormone (TH) also plays a pivotal role in Meth-induced hyperthermia and UCP3 regulation in SKM (Sprague et al. 2007; Sprague, Mallett, et al. 2004; Nicholls & Locke 1984b).

There are several components of sympathomimetic-induced hyperthermia, and in addition to SKM, it has also been proposed that BAT also plays an important role in this response. Although UCP3 protein expression can be found in SKM and BAT, its activity is not well studied. Indeed, UCP1 in BAT is recognized as the primary regulator of non-shivering thermogenesis in this tissue in response to cold (Nedergaard et al. 2000). The original postulation that adult humans did not possess significant amounts of BAT led researchers to believe that BAT did not contribute to adult thermogenic processes, including sympathomimetic-induced hyperthermia. However, advancements in medical imaging technology have revealed that BAT is not only present in adult humans (Nedergaard et al. 2007; Bar-Shalom et al. 2004), but also that certain depots of white adipose tissue can be converted to BAT with the treatment of certain sympathetic mimetics (Townsend & Tseng 2014). Furthermore, recent surgical BAT ablation experiments performed by Sanchez- Alavez et *al.* revealed that BAT contributes to 40% of Meth-induced hyperthermia (Sanchez-Alavez et al. 2013). In light of these new findings, characterizing the contribution of SKM UCP3 and BAT UCP1 in adult thermogenic processes will reveal key information about the interplay between different thermogenic pathways.

Herein, we utilize a transgenic $UCP3^{-/-}$ mouse model that specifically expresses human UCP3 at physiological levels in SKM (TgSKM $UCP3^{-/-}$) to demonstrate that SKM

UCP3 is key in regulating sympathomimetic-induced thermogenesis. We then focused on defining the role of SNS activation on UCP3-dependent thermogenesis in SKM. Lastly, we investigated the relationship of UCP1 and UCP3-dependent thermogenesis in response Meth-induced hyperthermia, and show that the presence of UCP1 and UCP3 are both key components in the development of hyperthermia in response to Meth.

3.2 Results

3.2.1 UCP3 expression in SKM is a key effector in sympathomimetic-induced thermogenesis

Given that SKM is thought to play a significant role in sympathomimetic-induced thermogenesis, we focused on investigating the thermogenic capacity of UCP3 in SKM. Although UCP3 can be found in SKM and BAT, its expression in BAT is relatively small, especially when compared to the concentrations of BAT UCP1, which accounts for 10% of total membrane protein (Brand & Esteves 2005). Therefore, the blunted Meth-induced thermogenic response previously seen in $UCP3^{-/-}$ mice (Sprague, Brutcher, et al. 2004) is likely due to the lack of UCP3 expression in SKM rather than BAT. Therefore, we directed our efforts to characterizing UCP3 activity in SKM by crossing the $UCP3^{-/-}$ line with the TgSKM $UCP3^{-/-}$ mice. The resulting TgSKM $UCP3^{-/-}$ strain was a UCP3 null mouse that overexpressed UCP3 specifically in SKM alone (Figure 3.1 A). Consistent with previous findings, the $UCP3^{-/-}$ mice demonstrated a blunted thermogenic response in response to Meth. Interestingly, the expression of UCP3 in SKM alone was

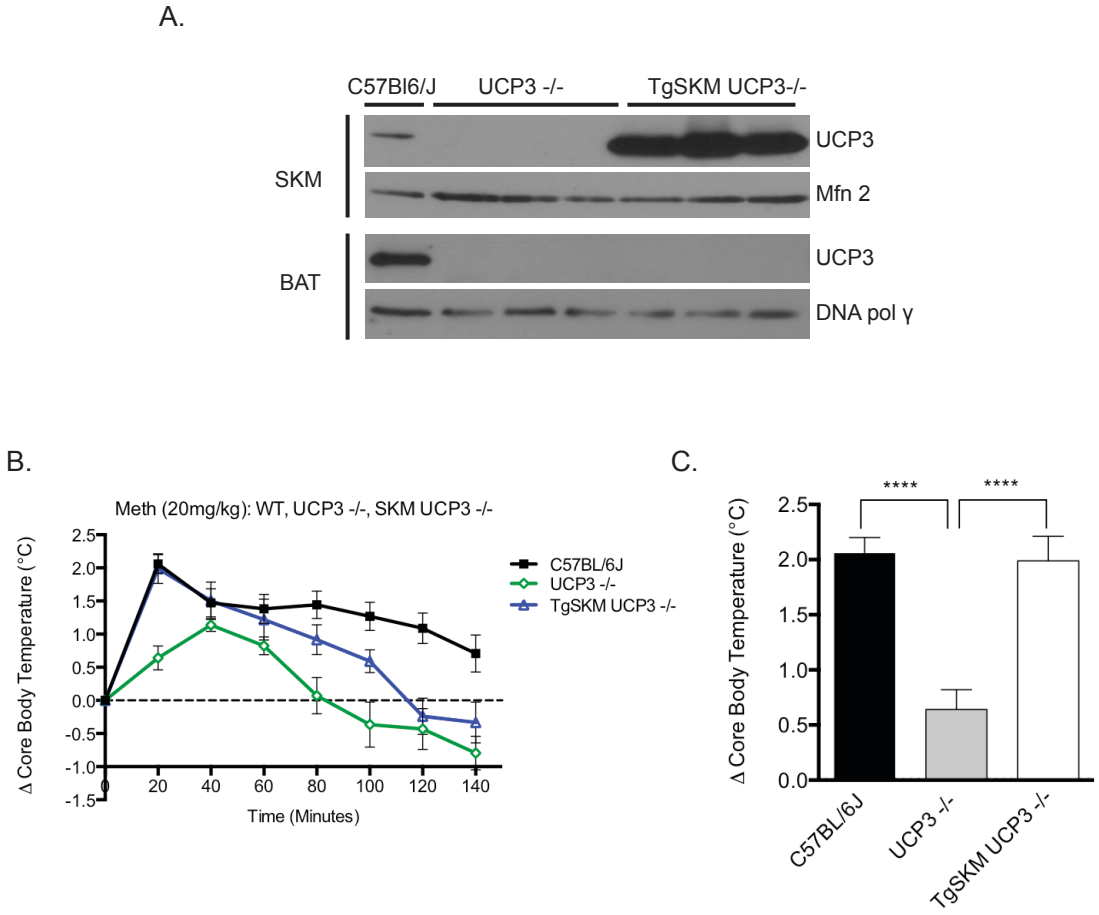

Figure 3.1 UCP3-dependent thermogenesis in Meth-induced hyperthermia

(A) UCP3 expression in mitochondrial lysates isolated from SKM (SKM) and brown adipose tissue (BAT). Mitofusion 2 (Mfn2) and DNA polymerase ϒ (DNA pol ϒ) were used as loading controls. (B) Changes in core body temperature from baseline after subcutaneous injection of Meth (20mg/kg). (C) Peak change in core body temperature from baseline after Meth injection (20 minutes).

Data are expressed as mean +/- SEM. ***p<0.01 (n=7)

able to restore Meth-induced thermogenesis in the TgSKM-UCP3 $^{-/-}$ mice similar to the wild-type group (C57BL/6J) (Figure 3.1 B-C).

Another important issue regarding the mechanisms of sympathomimetic-induced hyperthermia is whether UCP3 activation is directly or indirectly mediated by SNS via NE. Sympathomimetic drugs have the ability to increase thermogenesis through adrenergic stimulation. Data showing that levels of circulating NE spikes (35-fold) in the bloodstream 30 minutes prior to peak MDMA-induced hyperthermia (Sprague et al. 2005) suggests that adrenergic signaling through NE is key in mediating this thermogenic response. Furthermore, it has also been shown that combined antagonism of the α_1- and β_3 adrenergic receptors reverses and inhibits MDMA-induced hyperthermia(Sprague, Brutcher, et al. 2004). However, it is important to note that these drugs can also affect thermogenesis through their indirect actions on the hypothalamic-pituitary-adrenal and hypothalamic-pituitary-thyroid axes (Sprague, Brutcher, et al. 2004; Sprague et al. 2003). Additionally, the generation of ROS has also been implicated as a contributing regulator of Meth-induced hyperthermia, in a pathway independent of SNS activation (Sanchez-Alavez et al. 2013). Given that UCP3 activity has been linked to thyroid hormone (Solanes et al. 2005) and ROS (Echtay et al. 2003), it is possible that UCP3-dependent thermogenesis in response to Meth is not directly mediated through SNS activation. To test this, we administered NE (1mg/kg, s.c.) to UCP3$^{-/-}$ mice and found that even though peak-thermogenesis was slightly depressed in the UCP3$^{-/-}$ mice compared to the wild-type group, the difference was not statistically significant (Figure 3.2 A-B). These results demonstrate that NE is not a direct regulator of UCP3-dependent thermogenesis.

3.2.2 Interplay between UCP1 and UCP3 in sympathomimetic-induced thermogenesis

As previously discussed, BAT and SKM tissues have both been shown to contribute to Meth-induced hyperthermia. In order to characterize the effect of uncoupling-dependent thermogenesis in these distinct tissues we generated a global, double knockout strain lacking UCP3 and UCP1 (UCP1$^{-/-}$ + UCP3 $^{-/-}$). We then focused on further scrutinizing the thermogenic capacity of UCP3 in SKM by generating a novel double UCP1 and UCP3 global knockout mouse line, that specifically overexpressed human UCP3 in SKM (TgSKM UCP1$^{-/-}$ + UCP3$^{-/-}$) (Figure 3.3 A). In characterizing these mice, we found that body weight was significantly reduced in the TgSKM UCP3$^{-/-}$ and TgSKM UCP1$^{-/-}$ + UCP3$^{-/-}$ compared to the wild-type, single UCP-knockout, and double UCP-knockout mice (Figure 3.2 B). This was not too surprising given that it has been previously shown that mice expressing human UCP3 transgene off the α-skeletal actin promoter are leaner, and have a marked reduction in adiposity (Clapham et al. 2000). Furthermore, there were no significant differences in body weight among wild-type, UCP1$^{-/-}$, UCP3$^{-/-}$, and UCP1$^{-/-}$ + UCP3 $^{-/-}$ (Vidal-Puig et al. 2000; Gong et al. 2000).

Although, BAT has been previously shown to play an important role in Meth-induced hyperthermia, the direct contribution of UCP1 has not been defined. In order to investigate the significance of UCP1 in this thermogenic response we administered Meth

A.

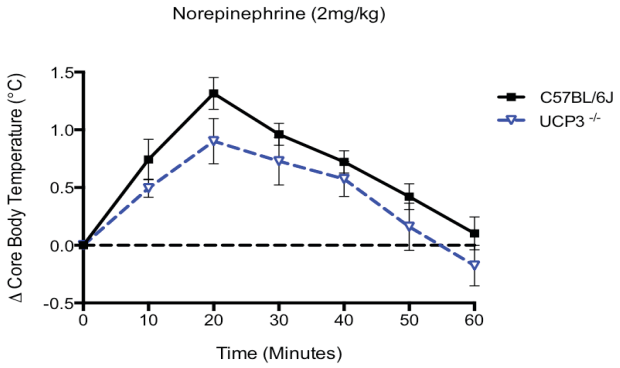

B.

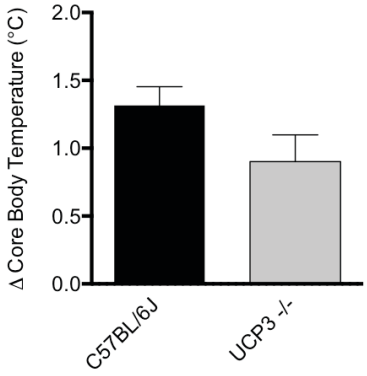

Figure 3.2 The sympathetic nervous system is not a direct regulator of UCP3-dependent thermogenesis

(A) Changes in core body temperature from baseline after subcutaneous injection of norepinephrine (NE, 2mg/kg). (D) Peak change in core body temperature from baseline after norepinephrine (20 minutes).

Data are expressed as mean +/- SEM. No significant difference between genotypes was detected (n=7).

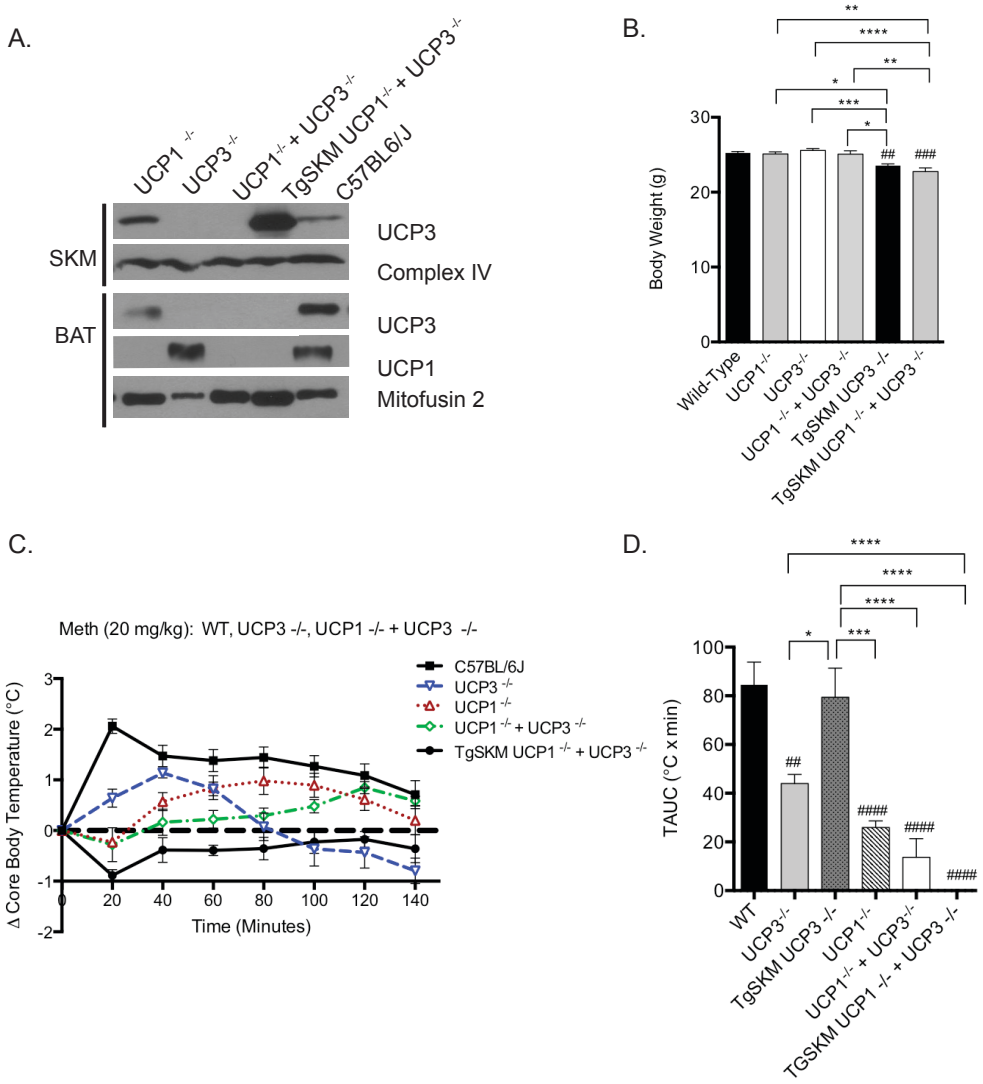

Figure 3.3 SKM UCP1 and UCP3 both contribute to Meth-induced thermogenesis

(A) UCP1 and UCP3 expression in mitochondrial lysates isolated from BAT and SKM tissues. (B) Body weights of mice between 7-8 weeks of age fed normal chow diet (n=9-42). (C) Changes in core body temperature from baseline after subcutaneous injection of Meth (20mg/kg). (D) The area under the curve (TAUC) for 60 minutes post injection (n=5-7).

Data are expressed as mean +/- SEM. ##p<0.01, ###p<0.001, differences compared to WT group. *p<0.05, **p<0.01, ***p<0.001, ****p<0.0001 differences between groups.

to UCP1$^{-/-}$ mice and found that they exhibited a delayed and blunted thermogenic response similar to the UCP3$^{-/-}$ (Figure 3.3 C). Indeed, 20 minutes post injection, the core body temperature of the UCP1$^{-/-}$ mice dropped below baseline. This data, taken with our previous findings that UCP3 in SKM is important in Meth-induced thermogenesis, argues that SKM UCP3 and BAT UCP1 both contribute to the hyperthermic response seen with Meth administration. We then focused on answering the question of whether regulation of UCP-dependent thermogenesis in these two distinct tissues was interrelated in response to Meth using our single, double UCP knockout, and transgenic SKM UCP3 mouse lines. As expected, the UCP1$^{-/-}$ + UCP3$^{-/-}$ double knockout mice displayed an even more exaggerated thermogenic phenotype post Meth injection than the single knockout strain. Interestingly, the TgSKM UCP1$^{-/-}$ + UCP3$^{-/-}$ mice also did not exhibit a hyperthermic response, despite the presence of UCP3 in SKM. Taken together, these results suggest that UCP1-dependent BAT thermogenesis plays a key role in regulating the contribution of UCP3-dependent thermogenesis in SKM.

Analysis of the area under the curve (AUC, Figure 3.3 D) of core body temperature in in the first 60 minutes post Meth injection was used to quantify the initial changes caused by Meth and the influence of BAT UCP1 and SKM UCP3. The AUC data revealed that UCP3 in SKM contributes to ~50% of METH-induced thermogenesis within the first 60 minutes, whereas UCP1 accounts for ~75% of the initial response.

3.3 Discussion

As discussed earlier, there are several lines of evidence to suggest that UCP3 regulates SKM thermogenesis in Meth-induced hyperthermia. Our observations strongly support the thermogenic capabilities of UCP3 in SKM by using a mouse model that specifically expresses human SKM UCP3 in a global UCP3 knockout background. In contrast, to the well-described pathways of SNS regulation of BAT UCP1-dependent thermogenesis in response to cold temperatures, the mechanisms that regulate UCP3-dependent thermogenesis in SKM are less characterized. Here we show that unlike BAT UCP1, NE is not a direct regulator of UCP3-dependent thermogenesis in sympathomimetic-induced hyperthermia. Therefore, it is likely that there are pathways independent of SNS activation that could be contributing to UCP3-dependent thermogenesis in SKM. These indirect pathways of Meth-induced hyperthermia could possibly be mediated through thyroid hormone or ROS generation, which are both physiological mediators that are also associated with UCP3 activation. Our data imply that strategies that target UCP3 function independent of SNS activation may be an effective therapeutic approach to treating toxicities seen with sympathomimetics.

We also demonstrate that UCP-dependent thermogenesis in BAT and SKM both contribute to Meth-induced hyperthermia. Furthermore, our findings imply that Meth-induced hyperthermia may be a result of an integrated response between uncoupling in BAT and SKM, where BAT UCP1 part of the initial response to Meth and also mediates UCP3 activation in SKM. These findings are consistent with additional studies that suggest crosstalk between SKM and BAT exists and is important in regulating whole

body thermogenesis (Lee et al. 2014). Taken together, the data suggests that UCP1-mediated crosstalk between SKM and BAT may represent a novel thermogenic axis that can be targeted in treating sympathomimetic-induced hyperthermia (Illustration 3.1).

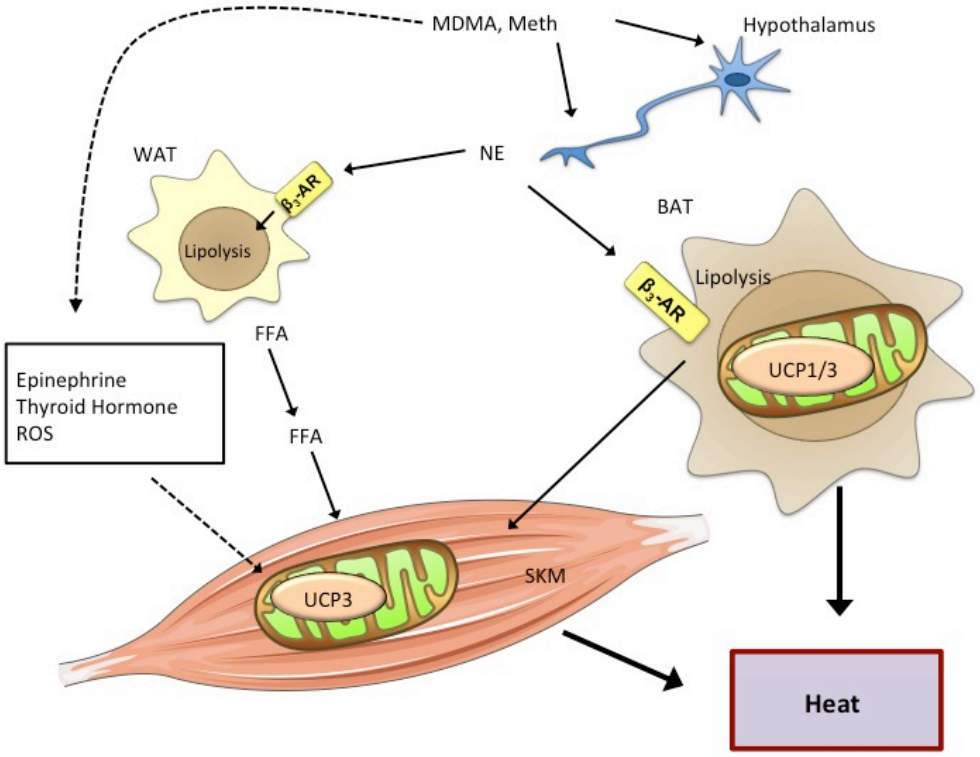

Illustration 3.1 Proposed model of UCP-dependent thermogenesis in response to amphetamines

There are several mechanisms that contribute to amphetamine-induced thermogenesis. In response to amphetamine-like agents (MDMA and Meth), hypothalamic neurons activate the sympathetic nervous system and leads to peripheral release of norepinephrine (NE). NE binds to the β_3- adrenergic receptors on target tissues including, white adipose tissue (WAT) and brown adipose tissue (BAT), to initiate a signaling cascade that leads to lipolysis of triglyceride stores and subsequent release of free fatty acids (FFA). The FFAs serve as substrates for mitochondrial β-oxidation and directly activate uncoupling in BAT and SKM tissues. In this model, UCP3 in SKM is part of an integrated response with UCP1 in BAT that contributes to hyperthermia. It is also possible that these amphetamine-like agents can have indirect thermoregulatory effects through UCP3 activity (via epinephrine, thyroid hormone, and ROS production).

Chapter 4: Identification of UCP3-protein interaction networks

4.1 Introduction

The ability of mitochondria to appropriately switch freely between different energetic substrates (lipids, glucose, amino acids) in various nutritional and physiological circumstances is thought to be a key factor in maintaining energy homeostasis and protecting against obesity-induced metabolic dysregulation. Thus, understanding the mechanisms that guide nutrient partitioning and metabolic flexibility in mitochondria is an attractive approach to treat obesity and its late stage complications.

There are numerous studies to support the importance of UCP3 in maintaining energy balance in various physiological contexts. Studies have shown that overexpression of UCP3 in SKM not only increases fatty acid metabolism and protects against oxidative stress (MacLellan, Gerrits, Gowing, P. J. S. Smith, Wheeler & Harper 2005b) but also improves glucose homeostasis (Choi et al. 2007; Huppertz et al. 2001). Indeed, there are numerous clinical studies that associate altered UCP3 expression and function to the pathophysiology of obesity, insulin resistance, and the development of type II diabetes (Schrauwen et al. 1999; Schrauwen et al. 2001; Y. J. Liu et al. 2005; Musa et al. 2011). However, little is known about the mechanisms by which UCP3 influences mitochondrial metabolism and contributes to energy homeostasis. To better understand the physiological regulation of UCP3 function in mitochondrial metabolism we coupled immunoprecipitation methods with mass spectrometry to identify interacting

partners of UCP3. The results showed that UCP3 associated with key mitochondrial metabolic enzymes involved in regulating fatty acid, glucose, and amino acid metabolism. These diverse interactions suggest that UCP3 may play a key role in coordinating the different pathways of substrate metabolism to maintain energy homeostasis.

4.2 Results

Information about candidate interacting partners of a protein can help characterize functional protein relationships and reveal details about new biological networks. Our lab has previously employed a yeast 2-hybrid assay to identify UCP3-interacting partners, however this type of screening inherently results in numerous false positives (Brückner et al. 2009). To circumvent this issue we employed a high-throughput immunoprecipitation-mass spectrometry approach and identified ~82 target proteins that either indirectly or directly interact with UCP3 (Table 4.1). Using the Scaffold Proteome Software, all targets were aligned to protein sequences in the NCBI database with protein and peptide probability thresholds set to 99% and 95%, respectively. The results were filtered for a minimum of 2 peptides with peak numbers representing how many unique peptides of a protein were identified within the sample. We then eliminated protein targets that were likely non-specific interacting partners based on the criteria that peak numbers in the wild-type samples were less than or equal to peak numbers in the $UCP3^{-/-}$ samples. In terms of the specificity of the immunoprecipitation pull down, a total of 42 peptides

unique to UCP3 were detected in our WT sample. In contrast, there were no detectable peaks identified in our UCP3$^{-/-}$ group, thus suggesting that we were able to successfully purify UCP3 in our immunoprecipitation.

Consistent with the well-established association between UCP3 function and fatty acid metabolism, we show that UCP3 interacts with numerous enzymes that regulate mitochondrial fatty acid transport and oxidation. Interestingly, the data also show that UCP3 interacts with key regulators of glucose and amino acid metabolism in the mitochondria. Taken together, the data suggests that UCP3 could play a key role in coordinating glucose, amino acid, and lipid metabolism through its association with key metabolic enzymes.

4.3 Discussion

Although there is no consensus regarding the thermogenic capabilities of UCP3, it has been proposed that UCP3 may have an alternative function by which its activity contributes to whole-body energy metabolism. The literature has shown that the beneficial metabolic effects of UCP3 overexpression in SKM are not limited to this particular tissue, and also protects against high fat diet-induced resistance in the liver (Choi et al. 2007). Given the strong association between mitochondrial dysfunction and insulin resistance in SKM, this effect can likely be attributed to the influence that UCP3 has on mitochondrial metabolism.

Herein, we are the first to demonstrate that UCP3 interacts with key enzymes that regulate glucose and fatty acid metabolism. Prevailing evidence indicates that efficient

fuel switching between fatty acid and glucose metabolism in response to the proper physiological and nutritional cues (i.e. transition from fasted to fed state) is crucial in maintaining energy homeostasis. Indeed, the importance of appropriate mitochondrial fuel selection is highlighted by studies showing that obese and diabetic patients fail to switch from fatty acid to glucose metabolism during the transition from a fasted to fed state (Kelley et al. 1999; Petersen et al. 2003; Befroy et al. 2007). According to Randle's proposed glucose-fatty acid cycle, in a fasted state fatty acid metabolism in SKM is dominant and suppresses glucose uptake as a survival mechanism to prevent hypoglycemia(Randle et al. 1963). In this model, by-products of fatty acid β-oxidation, such as acetyl-CoA, act as an allosteric inhibitor of PDH. Because pyruvate dehydrogenase is a key enzyme in regulating glycolytic flux, its inhibition results in a negative feedback of glucose uptake, which is especially critical during fasting when glucose should be spared for tissues that rely predominantly on this substrate, such as brain. In contrast, this cycle can also be counter-regulated in a fed state where insulin-stimulated glucose uptake increases flux through the TCA cycle and causes a surge in the mitochondrial efflux of citrate. In the cytoplasm the citrate is converted to acetyl-CoA and then to the CPT1 inhibitor malonyl-CoA(Muoio 2014). In this model, efficient fuel switching from glucose to fatty acid metabolism and vice versa relies heavily on the gatekeeping function of PDH and CPT1. Given that our mass spectrometry data shows that UCP3 interacts with PDH and CPT1, it is possible that UCP3 plays an important role in coordinating the fuel switch from glucose and fatty acid metabolism in the transition from a fasted and fed state. Based on these findings, it is likely that UCP3 could play a

role in coordinating fatty acid and glucose metabolism through its interactions with key gatekeeping enzymes. This idea is consistent with previous work showing that UCP3 overexpression in SKM can influence fatty acid metabolism and improve glucose homeostasis (Choi et al. 2007).

Our data also demonstrates that UCP3 interacts with numerous fatty acid metabolizing enzymes including acetyl-CoA acetyltransferase (Acat 1), medium chain specific acyl-CoA dehydrogenase (Acadm), subunits of trifunctional enzyme (Hadhb), short enoyl-CoA hydratase 1 (ECHs1), and enoyl-CoA delta isomerase 1 (ECI). Interestingly, ECI is a key enzyme involved in the complete degradation of unsaturated fatty acids, which have also been shown to be potent activators of UCP3 expression (Zackova et al. 2003; Thompson & D. Kim 2004). If UCP3 activity is important in unsaturated fatty acid metabolism, it likely that UCP3 interacts with other enzymes involved in the degradation of these particular fatty acid species. Indeed, our mass spectrometry data is consistent with our lab's previous work showing that UCP3 interacts with the auxiliary unsaturated fatty acid metabolizing enzyme enoyl-CoA hydratase 1 (ECH1), utilizing a yeast two-hybrid screen. The reason as to why our mass spectrometry data did not detect ECH1 as an interacting partner could be due to optimization of our affinity purification using our lab's custom-made UCP3 antibody. Regardless, our mass spectrometry data with our lab's detailed characterization of the ECH1:UCP3 complex (next chapter), further supports the link between UCP3 activity and unsaturated fatty acid metabolism.

In addition to fatty acids, mitochondrial degradation of amino acids also serves as an important alternative fuel source to glucose during prolonged fasting. Proteolysis and amino acid catabolism is regulated in part through mitochondrial branched-chain ketoacid dehydrogenase complex (BKCD). The first step in the degradation of branched chain amino acids is transanimation with α-ketoglutarate to form branched α-keto acids. These products are then irreversibly metabolized by BCKD and fed in to the TCA cycle for complete degradation. Interestingly, our mass spectrometry data shows that UCP3 also interacts with BCKD. Although there is little information regarding UCP3 function and amino acid metabolism, clinical studies in a African American population carrying a missense allele mutation that leads to a truncated form of UCP3 showed that these patients reduced plasma concentrations of α-ketoglutarate in SKM of subjects fasted overnight (Fiehn et al. 2010). Previous studies with this distinct population also showed a susceptibility in the development of severe obesity with whole-body lipid oxidation being significantly reduced (Argyropoulos et al. 1998).

Our findings, which demonstrate that UCP3 interacts with key enzymes involved in efficient mitochondrial substrate metabolism corresponds with the extensive literature regarding UCP3 in the protection against obesity-related diseases through mediation of whole-body energy balance. Future work is needed to characterize these interactions, as well as the complex mechanisms linking mitochondrial function and efficient fuel selection with the pathophysiology of obesity-related diseases.

Table 4.1 Interacting partners of UCP3 identified by mass spectrometry

Identified Proteins	Accession Number	WT	UCP3 $^{-/-}$
Mitochondrial uncoupling protein 3 OS=Mus musculus GN=Ucp3 PE=2 SV=1	sp|P56501|UCP3_MOUSE	42	0
Isoform 2 of 2-oxoglutarate dehydrogenase, mitochondrial OS=Mus musculus GN=Ogdh	sp|Q60597-2|ODO1_MOUSE (+3)	9	0
ATP synthase subunit O, mitochondrial OS=Mus musculus GN=Atp5o PE=1 SV=1	sp|Q9DB20|ATPO_MOUSE	15	0
Trifunctional enzyme subunit beta, mitochondrial OS=Mus musculus GN=Hadhb PE=1 SV=1	sp|Q99JY0|ECHB_MOUSE	12	0
Carnitine O-palmitoyltransferase 1, muscle isoform OS=Mus musculus GN=Cpt1b PE=2 SV=1	sp|Q924X2|CPT1B_MOUSE	11	0
Acetyl-CoA acetyltransferase, mitochondrial OS=Mus musculus GN=Acat1 PE=1 SV=1	sp|Q8QZT1|THIL_MOUSE	8	0
60 kDa heat shock protein, mitochondrial OS=Mus musculus GN=Hspd1 PE=1 SV=1	sp|P63038|CH60_MOUSE	5	0
Dihydrolipoyl dehydrogenase, mitochondrial OS=Mus musculus GN=Dld PE=1 SV=2	sp|O08749|DLDH_MOUSE	9	0
Myosin light chain 1/3, skeletal muscle isoform OS=Mus musculus GN=Myl1 PE=1 SV=2	sp|P05977|MYL1_MOUSE (+1)	6	0
ATP synthase gamma chain OS=Mus musculus GN=Atp5c1 PE=3 SV=1	tr|A2AKU9|A2AKU9_MOUSE	7	0
Histone H1.4 OS=Mus musculus GN=Hist1h1e PE=1 SV=2	sp|P43274|H14_MOUSE	2	0
Electron transfer flavoprotein subunit beta OS=Mus musculus GN=Etfb PE=1 SV=3	sp|Q9DCW4|ETFB_MOUSE	4	0
Beta-globin OS=Mus musculus GN=Hbb-b1 PE=3 SV=1	tr|A8DUK4|A8DUK4_MOUSE (+1)	7	0
Isoform 2 of Sacsin OS=Mus musculus GN=Sacs	sp|Q9JLC8-2|SACS_MOUSE-R (+3)	3	0
Malate dehydrogenase, mitochondrial OS=Mus musculus GN=Mdh2 PE=1 SV=3	sp|P08249|MDHM_MOUSE	4	0
AMP deaminase 1 OS=Mus musculus GN=Ampd1 PE=2 SV=1	sp|Q3V1D3|AMPD1_MOUSE (+2)	4	0
Histone H2B type 1-F/J/L OS=Mus musculus GN=Hist1h2bf PE=1 SV=2	sp|P10853|H2B1F_MOUSE (+12)	4	0
Thioredoxin-dependent peroxide reductase, mitochondrial OS=Mus musculus GN=Prdx3 PE=1 SV=1	sp|P20108|PRDX3_MOUSE	4	0
Lipoamide acyltransferase component of branched-chain alpha-keto acid dehydrogenase complex, mitochondrial OS=Mus musculus GN=Dbt PE=2 SV=2	sp|P53395|ODB2_MOUSE	5	0
Glycogen [starch] synthase, muscle OS=Mus musculus GN=Gys1 PE=1 SV=2	sp|Q9Z1E4|GYS1_MOUSE (+1)	5	0
Isocitrate dehydrogenase [NADP], mitochondrial OS=Mus musculus GN=Idh2 PE=1 SV=3	sp|P54071|IDHP_MOUSE	5	0
Ig gamma-2A chain C region secreted form OS=Mus musculus PE=1 SV=1	sp|P01864|GCAB_MOUSE (+1)	3	0
GrpE protein homolog 1, mitochondrial OS=Mus musculus GN=Grpel1 PE=1 SV=1	sp|Q99LP6|GRPE1_MOUSE	3	0
NADH dehydrogenase [ubiquinone] iron-sulfur protein 3, mitochondrial OS=Mus musculus GN=Ndufs3 PE=1 SV=2	sp|Q9DCT2|NDUS3_MOUSE	3	0
Aldehyde dehydrogenase, mitochondrial OS=Mus musculus GN=Aldh2 PE=1 SV=1	sp|P47738|ALDH2_MOUSE	4	0
Chaperone activity of bc1 complex-like, mitochondrial OS=Mus musculus GN=Adck3 PE=2 SV=2	sp|Q60936|ADCK3_MOUSE (+1)	5	0

Table 4.1 (continued)

MCG140437, isoform CRA_d OS=Mus musculus GN=Myh2 PE=4 SV=1	tr|G3UW82|G3UW82_MOUSE	4	0
ATP synthase subunit d, mitochondrial OS=Mus musculus GN=Atp5h PE=1 SV=3	sp|Q9DCX2|ATP5H_MOUSE (+1)	5	0
Ubiquitin-protein ligase E3A OS=Mus musculus GN=Ube3a PE=2 SV=1	sp|O08759|UBE3A_MOUSE (+1)	0	0
Isoform 2 of DnaJ homolog subfamily A member 3, mitochondrial OS=Mus musculus GN=Dnaja3	sp|Q99M87-2|DNJA3_MOUSE (+2)	2	0
Isoform Cytoplasmic of Fumarate hydratase, mitochondrial OS=Mus musculus GN=Fh	sp|P97807-2|FUMH_MOUSE (+1)	3	0
Glycogen phosphorylase, muscle form OS=Mus musculus GN=Pygm PE=1 SV=3	sp|Q9WUB3|PYGM_MOUSE (+1)	3	0
Medium-chain specific acyl-CoA dehydrogenase, mitochondrial OS=Mus musculus GN=Acadm PE=1 SV=1	sp|P45952|ACADM_MOUSE	3	0
Aspartate-beta-hydroxylase OS=Mus musculus GN=Asph PE=4 SV=1	tr|A2AL78|A2AL78_MOUSE	4	0
Enoyl-CoA hydratase, mitochondrial OS=Mus musculus GN=Echs1 PE=1 SV=1	sp|Q8BH95|ECHM_MOUSE	3	0
60S acidic ribosomal protein P0 OS=Mus musculus GN=Rplp0 PE=1 SV=3	sp|P14869|RLA0_MOUSE (+1)	3	0
Triosephosphate isomerase OS=Mus musculus GN=Tpi1 PE=3 SV=1	tr|H7BXC3|H7BXC3_MOUSE (+1)	4	0
Alpha globin 1 OS=Mus musculus GN=Hba-a1 PE=2 SV=1	tr|Q91VB8|Q91VB8_MOUSE	4	0
Tubulin alpha-1B chain OS=Mus musculus GN=Tuba1b PE=1 SV=2	sp|P05213|TBA1B_MOUSE (+1)	2	0
[Pyruvate dehydrogenase [lipoamide]] kinase isozyme 4, mitochondrial OS=Mus musculus GN=Pdk4 PE=2 SV=1	sp|O70571|PDK4_MOUSE	3	0
Tropomyosin beta chain OS=Mus musculus GN=Tpm2 PE=1 SV=1	sp|P58774|TPM2_MOUSE (+1)	3	0
Tubulin beta-4B chain OS=Mus musculus GN=Tubb4b PE=1 SV=1	sp|P68372|TBB4B_MOUSE (+1)	3	0
Nuclear pore membrane glycoprotein 210 OS=Mus musculus GN=Nup210 PE=1 SV=2	sp|Q9QY81|PO210_MOUSE-R	2	0
Fumarylacetoacetate hydrolase domain-containing protein 2A OS=Mus musculus GN=Fahd2 PE=1 SV=1	sp|Q3TC72|FAHD2_MOUSE	2	0
Isoform 2 of Neuralized-like protein 4 OS=Mus musculus GN=Neurl4	sp|Q5NCX5-2|NEUL4_MOUSE (+3)	2	0
Hexaprenyldihydroxybenzoate methyltransferase, mitochondrial OS=Mus musculus GN=Coq3 PE=2 SV=1	sp|Q8BMS4|COQ3_MOUSE	2	0
Mitochondrial 2-oxoglutarate/malate carrier protein OS=Mus musculus GN=Slc25a11 PE=1 SV=3	sp|Q9CR62|M2OM_MOUSE (+1)	2	0
Protein Pcdhb12 OS=Mus musculus GN=Pcdhb12 PE=3 SV=1	tr|F6V243|F6V243_MOUSE	2	0
Myosin-4 OS=Mus musculus GN=Myh4 PE=1 SV=1	sp|Q5SX39|MYH4_MOUSE	30	2
Isoform 2 of Ig gamma-2B chain C region OS=Mus musculus GN=Igh-3	sp|P01867-2|IGG2B_MOUSE (+1)	4	3
Tripartite motif-containing protein 72 OS=Mus musculus GN=Trim72 PE=1 SV=1	sp|Q1XH17|TRI72_MOUSE	13	3
Creatine kinase S-type, mitochondrial OS=Mus musculus GN=Ckmt2 PE=1 SV=1	sp|Q6P8J7|KCRS_MOUSE	10	3
Isocitrate dehydrogenase [NAD] subunit gamma 1, mitochondrial OS=Mus musculus GN=Idh3g PE=1 SV=1	sp|P70404|IDHG1_MOUSE	9	3
Desmoplakin OS=Mus musculus GN=Dsp PE=3 SV=1	sp|E9Q557|DESP_MOUSE	5	3

Table 4.1 (continued)

Succinyl-CoA ligase [ADP-forming] subunit beta, mitochondrial OS=Mus musculus GN=Sucla2 PE=1 SV=2	sp|Q9Z2I9|SUCB1_MOUSE	27	4
Trifunctional enzyme subunit alpha, mitochondrial OS=Mus musculus GN=Hadha PE=1 SV=1	sp|Q8BMS1|ECHA_MOUSE	21	4
Calcium-binding mitochondrial carrier protein Aralar1 OS=Mus musculus GN=Slc25a12 PE=1 SV=1	sp|Q8BH59|CMC1_MOUSE	14	4
Elongation factor Tu, mitochondrial OS=Mus musculus GN=Tufm PE=1 SV=1	sp|Q8BFR5|EFTU_MOUSE (+1)	20	5
Ryanodine receptor 1 OS=Mus musculus GN=Ryr1 PE=1 SV=1	sp|E9PZQ0|RYR1_MOUSE (+1)	16	5
Glycerol-3-phosphate dehydrogenase, mitochondrial OS=Mus musculus GN=Gpd2 PE=1 SV=2	sp|Q64521|GPDM_MOUSE (+1)	13	5
Enoyl-CoA delta isomerase 1, mitochondrial OS=Mus musculus GN=Eci1 PE=2 SV=2	sp|P42125|ECI1_MOUSE	10	5
NADH dehydrogenase [ubiquinone] 1 alpha subcomplex subunit 4 OS=Mus musculus GN=Ndufa4 PE=1 SV=2	sp|Q62425|NDUA4_MOUSE	10	6
Glyceraldehyde-3-phosphate dehydrogenase OS=Mus musculus GN=Gapdh PE=1 SV=2	sp|P16858|G3P_MOUSE	15	7
Very long-chain specific acyl-CoA dehydrogenase, mitochondrial OS=Mus musculus GN=Acadvl PE=1 SV=3	sp|P50544|ACADV_MOUSE	45	8
Succinyl-CoA ligase [ADP/GDP-forming] subunit alpha, mitochondrial OS=Mus musculus GN=Suclg1 PE=1 SV=4	sp|Q9WUM5|SUCA_MOUSE	16	8
Complement C1q subcomponent subunit C OS=Mus musculus GN=C1qc PE=2 SV=2	sp|Q02105|C1QC_MOUSE	11	8
Actin, alpha skeletal muscle OS=Mus musculus GN=Acta1 PE=1 SV=1	sp|P68134|ACTS_MOUSE	18	9
Isoform 2 of Sarcalumenin OS=Mus musculus GN=Srl	sp|Q7TQ48-2|SRCA_MOUSE (+1)	15	10
Electron transfer flavoprotein subunit alpha, mitochondrial OS=Mus musculus GN=Etfa PE=1 SV=2	sp|Q99LC5|ETFA_MOUSE	18	11
Succinate dehydrogenase [ubiquinone] flavoprotein subunit, mitochondrial OS=Mus musculus GN=Sdha PE=1 SV=1	sp|Q8K2B3|DHSA_MOUSE	28	12
Complement C1q subcomponent subunit A OS=Mus musculus GN=C1qa PE=1 SV=2	sp|P98086|C1QA_MOUSE	18	12
Pyruvate dehydrogenase E1 component subunit beta, mitochondrial OS=Mus musculus GN=Pdhb PE=1 SV=1	sp|Q9D051|ODPB_MOUSE	22	13
3-ketoacyl-CoA thiolase, mitochondrial OS=Mus musculus GN=Acaa2 PE=1 SV=3	sp|Q8BWT1|THIM_MOUSE	22	13
Calsequestrin-1 OS=Mus musculus GN=Casq1 PE=2 SV=3	sp|O09165|CASQ1_MOUSE	20	16
Isocitrate dehydrogenase [NAD] subunit alpha, mitochondrial OS=Mus musculus GN=Idh3a PE=1 SV=1	sp|Q9D6R2|IDH3A_MOUSE	22	17
Isocitrate dehydrogenase 3 (NAD+) beta OS=Mus musculus GN=Idh3b PE=2 SV=1	tr|Q91VA7|Q91VA7_MOUSE	38	20
Aconitate hydratase, mitochondrial OS=Mus musculus GN=Aco2 PE=1 SV=1	sp|Q99KI0|ACON_MOUSE	80	22
Dihydrolipoyllysine-residue acetyltransferase component of pyruvate dehydrogenase complex, mitochondrial OS=Mus musculus GN=Dlat PE=1 SV=2	sp|Q8BMF4|ODP2_MOUSE	27	23
ADP/ATP translocase 1 OS=Mus musculus GN=Slc25a4 PE=1 SV=4	sp|P48962|ADT1_MOUSE	49	29
Sarcoplasmic/endoplasmic reticulum calcium ATPase 1 OS=Mus musculus GN=Atp2a1 PE=2 SV=1	sp|Q8R429|AT2A1_MOUSE	134	69
ATP synthase subunit alpha, mitochondrial OS=Mus musculus GN=Atp5a1 PE=1 SV=1	sp|Q03265|ATPA_MOUSE	146	73
ATP synthase subunit beta, mitochondrial OS=Mus musculus GN=Atp5b PE=1 SV=2	sp|P56480|ATPB_MOUSE	112	106

Chapter 5: The novel interaction between UCP3 and ECH1

5.1 Introduction

The interplay between mitochondrial bioenergetics and fatty acid metabolism has been intricately linked to the pathophysiology of obesity and –related metabolic complications. The observation that the accumulation of toxic intramuscular lipid intermediates including diacylglycerol and ceramide negatively correlates with insulin sensitivity, led researchers to believe that diminished mitochondrial fatty acid oxidation is the underlying mechanism of obesity-related complications (Krssak et al. 1998; Pan et al. 1997; Roden et al. 1996; Boden 2011). However, therapeutic approaches that focus on increasing fatty acid metabolism alone as a means to relieve mitochondrial congestion and counteract the effects of lipotoxicity have been met with conflicting results. A new theory that has emerged in recent years is centered on the premise of relieving nutrient overload and restoring energy dysregulation through targeting mitochondrial bioenergetics. In this model, nutrient overload induces an energetic imbalance where the rate of fatty acid catabolism exceeds the capacity of the ETC. Therefore, adjusting the flux rate through β-oxidation in the absence of a corresponding change in energy utilization will just impinge additional pressure on mitochondrial respiration (Muoio & Neufer 2012). Thus, strategies that coordinate an increase in the rates of fatty acid

oxidation with energy demand as a means to relieve mitochondrial overload are promising therapeutic strategies for combating metabolic disease.

There are several studies to support that UCP3 functions to regulate lipid metabolism and lower metabolic efficiency. First, being the induction of UCP3 expression in physiological states where fatty acid levels are high, such as high fat feeding and fasting, which suggests that UCP3 is important in mediating lipid handling and preventing mitochondrial overload (Bézaire et al. 2001) (Felipe et al. 2003; Chou et al. 2001) and fasting (Samec et al. 1999). Additionally, transgenic mice that overexpress UCP3 in SKM at physiological levels were found to be lean despite being hyperphagic (Clapham et al. 2000), and showed lower levels of intramuscular triacylglycerol stores (Bézaire et al. 2005). From these findings, it has been suggested that in conditions where fatty acid supply exceeds the oxidation capacity of SKM, up-regulation of UCP3 expression facilitates an overflow pathway to increase the fatty acid oxidation capacity of SKM. Although, there are several studies to implicate UCP3 involvement in regulating mitochondrial fatty acid transport and metabolism in certain physiological contexts the regulatory mechanisms are unclear.

This study sheds light on the link between UCP3 function and mitochondrial fatty acid metabolism in SKM mitochondria. As discussed earlier, our lab has previously shown that UCP3 directly interacts with the auxiliary, unsaturated fatty acid metabolizing enzyme enoyl CoA hydratase 1 (ECH1). Unsaturated fatty acids with double bonds in the odd position must have these double bonds isomerized to even positions to allow their complete oxidation. This is accomplished through either the isomerase dependent

pathway or the reductase dependent pathway. In the reductase-pathway, ECH1 catalyzes the isomerization of the 3-trans, 5–cis dienoyl-CoA substrate to the 2-trans, 4-trans dienoyl-CoA substrate (Filppula 1998; Luthria et al. 1995). Although little is known about the physiological relevance of ECH1, it has been proposed that flux through the reductase-dependent pathway is important in preventing the depletion of free coenzyme A, thus protecting mitochondrial oxidative function and maintaining energy balance (Shoukry & Schulz 1998). It has been shown that bacteria that do not express ECH1 rely upon fatty acid export to defend against the accumulation of unmetabolizeable enoyl-CoA derivatives which could stall β-oxidation (Ren et al. 2004). Additionally, fatty acid levels are significantly increased after ECH1-knockdown in C. elegans roundworms compared to wild-type. Furthermore, studies in mice lacking 2,4-dienoyl-CoA reductase (DECR), another auxiliary enzyme involved in unsaturated fatty acid oxidation, showed a compromised thermoregulatory response when challenged by fasting and cold exposure (Miinalainen et al. 2009). Together, these studies indicate that the auxiliary enzymes involved in the complete breakdown of unsaturated fatty acids are critical in that adaptation to metabolic stress (e.g. fasting) by maintaining balanced fatty acid and energy metabolism.

Herein, we demonstrate a mechanism by which UCP3 mediates fatty acid oxidation and mitochondrial metabolism via its interaction with the auxiliary unsaturated fatty acid metabolizing enzyme ECH1. The physiological relevance of this work is supported by observations that UCP3 and ECH1 directly interact at endogenous concentrations in SKM to enhance uncoupled respiration and unsaturated fatty acid

oxidation. With the use of UCP3 and ECH1-knockout mouse models, our work demonstrates that both proteins are important regulators of cold-induced thermogenesis during periods of metabolic stress.

5.2 Results

5.2.1 Identifying the interaction between UCP3 and ECH1

The endogenous function(s) of ECH1 in a physiological context are unclear. Interestingly, ECH1 exhibited an overlapping protein expression profile with UCP3 in highly metabolic tissues including BAT, SKM, and heart (HRT) (Figure 5.1 A). Previous work in our lab has shown that ECH1 and UCP3 interact when overexpressed, and also form a direct complex with each other *in vitro*. Considering the substantial role of SKM in whole body energy metabolism, we then tested whether the ECH1:UCP3 complex could be detected in differentiated C2C12 myotubes. C2C12s mouse myoblasts were subjected to low serum-induced differentiation (2% equine serum) to induce UCP3 mRNA and protein expression (Figure 5.1 C, upper blot, days 2-6) as previously shown (Nagase et al. 2001; Solanes et al. 2000; Son et al. 2001). Interestingly, that data showed that endogenous ECH1 mRNA and protein levels did not change upon differentiation (Figure 5.1 B). Using lysates from differentiated myotubes, we found that endogenous ECH1 could be detected when immunoprecipitated with anti-UCP3, but not with rabbit anti-IgG in C2C12 myotubes (Figure 5.1D).

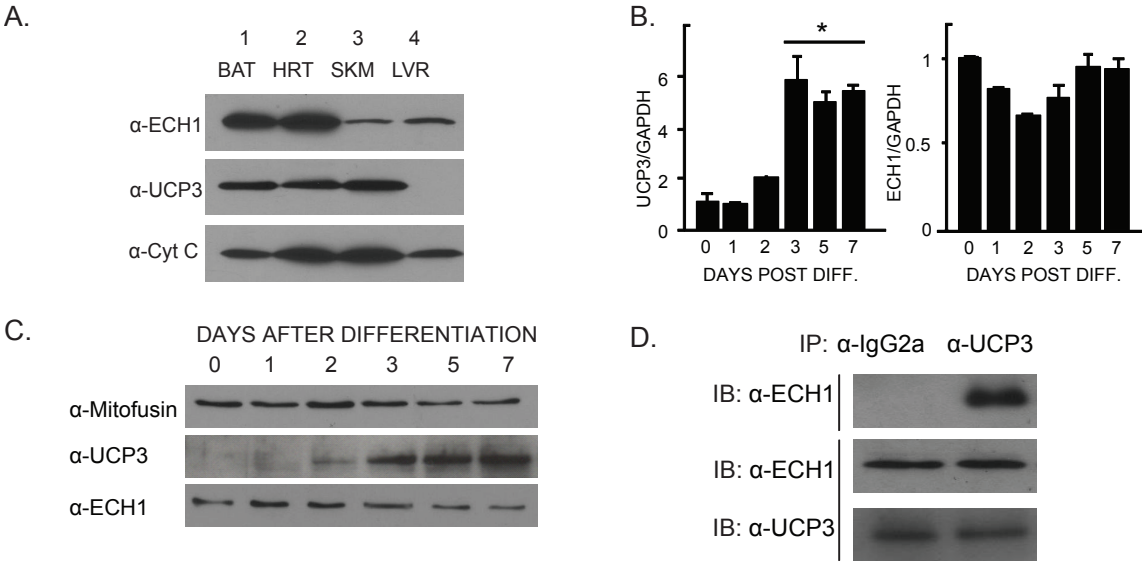

Figure 5.1 Characterizing the interaction between ECH1 and UCP3

(A) ECH1 and UCP3 protein expression profiles in mitochondrial lysates isolated from brown adipose tissue (BAT), SKM (SKM), heart (HRT), and liver (LVR) tissues (n=5). (B-C) Endogenous mRNA and protein expression levels of ECH1 and UCP3 in differentiating mouse myoblasts C2C12s. (D) Mitochondrial lysates isolated from myotubes were immunoprecipitated with anti-UCP3 or negative control IgG. Co-immunoprecipitating proteins were detected by immunoblotting with anti-ECH1.

An interesting characteristic of ECH1 is that it contains both mitochondrial and peroxisomal targeting sequences that flank the catalytic and trimerization domains (Modis et al. 1998; Zhang et al. 2001). Previous studies investigating ECH1 function have primarily focused on its characterization in liver and heart therefore its subcellular localization in SKM has not been defined. To examine whether ECH1 localizes predominantly to the mitochondria or peroxisomes, immunocytochemistry was performed on C2C12 myocytes that were co-transfected with ECH1-Myc and either Mito-GFP or the empty vector control plasmid (Figure 5.2 A). Pearson's correlation coefficient was calculated to quantify ECH1's subcellular localization, and revealed that ECH1 localizes predominantly to mitochondria based on the co-localization of ECH1's immunofluorescent stain with Mito-GFP (Figure 5.2 B). Endogenous staining of catalase was used as a peroxisomal marker.

5.2.2 Fatty acid regulation of ECH1 and UCP3

After confirming that ECH1 localizes primarily to mitochondria and that UCP3 endogenously interacts in C2C12 myotubes, we then focused on defining the biochemical and physiological factors that regulate ECH1 and UCP3 complex formation. We generated Myc-tagged ECH1 catalytic mutants to address whether the mutants could be co-immunoprecipitated with UCP3-V5 in lysates extracted from co-transfected cells (Figure 5.3 A). According to structural and mechanistic studies of ECH1, the aspartic acid 204 (D204) and glutamic acid 196 (E196) residues located in the active site of ECH1 are essential for catalysis (Modis et al. 1998). The aspartic acid 276 (D176) residue is

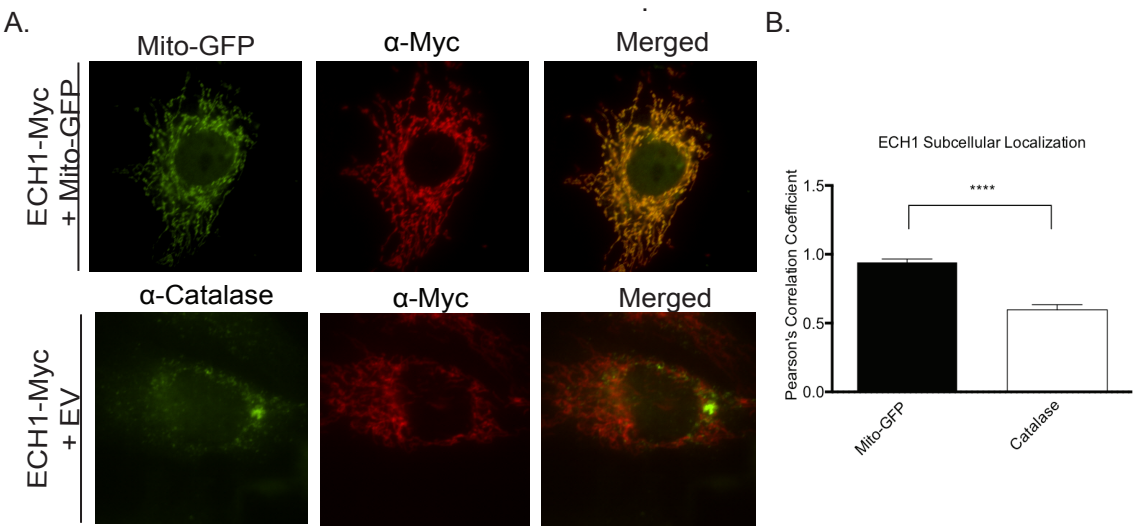

Figure 5.2 Subcellular localization of ECH1 in C2C12 myoblasts

(A) Representative immunocytochemistry images of C2C12 myoblasts co-transfected with ECH1-Myc and either the GFP fusion protein containing a mitochondrial targeting sequence (Mito-GFP, mitochondrial marker) or empty vector control. Cells were incubated with primary antibodies anti-Myc (ECH1-Myc) and anti-catalase (peroxisome marker), followed by incubation with corresponding fluorescent secondary antibodies anti-mouse (red, mECH1-Myc) and anti-rabbit (green, bottom panel, catalase). (B) Pearson's correlation coefficient for co-localization of ECH1-Myc (red) and Mito-GFP or catalase (green) (n= 6-7 cells). Data are expressed as mean ± SEM from three independent experiments. *$p<0.05$ ***$p<0.001$.

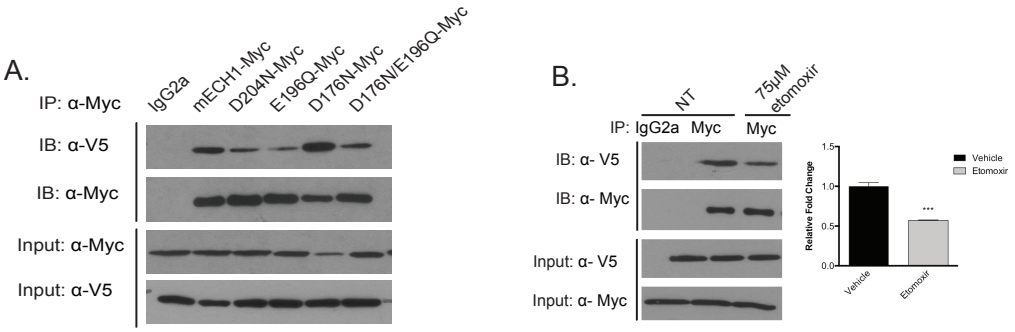

Figure 5.3 Fatty acid regulation of the ECH1 and UCP3 interaction

(A) Lysates were immunoprecipitated with either IgG or anti-Myc from cells co-transfected with UCP3-V5 and either ECH1-Myc or the Myc-tagged ECH1 catalytic mutant constructs (D204N-Myc and E196Q-Myc). To rule out any effects independent of catalytic activity we generated an ECH1 mutant that has been previously shown to retain enzymatic activity (D176N-Myc) and the ECH1 double mutant that re-introduced the E196Q catalytic mutation (D176N/E196Q-Myc). Co-immunoprecipitated UCP3-V5 was detected by immunoblotting with anti-V5. (B) Co-transfected cells were treated for 18hrs with either vehicle (lane 1-2) or 75 μM etomoxir the CPT1 inhibitor. Co-immunoprecipitations were performed as previously described. For densitometry precipitated UCP3-V5 (top panel) was normalized to pull down of ECH1-Myc. Data represent means ± SEM from 3 independent experiments. ***$p< 0.001$. (C) Protein expression levels of UCP3 and ECH1 are both elevated in SKM of wild type mice fed high fat diet (60% kCal). For densitometry ECH1 and UCP3 protein expression was normalized to mitofusin 2. Data expressed as mean ± SEM (n=6). *$p< 0.05$.

also located in the active site of ECH1, but is shown to have little effect on catalytic activity (Zhang et al. 2001). Both Myc-tagged ECH1 catalytic mutants D204N-Myc and E196-Myc, demonstrated a diminished interaction with UCP3-V5 in comparison to ECH1-Myc. Interestingly, the ECH1 mutant D176N-Myc, that still possessed catalytic activity, did not have the same attenuated effect on complex formation with UCP3-V5. Furthermore, the double mutant construct D176N/E196Q-Myc was not able to interact with UCP3-V5 to the same extent as ECH1-Myc, thus highlighting the importance of ECH1 catalytic activity in complex formation with UCP3.

If ECH1 catalytic activity greatly affects ECH1 and UCP3 complex formation, then it is possible that flux through the mitochondrial pathways of fatty acid metabolism may play an important role in regulating the ECH1:UCP3 interaction. To test this idea, we blocked mitochondrial fatty acid import by inhibiting the key mitochondrial fatty acid transporter, carnitine palmitoyl transferase I (CPT1) with the drug etomoxir. Co-immunoprecipitation experiments were performed in lysates extracted from HEK293T cells previously co-transfected with UCP3-V5 and ECH1-Myc, and treated with 75μM etomoxir. Densitometry analyses of immunoblots detecting the amount of UCP3-V5 co-immunoprecipitated with ECH1-Myc showed a ~2 fold decrease in complex formation with the etomoxir treated cells compared to vehicle treated (Figure 5.3 B).

5.2.3 Functional implications of ECH1:UCP3 complex in SKM metabolism

Given our previous data indicating that fatty acids play a key role in stimulating ECH1:UCP3 complex formation, we predicted that this interaction could be particularly

important in physiologically relevant conditions that require high levels of fatty acid metabolism (e.g. fasting and high fat feeding). Indeed, we observed a ~1.5 and 2 fold increase in ECH1 and UCP3 protein expression levels, respectively, in isolated SKM mitochondria from mice fed high-fat diets for 6 weeks (Figure 5.4A). In order to characterize the functional influence of the ECH1:UCP3 complex on mitochondrial metabolism in SKM we utilized the Precision Lenti-ORF plasmids (pLOC) to generate stable cell lines in C2C12 myoblasts that either overexpresses ECH1 (C2C12-ECH1) or empty vector, pLOC (C2C12-EV). Stables colonies of both cell lines were selected and densitometry analyses confirmed protein overexpression of ECH1 in the C212-ECH1 cell lines at physiological levels (Figure 5.4 B) similar to the induction of ECH1 expression in SKM of mice fed high fat diets (Figure 5.4 A). Considering that UCP3 function is closely tied to fatty acid metabolism, if ECH1 forms a direct complex with UCP3 in the presence of fatty acids it is possible that complex formation could regulate UCP3 activity and thus enhance uncoupled respiration. To investigate this notion we transfected UCP3-V5 in to our stable cell lines C2C12-ECH1 and -EV and measured uncoupled respiration using a fiber-optic fluorescence oxygen monitoring system. As shown in Figure 5.4 C oligomycin-induced uncoupled respiration was higher in cells overexpressing ECH1 and UCP3-V5 compared to cells expressing UCP3-V5 alone. We then set out to examine the consequences of the ECH1:UCP3 complex formation on ECH1-dependent metabolism of unsaturated fatty acids through quantification of radiolabeled oleate oxidation in our

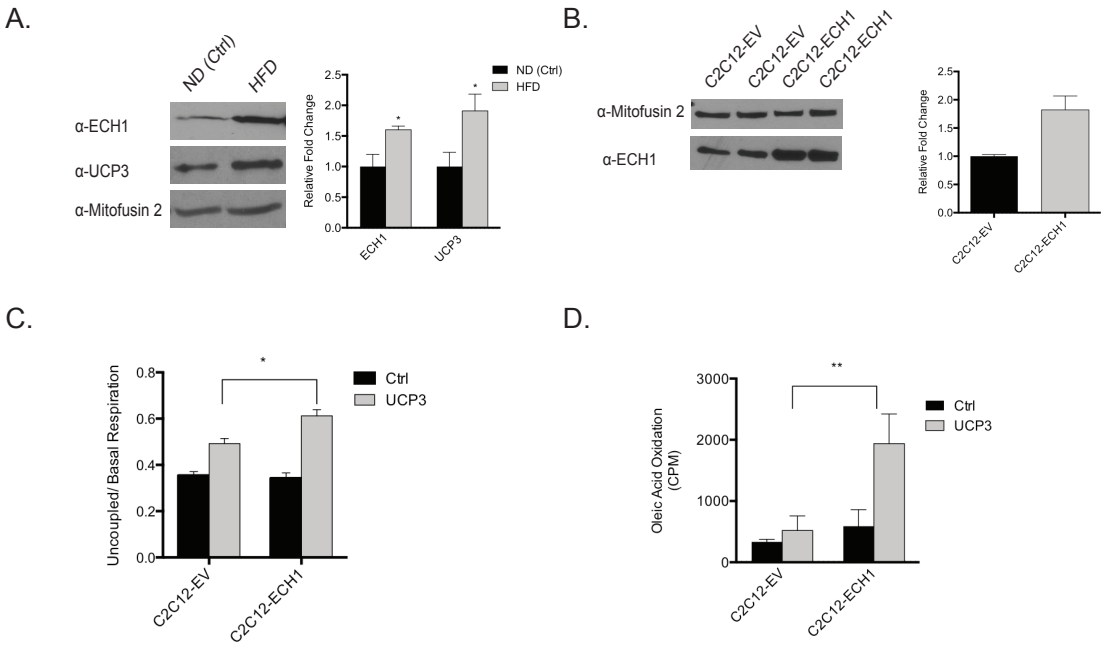

Figure 5.4 Functional implications of ECH1:UCP3 complex on fatty acid metabolism and uncoupled respiration

(A) Protein expression levels of UCP3 and ECH1 are both elevated in SKM of wild type mice fed high fat diet (60% kCal). For densitometry ECH1 and UCP3 protein expression was normalized to mitofusin 2. Data expressed as mean ± SEM (n=6). *p< 0.05. (B) Lentiviral overexpression of ECH1 in C2C12. For lentiviral transduction, C2C12s were incubated with lentiviral particles containing either the empty vector Precision Lenti-ORF plasmid (pLOC) or pLOC-ECH1 construct. Stable colonies of C2C12s expressing empty vector pLOC (C2C12-EV) or pLOC-ECH1 (C2C12-ECH1) were selected with blasticidin and grown up. Densitometry analyses of immunoblots detecting ECH1 protein expression normalized to mitofusin 2 confirmed stable overexpression of ECH1 in C2C12-ECH1 lines. (C) ECH1 expression enhances uncoupled respiration. C2C12-EV and C2C12-ECH1 cells were transfected with UCP3-V5 (UCP3) or empty vector (Ctrl). Uncoupled respiration was normalized to basal respiration rates. (D) ECH1 and UCP3 expression increased unsaturated fatty acid oxidation. Data are expressed as mean ± SEM. *p< 0.05, **p< 0.01

stable cell lines transfected with UCP3-V5. Consistent with previous observations, UCP3 expression alone led to a slight increase in oleate metabolism (Figure 5.4 D). Interestingly, ECH1 and UCP3 overexpression led to a synergistic increase in oleate oxidation.

5.2.4 Characterization of the ECH$^{-/-}$ mouse model

In order to further investigate the role of physiological relevance of ECH1 in whole body energy metabolism a global ECH1 knockout mouse model (ECH1$^{-/-}$) utilizing a zinc finger nucleases (ZFNs)-based genomic approach. Engineered ZFNs have been successfully employed to generate gene knockout models by introducing sequence-specific double strand breaks that lead to nonhomologous end joining (NHEJ)-mediated deletions or insertions at the target site (Cui et al. 2011). The custom made ECH1-ZFNs compromised of a DNA binding domain, targeted to exon 3 of the mouse ECH1 gene located on chromosome 7, was fused to a Fok I nuclease domain. Genomic PCR confirmed ZFN-mediated mutations (Figure 5.5 A). Two founder lines were then selected (line 3 and ll) based on sequence analysis of verified targeted ZFN-induced deletions or insertions (Figure 5.6 B-C). Analyses of ECH1 expression by western blot confirmed a complete loss of ECH1 expression in SKM, BAT, and HRT in both founder lines (Figure 5.6 D, line 3 data not shown). The data presented in the following experiments were performed with the fully back-crossed line 11-founder line (ECH1$^{-/-}$).

5.2.5 Physiological relevance of ECH1 and UCP3 in metabolic stress

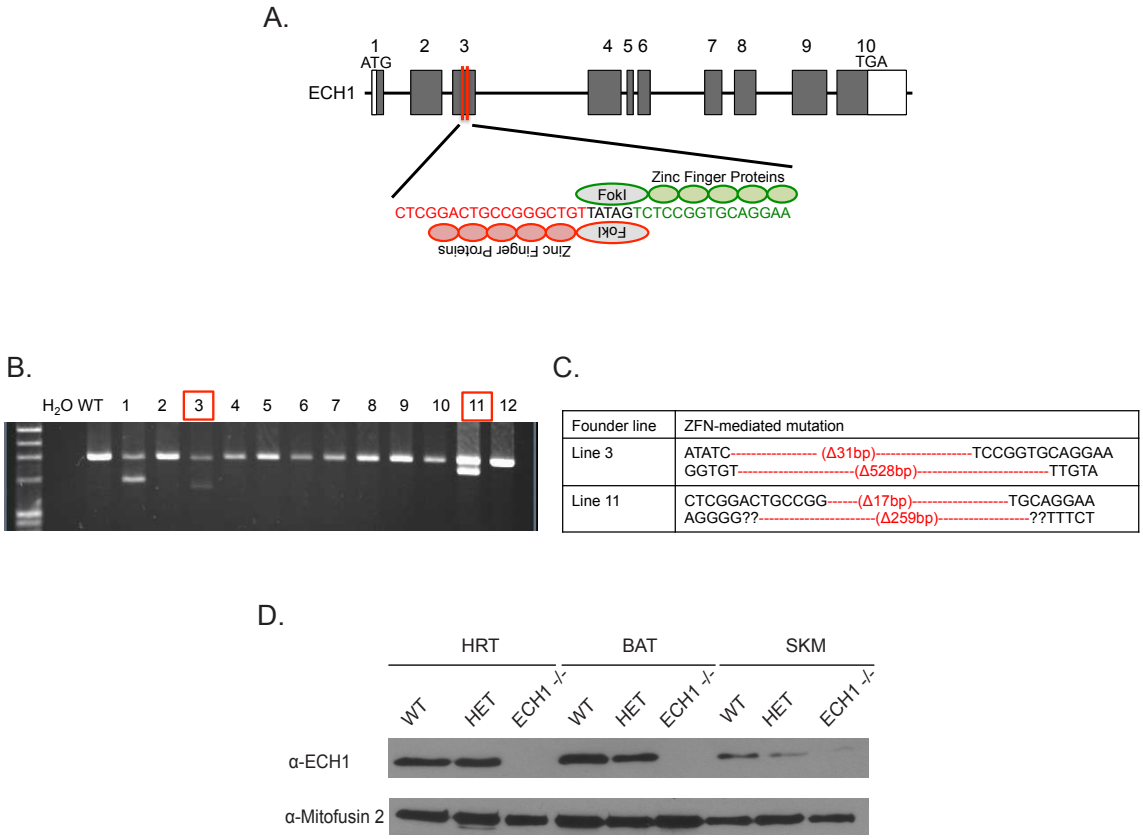

Figure 5.5 Generation of the ECH-knockout mouse model

(A) Schematic of zinc finger nucleases (ZFNs) target site. Nuclease cleavage domain indicated by Fok I site. (B) PCR analysis of ZFN-induced mutations. Wild-type (WT) was included as a positive control Lane 3 and 11 represent the selected founder lines. (C) Sequences of ZFN-induced mutations in founder lines. (D) ECH1 protein expression in wild-type (WT), heterozygotes (HET), and ECH1 knockout mice (ECH1$^{-/-}$, line 11).

Similar to UCP3, it has been proposed that ECH1 may play a crucial role in the protection against lipid overload in conditions of high metabolic stress where fatty acids serves as the primary source of energy. Given that fatty acid metabolism and transport is essential in driving cold-induced thermogenesis, it is not surprising that the most common phenotype seen with whole body knockout mouse models of different fatty acid metabolizing enzymes is severe cold intolerance with prior fasting (Miinalainen et al. 2009; Janssen & Stoffel 2002). In order to explore the physiological relevance of ECH1 and UCP3 in conditions of metabolic stress, we utilized the UCP3 and ECH1 knockout mouse models to investigate whether these mice would have similar thermogenic phenotypes in response to prolonged periods of fasting.

Even though $UCP3^{-/-}$ mice do not exhibit susceptibility to cold exposure or obesity, there is significant evidence to support the role of UCP3 in maintaining energy balance in metabolically challenging conditions that require higher rates of fatty acid oxidation. Indeed, experiments demonstrating that fasted $UCP3^{-/-}$ mice exhibited impaired rates of fatty acid oxidation along with elevated levels of lipid accumulation in the matrix, suggest that UCP3 is necessary for mitochondrial adaptation to fasting (Seifert et al. 2008). Interestingly, following an 18hrs fasting period we found that the fasted $UCP3^{-/-}$ mice were more sensitive to cold after 6hrs compared to the wild-type group (Figure 5.6).

We then focused on characterizing the role of ECH1 in metabolic stress. Similar to the wild-type, the fed $ECH1^{-/-}$ mice showed a slight decrease in body temperature following fasting treatment compared to the fed groups (Figure 5.7 A). However, the

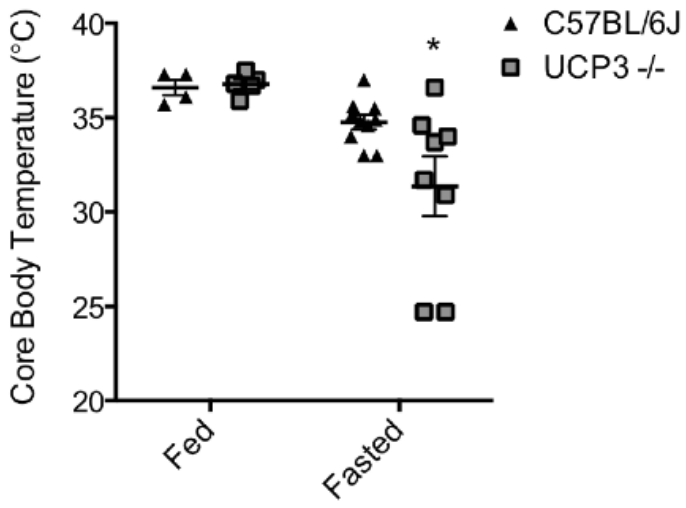

Figure 5.6 UCP3 is important in maintaining core body temperature in conditions of severe metabolic stress

Data represents the core body temperatures of individual UCP3$^{-/-}$ and C57BL/6J mice following 6hr cold exposure (4°C). Fasted groups underwent 18hr fasting challenge before cold exposure. Error bars are means of +/- SEM (n= 4-10).

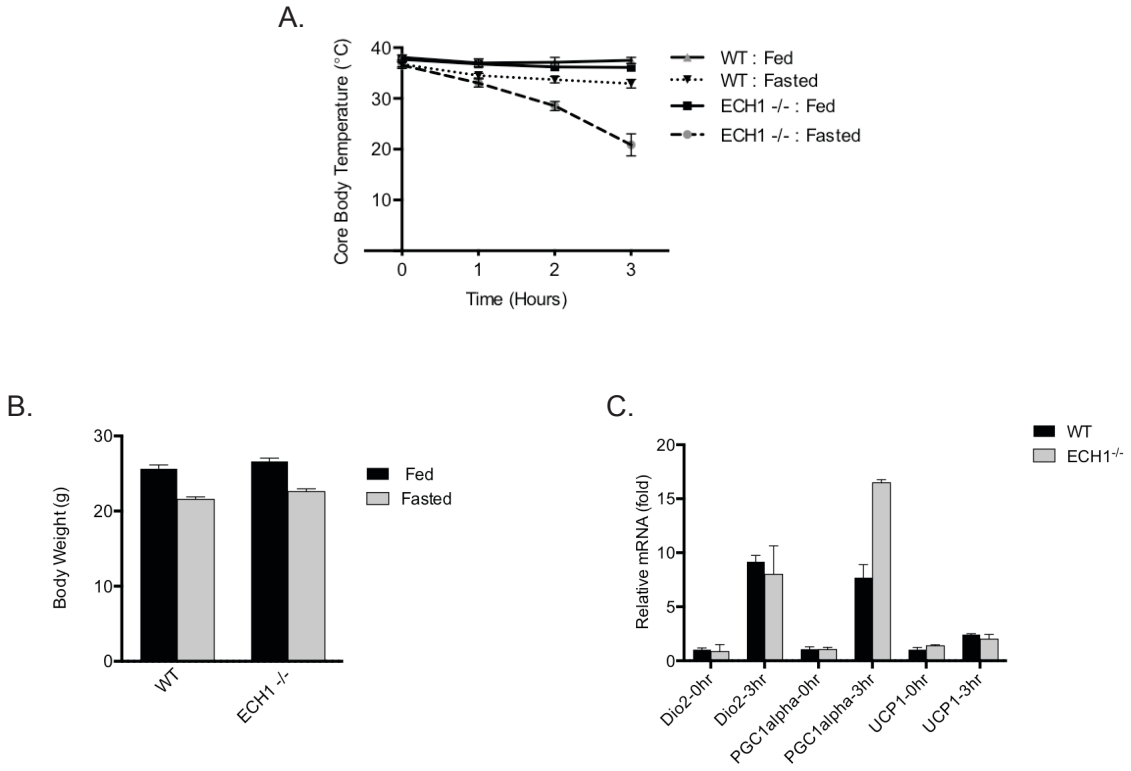

Figure 5.7 Thermogenesis in ECH1$^{-/-}$ mice in conditions of severe metabolic stress
(A) Body temperatures of WT and ECH1 $^{-/-}$ mice following 18hr fast and 3hr cold challenge at 4°C. * $p< 0.05$, statistical significance was was detected by two way analysis of variance (ANOVA) followed by Tukey's *post hoc* test. (B) Body weights of WT and ECH1$^{-/-}$ before (fed) and after 18hr fast (fasted) (n=4-5). *$p< 0.05$, statistical significance was detected by student's t test (C) mRNA expression levels of canonical cold-induced genes (n=4-5).
Data are expressed as +/- SEM and representative of experiments performed with the fully backcrossed ECH1 $^{-/-}$ founder line, Line 11.

Fasted ECH1$^{-/-}$ mice were unable to maintain core body temperature during acute cold exposure at 4°C, reaching critical hypothermia (<25°C) after 3 hours. Interestingly, the body weights of the wild-type and ECH1$^{-/-}$ mice were not different in the fasted and fed groups, thus indicating that the thermogenic phenotype seen in the ECH1$^{-/-}$ mice was independent of any differences in body weight following fasting (Figure 5.7 B). To further characterize the thermogenic phenotype in the ECH1$^{-/-}$ mice, we focused on determining whether this effect was due to impaired adrenergic stimulation of BAT thermogenesis by examining the expression of canonical cold-induced thermogenic genes. Compared to the wild-type group we found that the ECH1$^{-/-}$ mice did not exhibit a difference in mRNA expression levels of cold-induced BAT thermogenic genes including UCP1 and Dio2 (Figure 5.7 C). These results suggest that the signaling downstream of adrenergic stimulation of BAT in response to cold exposure is intact in the ECH1$^{-/-}$ mice and is not likely contributing to the severe cold-intolerant phenotype.

5.2.5 Characterization of ECH1 in brown adipose tissue

Given that BAT is another important site of regulated energy expenditure and inducible proton leak, we then focused on characterizing the physiological function of ECH1 in BAT. Considering that UCP1 and UCP3 are both expressed in BAT and shares 57% amino acid sequence homology (Vidal-Puig et al. 1997), we reasoned that ECH1 could interact with both UCP-homologues in BAT to regulate whole-body metabolism. Accordingly, co-immunoprecipitation assays performed with mitochondria isolated from

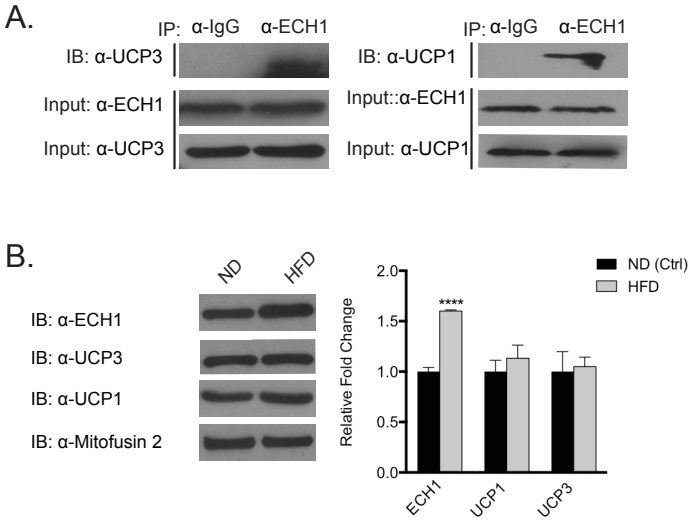

Figure 5.8 Characterization of ECH1 in BAT

(A) ECH1 interacts with UCP1 and UCP1 in BAT. Co-immunoprecipitating proteins were detected by immunoblotting with either anti-UCP3 or anti-UCP1. (B) Protein expression levels of ECH1, UCP3, and UCP1 of wild type mice fed high fat diet (60% kCal). For densitometry ECH1, UCP3 protein expression was normalized to mitofusin 2. Data expressed as mean ± SEM (n=6). *p< 0.05.

BAT showed that ECH1 interacts with UCP1 and UCP3 at endogenous levels (Figure 5.8 A).

As previously discussed, we have shown that UCP3 and ECH1 protein expression is induced in SKM in response to high fat feeding, thus implicating the physiological relevance of ECH1:UCP3 complex formation in fatty acid-induced pathologies. In contrast, we did not see a similar pattern in BAT with UCP1 and UCP3 protein expression levels remaining relatively unchanged, despite a statistically significant increase ($p<0.0001$) in ECH1 expression with mice fed high fat diets for 6 weeks (Figure 5.8 B). The lack of early induction of UCP1 and UCP3 protein expression could suggest that BAT uncoupling activity is not relevant at the early stages of obesity. Regardless, it is clear from this data that regulation of complex formation of ECH1 with UCP1 and/or UCP3 in BAT is different in SKM.

5.3 Discussion

There is considerable evidence to support that UCP3 has the ability to lower metabolic efficiency and facilitate higher rates of fatty acid metabolism in order to protect SKM mitochondria from nutrient overload, but only when activated in certain physiological contexts. Fatty acids have been implicated as potent activators of UCP function (Jiménez-Jiménez et al. 2006; Skulachev 1999; Hagen & Lowell 2000), however significant debate exists regarding the mechanisms by which fatty acids activate UCP3, and by which UCP3 regulates fatty acid metabolism. Our work demonstrating that the

auxiliary unsaturated fatty acid metabolizing enzyme ECH1 interacts with UCP3 in the mitochondrial matrix, at endogenous levels, supports a mechanism by which UCP3 can coordinate an increase in fatty acid metabolism with energy expenditure through uncoupling. Importantly, we also demonstrate that UCP3 and ECH1 are both important in facilitating an adaptive response to metabolic stress, and that complex formation between these proteins is key in regulating a thermogenic response to acute cold exposure in a fasted state.

The characterization of the ECH1:UCP3 complex sheds new light on how the specific metabolism of polyunsaturated fatty acids with odd-numbered double bonds contributes to mitochondrial energy balance. ECH1 is a unique enzyme in that it demonstrates dual-organelle distribution to the peroxisomes and mitochondria in mammalian cells in liver and heart. The enzyme contains a known type I peroxisomal targeting sequence (SKL) in its C-terminus (Filppula 1998), and it has also been shown that the first 40 amino acids in the N terminus resembles a cleavable mitochondrial targeting signal as predicted by Mitoprot II analysis (Claros & Vincens 1996). While mitochondrial fatty acidmetabolism is a major contributor to energy production and balance, peroxisomal fatty acid oxidation is only capable of shortening the fatty acyl-CoA chains, while the complete degradation of the fatty acyl-CoA chain to generate ATP occurs exclusively in the mitochondria (Borgne & Demarquoy 2012). Therefore, our finding that ECH1 localizes primarily to the mitochondria rather than peroxisomes is consistent with previous studies that ECH1 is important in maintaining pools of coenzyme A and regulating energy balance.

It has been proposed that ECH1 plays an important role in the disposal of unmetabolizable fatty acid metabolites (Shoukry & Schulz 1998). ECH1 is an essential auxiliary enzyme in the reductase-dependent pathway that is responsible for catalyzing the isomerization of the 3,5-dienoyl-CoA substrate to 2,4-dienoyl-CoA. This is regarded as a crucial step in the reductase-dependent pathway because unlike other fatty acid-intermediates that can be metabolized by redundant fatty acid enzymes, the 3,5-dienoyl-CoA substrate is a "dead end metabolite" that is exclusively metabolized by ECH1. Based on these realizations it was later suggested that the reductase-dependent pathway be renamed to the ECH1-dependent pathway (Shoukry & Schulz 1998) given that in the absence of ECH1 activity, the "dead end metabolite" would accumulate, sequester coenzyme A, and halt mitochondrial β-oxidation.

Interestingly, the proposed physiological function of ECH1 is similar to previous theories by Harper et al. that suggest UCP3 also protects against lipotoxicity by facilitating fatty acid transport to maintain coenzyme A availability in conditions that require high levels of fatty acid oxidation. In support of this notion, UCP3 expression is induced in response to high fat feeding and fasting, thus suggesting a role for UCP3 in conditions where the rates of mitochondrial fatty acid oxidation are high. Furthermore, it has also been shown that UCP3 overexpression in SKM can lower circulating levels of acylcarnitines and thus facilitate complete fatty acid oxidation (Aguer et al. 2013). Based on these findings, it makes sense that UCP3 would interact with a fatty acid metabolizing enzyme to mediate efficient fatty acid oxidation. Accordingly, our data demonstrating that ECH1:UCP3 complex formation is regulated through fatty acids and is likely

activated in conditions that require enhanced levels of fatty acid oxidation e.g. high fat feeding, suggests these two proteins could be facilitating a compensatory response to metabolic fatty acid overload. Indeed, we propose a modified model by which UCP3 functions to maintain coenzyme A availability in part through ECH1-dependent metabolism of unsaturated fatty acids. The finding that UCP3 and ECH1 expression synergistically increases oleic acid oxidation suggests that UCP3 binding could enhance ECH1 activity and promote unsaturated fatty acid oxidation. In addition to this, we also demonstrate that ECH1 and UCP3 expression synergistically enhances uncoupled respiration in C2C12 myocytes. Taken together, it is tempting to speculate that complex formation between ECH1 and UCP3 functions to coordinate fatty acid oxidation and uncoupling activity in a compensatory pathway that is activated in situations that require enhanced levels of fatty acid oxidation.

Despite the numerous debates regarding the thermogenic capabilities of UCP3 in SKM, results herein demonstrate the UCP3 is important in mediating an adaptive thermogenic response to cold temperatures, in a fasted state. The assumption that UCP3 is not a physiological thermogenic regulator stems from the finding that UCP3$^{-/-}$ mice are able to maintain core body temperature in response to cold. However, the lack of a cold-phenotype may be due to a compensatory process, but it does not necessarily exclude the possibility that UCP3 can contribute to whole-body thermogenesis through alternative mechanisms that may be crucial in different physiological contexts. Indeed, UCP3 has been shown to be a crucial molecular mediator of non-shivering thermogenesis in response pharmacological amphetamines (Mills et al. 2003), and thyroid hormone

(Flandin et al. 2009) which is arguably one of the most important hormonal regulators of whole body thermogenesis and energy metabolism. Indeed, observed changes in UCP3 expression in certain physiological contexts where mitochondria rely predominantly on fatty acid metabolism, along with mechanistic studies in fasted mice, suggest that UCP3 may be relevant in mediating an adaptive increase in fatty acid oxidation capacity in SKM (Seifert et al. 2008). Given that fasting and cold exposure are both stimulators of fatty acid oxidation, it is likely that the absence of UCP3 diminishes efficient fatty acid handling in response to these metabolic stressors, thus diminishing optimal cold-induced thermogenesis in UCP3$^{-/-}$ in a fasted stated.

Lastly, we demonstrate for the first time that unsaturated fatty acid metabolism through the reductase/ECH1-dependent pathway is essential for thermogenesis in conditions of severe metabolic stress. The impaired thermogenic phenotype seen in the ECH1$^{-/-}$ mice in response to fasting is similar to previous studies with mice lacking dienoyl-CoA reductase, an auxiliary enzyme involved in the metabolism of all species of unsaturated fatty acids (odd- and even-numbered double bonds) (Miinalainen et al. 2009). Despite previous work indicating that the reductase/ECH1-dependent pathway contributes to a minor portion of mitochondrial β-oxidation of unsaturated fatty acids with odd-numbered double bonds (Shoukry & Schulz 1998), our work clearly shows that impairment of this metabolic pathway can have a significant effect on whole-body thermogenesis in fasted conditions. Taken together, this data shows that ECH1 is an essential regulator of cold-induced thermogenesis in a fasted state, through a mechanism that is mediated in part through UCP3-dependent activity in SKM.

The present study is the first to establish a molecular mechanism by which UCP3 can facilitate fatty acid metabolism in SKM and combat lipid-induced toxicity through complex formation with the auxiliary unsaturated fatty acid metabolism enzyme ECH1. Our work demonstrating that the ECH1:UCP3 complex can synergistically increase unsaturated fatty oxidation and uncoupled respiration provides the foundation for developing new treatments to combat obesity and related metabolic diseases. In our proposed model, we predict that complex formation between ECH1 and UCP3 is key in coordinating a compensatory pathway that increases SKM capacity for fatty acid oxidation by facilitating efficient mitochondrial fatty acid transport and metabolism in conditions of severe metabolic stress (Illustration 5.1). This work lays the foundation for the development of new anti-obesity therapies that focus on restoring energy balance by increasing SKM metabolic inefficiency through mitochondrial uncoupling.

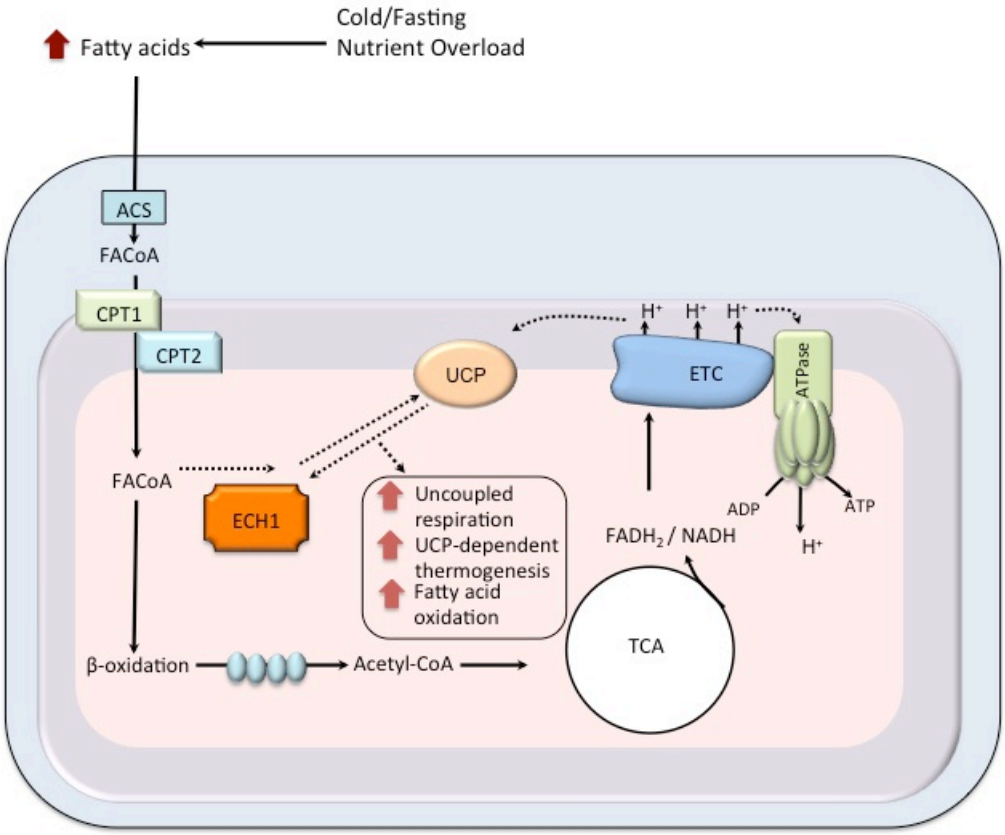

Illustration 5.1 Proposed model of ECH1 and UCP3 complex formation in protecting against metabolic stress

In physiological conditions where fatty acid metabolism is elevated, ECH1:UCP3 complex formation protects mitochondrial function by coordinating an increase in fatty acid oxidation and uncoupled respiration. The thermogenic effects of UCP3 on proton conductance and mitochondrial respiration allows the electron transport chain to handle the excess supply of reduced cofactors (NADH and $FADH_2$) generated from the increased flux though β-oxidation. This coordinated response protects against the detrimental effects of metabolic stress caused from mitochondrial overload.

Chapter 6: Concluding remarks and future directions

Since its discovery, UCP3 has remained an attractive target in treatment of obesity and related metabolic disorders despite the controversy surrounding its physiological relevance and thermogenic capabilities. The early observation that UCP3 knockout mice exhibit normal thermoregulatory responses to cold, led many to believe that unlike BAT UCP1, UCP3 does not regulate thermogenesis. However, the lack of a "cold-induced" phenotype in UCP3$^{-/-}$ mice could be explained by compensatory pathways (most likely UCP1) that mask any UCP3-dependent effects. In addition to this, it is also possible that UCP3 activity may be more important in other thermogenic responses. Indeed, previous work has shown that UCP3 knockout mice lack thermogenic responses to various pharmacological amphetamines (Mills et al. 2003; Sprague, Mallett, et al. 2004). Herein, our work further substantiates the thermogenic capabilities of SKM UCP3 in sympathomimetic-induced hyperthermia, and also demonstrates that activation of UCP3-dependent thermogenesis is particularly important conditions of severe metabolic stress (e.g. prolonged periods of fasting). The thermogenic effects of UCP3 are likely mediated in part through the identified interactions with key metabolic enzymes involved fatty acid metabolism (particularly ECH1), and efficient substrate selection in certain physiological contexts. Future studies that focus on further characterizing how these UCP3-regulated protein complexes can influence mitochondrial substrate preference and energetics could provide new therapeutic approaches to treat obesity and –related metabolic disorders.

An attractive area of research that has gained momentum in recent years deals with the interplay between thermogenesis in BAT and SKM. Although it was originally postulated that the role of SKM in regulating core body temperature was limited to shivering thermogenesis, it is now clear that SKM also possesses mechanisms of non-shivering thermogenesis that greatly contribute to thermoregulation and energy balance (Kozak & Young 2012). Interestingly, BAT and SKM originate from the same progenitor cells that diverge along separate lineages to give rise to either myoblasts or brown adipocytes (Seale et al. 2008). Indeed, certain brown adipocyte "like" cells that correlate with increased energy expenditure have actually been identified in SKM tissue (Almind et al. 2007). Although, the function of these specialized brown adipocytes requires additional investigation, it has been suggested that these cells might function to increase the oxidative capacity of SKM (Farmer 2008).

Given the similar origins and metabolic features of BAT and SKM, it has been proposed that these distinct organs could have an interrelated role in regulating whole-body thermogenesis. The idea that crosstalk between BAT and SKM exists, and plays a significant role in contributing to whole body thermogenesis is further supported by the observation that secretion of irisin and natriuretic peptide from SKM influences whole body thermogenesis by inducing brown adipocyte depots that are intersperse among white adipose tissue (Lee et al. 2014; Kozak & Young 2012). Our data not only supports the possibility of interplay between these two distinct organs, but also suggest a new mechanism of crosstalk between BAT and SKM that is mediated through UCP1 and

UCP3. Given that various stimulants of thermogenesis activate BAT and SKM to different extents in humans (Cypess et al. 2012; Astrup et al. 1984; Astrup et al. 1985) understanding the underlying mechanisms that regulate the relative contribution of the these two organs in whole body thermogenesis can be useful developing new treatments for obesity.

With regard to the role of UCP3 in fatty acid metabolism, to our knowledge we are the first to show a detailed mechanism by which UCP3 influences fatty acid oxidation through its interaction with ECH1. Furthermore, our work argues that complex formation between ECH1 and UCP3 opposes obesity-induced metabolic derangements in SKM by coordinating changes in fatty acid metabolism and energy demand. Related studies with animals that specifically overexpress peroxisome proliferator-activated receptor-α (PPARα) in SKM support this view. Even though these mice exhibited a higher rates of fatty acid oxidation due to PPAR-α overexpression, these mice were surprisingly more susceptible to diet-induced insulin resistance (Finck et al. 2005). However, in the same study, the repressive effects of PPAR-α on glucose uptake were completely reversed in when L6 myotubes were treated with the chemical uncoupler DNP (Finck et al. 2005). These studies highlight the importance developing new obesity treatments that center on coordinating alterations in fatty acid metabolism with mitochondrial bioenergetics.

A key feature in understanding mitochondrial bioenergetics is that all metabolic processes are interconnected and stimulating fuel oxidation, as a means to relieve nutrient overload, without increasing energy utilization will further exacerbate energy homeostasis. Therefore, normal mitochondrial bioenergetics requires coordination

between mitochondrial transporters, enzymes involved substrate catabolism (β-oxidation, TCA cycle, glycolysis), and the ETC. It has been proposed that all these metabolic proteins and enzymes can function as monomeric units, or be arranged in large multi-enzyme complexes that are capable of efficient substrate channeling (Goetzman 2011). Formation of these organized multi-enzyme complexes could play a role in regulating enzyme activity and would provide a clear kinetic advantage especially in conditions where flux through certain pathways is extremely high. The data shown here is consistent with the growing literature that supports the importance of UCP3 activity in conditions where fatty acid oxidation levels are elevated. In addition to its interactions with key enzymes involved in fatty acid metabolism (CPT1, ECHs1, Acat1, Acadm), UCP3 could possibly influence energy metabolism through its interaction with malate dehydrogenase 2 (MDH2) and other TCA cycle enzymes. MDH2 is involved in the malate-aspartate shuttle that is responsible for the transport of reducing equivalents from cytosol to the mitochondria (LaNoue & Tischler 1974; LaNoue & Schoolwerth 1979). This shuttle system can also function in reverse and export NADH from mitochondria (Safer 1975) in situations where fatty acid supply and β-oxidation generation of NADH exceeds the energy demand (e.g. fasting). Thus, coordination between UCP3 and MDH2 could function to prevent inhibition of oxidative phosphorylation by alleviating the intramitochondrial accumulation of NADH when fatty acid oxidation is high. Future investigations to understand how formation of these UCP3 complexes are affected by changes in diet or nutritional status will reveal useful information of the underlying mechanisms of UCP3-dependent thermogenesis.

Another possibility that has yet to be investigated is the role of UCP3 in regulating cross talk between glucose and fatty acid metabolism. It is likely that this would be particularly important in conditions that require efficient substrate switching i.e. metabolic flexibility. The Randle cycle suggests that glucose and fatty acid metabolism oppose each other (Randle et al. 1963). Therefore, in a fasted stated where fatty acids are the primary fuel substrate acetyl-CoA produced from β-oxidation will inhibit PDH activity and glycolysis. However, when re-feeding begins insulin stimulated glucose uptake and catabolism leads to a surge in TCA cycle flux that is caused by acetyl-CoA generated from glycolysis and fatty acid metabolism. This action results in mitochondrial efflux of the TCA cycle intermediate citrate and ultimately inhibits fatty acid uptake and oxidation through the malonyl-CoA / CPT1 axis.

The counter regulatory actions between glucose and fatty acid metabolism are important in preventing the excessive generation of reducing equivalents produced from different catabolic substrates being fluxed into the same energetic pathways (TCA and ETC cycle). The effectiveness of the Randle cycle centers on the allosteric inhibition of PDH and CPT1. Interestingly, mechanisms that ease inhibition of PDH and facilitate a more rapid transition from fatty acid to glucose metabolism can improve overall mitochondrial bioenergetics (Muoio et al. 2012). Our data supports a possible mechanism by which UCP3 influences insulin sensitivity and glucose homeostasis is by facilitating efficient substrate selection through its interaction with PDH and CPT1.

Taken together, the work herein provides novel mechanistic information regarding how UCP3 influences SKM thermogenesis and bioenergetics through its broad

interactions with key enzymes involved in interconnected pathways of metabolism. Although numerous studies have suggested a fascinating link between defects in fatty acid metabolism and obesity-induced resistance, complications seen with obesity-induced insulin resistance are now recognized as disorders of metabolic flexibility. In these conditions, nutrient overload increases substrate competition to a point where clear metabolic signaling between substrate catabolism and energy utilization is compromised. This action can have complex, detrimental effects on mitochondrial function and insulin signaling in SKM. Our interaction and mechanistic studies suggest that UCP3 can counteract the effects of metabolic inflexibility by coordinating an increase in fatty acid oxidation and energy demand through its thermogenic actions. The work shown here also raises intriguing questions as to the direct effects that UCP3 may have on maintaining glucose homeostasis through complex formation with key enzymes involved in various catabolic pathways. Ultimately, the diverse effects of UCP3 in SKM encompass diverse mechanisms that counteract the metabolic derangements seen with obesity-induced resistance.

References

Aguer, C. et al., 2013. Muscle uncoupling protein 3 overexpression mimics endurance training and reduces circulating biomarkers of incomplete β-oxidation. *The FASEB Journal*, 27(10), pp.4213–4225.

Almind, K. et al., 2007. Ectopic brown adipose tissue in muscle provides a mechanism for differences in risk of metabolic syndrome in mice. *Proceedings of the National Academy of Sciences of the United States of America*, 104(7), pp.2366–2371.

Argyropoulos, G. et al., 1998. Effects of mutations in the human uncoupling protein 3 gene on the respiratory quotient and fat oxidation in severe obesity and type 2 diabetes. *Journal of Clinical Investigation*, 102(7), pp.1345–1351.

Astrup, A. et al., 1985. Contribution of BAT and skeletal muscle to thermogenesis induced by ephedrine in man. *The American journal of physiology*, 248(5 Pt 1), pp.E507–15.

Astrup, A. et al., 1984. Ephedrine-induced thermogenesis in man: no role for interscapular brown adipose tissue. *Clinical Science*, 66(2), pp.179–186.

Bal, N.C. et al., 2012. Sarcolipin is a newly identified regulator of muscle-based thermogenesis in mammals. *Nature Medicine*, 18(10), pp.1575–1579.

Bar-Shalom, R. et al., 2004. Non-malignant FDG uptake in infradiaphragmatic adipose tissue: a new site of physiological tracer biodistribution characterised by PET/CT. *European journal of nuclear medicine and molecular imaging*, 31(8), pp.1105–1113.

Barnett, M., Collier, G.R. & O'Dea, K., 1992. The longitudinal effect of inhibiting fatty acid oxidation in diabetic rats fed a high fat diet. *Hormone and metabolic research = Hormon- und Stoffwechselforschung = Hormones et métabolisme*, 24(8), pp.360–362.

Barre, H. & Rouanet, J.L., 1983. Calorigenic effect of glucagon and catecholamines in king penguin chicks. *The American journal of physiology*, 244(6), pp.R758–63.

Barreiro, E. et al., 2009. UCP3 overexpression neutralizes oxidative stress rather than nitrosative stress in mouse myotubes. *FEBS letters*, 583(2), pp.350–356.

Befroy, D.E. et al., 2007. Impaired mitochondrial substrate oxidation in muscle of insulin-resistant offspring of type 2 diabetic patients. *Diabetes*, 56(5), pp.1376–1381.

Bézaire, V. et al., 2005. Constitutive UCP3 overexpression at physiological levels increases mouse skeletal muscle capacity for fatty acid transport and oxidation. *The*

FASEB Journal, 19(8), pp.977–979.

Bézaire, V. et al., 2001. Effects of fasting on muscle mitochondrial energetics and fatty acid metabolism in Ucp3(-/-) and wild-type mice. *American journal of physiology Endocrinology and metabolism*, 281(5), pp.E975–82.

Block, B. & Franzini-Armstrong, C., 1988. The structure of the membrane systems in a novel muscle cell modified for heat production. *The Journal of Cell Biology*, 107(3), pp.1099–1112.

Boden, G., 2011. Obesity, insulin resistance and free fatty acids. *Current opinion in endocrinology, diabetes, and obesity*, 18(2), pp.139–143.

Borgne, F.L. & Demarquoy, J., 2012. Interaction between peroxisomes and mitochondria in fatty acid metabolism. *Open Journal of Molecular and Integrative Physiology*, 02(01), pp.27–33.

Boss, O., Hagen, T. & Lowell, B.B., 2000. Uncoupling proteins 2 and 3: potential regulators of mitochondrial energy metabolism. *Diabetes*, 49(2), pp.143–156.

Brand, M.D. & Esteves, T.C., 2005. Physiological functions of the mitochondrial uncoupling proteins UCP2 and UCP3. *Cell Metabolism*, 2(2), pp.85–93.

Brand, M.D. & Nicholls, D.G., 2011. Assessing mitochondrial dysfunction in cells. *Biochemical Journal*, 435(2), pp.297–312.

Brand, M.D. et al., 2002. Oxidative damage and phospholipid fatty acyl composition in skeletal muscle mitochondria from mice underexpressing or overexpressing uncoupling protein 3. *Biochemical Journal*, 368(Pt 2), pp.597–603.

Brückner, A. et al., 2009. Yeast Two-Hybrid, a Powerful Tool for Systems Biology. *International Journal of Molecular Sciences*, 10(6), pp.2763–2788.

Cannon, B. & Nedergaard, J., 2004. Brown Adipose Tissue: Function and Physiological Significance. *Physiological Reviews*, 84(1), pp.277–359.

Cannon, B., Hedin, A. & Nedergaard, J., 1982. Exclusive occurrence of thermogenin antigen in brown adipose tissue. *FEBS letters*, 150(1), pp.129–132.

Chakraborti, S. & Chakraborti, T., 1998. Oxidant-mediated activation of mitogen-activated protein kinases and nuclear transcription factors in the cardiovascular system: a brief overview. *Cellular signalling*, 10(10), pp.675–683.

Chan, T.C., Evans, S.D. & Clark, R.F., 1997. Drug-induced hyperthermia. *Critical care clinics*, 13(4), pp.785–808.

Charkoudian, N., 2003. Skin blood flow in adult human thermoregulation: how it works, when it does not, and why., 78(5), pp.603–612.

Choi, C.S. et al., 2007. Overexpression of uncoupling protein 3 in skeletal muscle protects against fat-induced insulin resistance. *Journal of Clinical Investigation*, 117(7), pp.1995–2003.

Chou, C.J. et al., 2001. High-fat diet feeding elevates skeletal muscle uncoupling protein 3 levels but not its activity in rats. *Obesity research*, 9(5), pp.313–319.

Clapham, J.C. et al., 2000. Mice overexpressing human uncoupling protein-3 in skeletal muscle are hyperphagic and lean. *Nature*, 406(6794), pp.415–418.

Claros, M.G. & Vincens, P., 1996. Computational method to predict mitochondrially imported proteins and their targeting sequences. *European journal of biochemistry / FEBS*, 241(3), pp.779–786.

Cui, X. et al., 2011. Targeted integration in rat and mouse embryos with zinc-finger nucleases. *Nature biotechnology*, 29(1), pp.64–67.

Cypess, A.M. et al., 2012. Cold but not sympathomimetics activates human brown adipose tissue in vivo. *Proceedings of the National Academy of Sciences of the United States of America*, 109(25), pp.10001–10005.

Cypess, A.M. et al., 2009. Identification and importance of brown adipose tissue in adult humans. *The New England journal of medicine*, 360(15), pp.1509–1517.

Dao, C.K., Nowinski, S.M. & Mills, E.M., 2014. The heat is on: Molecular mechanisms of drug-induced hyperthermia. *Temperature*, 1(3), pp.183–191.

De Witte, J., 2002. Perioperative Shivering. *Anesthesiology*, pp.1–18.

Deems, R.O., Anderson, R.C. & Foley, J.E., 1998. Hypoglycemic effects of a novel fatty acid oxidation inhibitor in rats and monkeys. *The American journal of physiology*, 274(2 Pt 2), pp.R524–8.

DeFronzo, R.A. et al., 1981. Synergistic interaction between exercise and insulin on peripheral glucose uptake. *Journal of Clinical Investigation*, 68(6), pp.1468–1474.

Echtay, K.S. et al., 2003. A signalling role for 4-hydroxy-2-nonenal in regulation of mitochondrial uncoupling. *The EMBO journal*, 22(16), pp.4103–4110.

Echtay, K.S. et al., 2002. Superoxide activates mitochondrial uncoupling proteins. *Nature*, 415(6867), pp.96–99.

Enerback, S. et al., 1997. Mice lacking mitochondrial uncoupling protein are cold-sensitive but not obese. *Nature*.

Esteves, T.C. & Brand, M.D., 2005. The reactions catalysed by the mitochondrial uncoupling proteins UCP2 and UCP3. *Biochimica et biophysica acta*, 1709(1), pp.35–44.

Farmer, S.R., 2008. Brown fat and skeletal muscle: unlikely cousins? *Cell*, 134(5), pp.726–727.

Fedorenko, A., Lishko, P.V. & Kirichok, Y., 2012. Mechanism of Fatty-Acid-Dependent UCP1 Uncoupling in Brown Fat Mitochondria. *Cell*, 151(2), pp.400–413.

Feldmann, H.M. et al., 2009. UCP1 ablation induces obesity and abolishes diet-induced thermogenesis in mice exempt from thermal stress by living at thermoneutrality. *Cell Metabolism*, 9(2), pp.203–209.

Felipe, F. et al., 2003. Up-regulation of muscle uncoupling protein 3 gene expression in mice following high fat diet, dietary vitamin A supplementation and acute retinoic acid-treatment. *International Journal of Obesity*, 27(1), pp.60–69.

Fiehn, O. et al., 2010. Plasma metabolomic profiles reflective of glucose homeostasis in non-diabetic and type 2 diabetic obese African-American women. J. M. Gimble, ed. *PLoS ONE*, 5(12), p.e15234.

Filppula, S.A., 1998. Delta 3,5-Delta 2,4-Dienoyl-CoA Isomerase from Rat Liver. MOLECULAR CHARACTERIZATION. *Journal of Biological Chemistry*, 273(1), pp.349–355.

Finck, B.N. et al., 2005. A potential link between muscle peroxisome proliferator-activated receptor-alpha signaling and obesity-related diabetes. *Cell Metabolism*, 1(2), pp.133–144.

Fisher-Wellman, K.H. & Neufer, P.D., 2012. Linking mitochondrial bioenergetics to insulin resistance via redox biology. *Trends in Endocrinology & Metabolism*, 23(3), pp.142–153.

Flandin, P. et al., 2009. Uncoupling protein-3 as a molecular determinant of the action of 3,5,3'-triiodothyronine on energy metabolism. *Endocrine*, 36(2), pp.246–254.

Fredriksson, J.M. et al., 2001. Analysis of inhibition by H89 of UCP1 gene expression and thermogenesis indicates protein kinase A mediation of beta(3)-adrenergic signalling rather than beta(3)-adrenoceptor antagonism by H89. *Biochimica et biophysica acta*, 1538(2-3), pp.206–217.

Goetzman, E.S., 2011. Modeling disorders of fatty acid metabolism in the mouse. *Progress in Molecular Biology and Translational Science*, 100, pp.389–417.

Golozoubova, V. et al., 2001. Only UCP1 can mediate adaptive nonshivering thermogenesis in the cold. *Faseb Journal*, 15(11), pp.2048–2050.

Gong, D.W. et al., 2000. Lack of obesity and normal response to fasting and thyroid hormone in mice lacking uncoupling protein-3. *The Journal of biological chemistry*, 275(21), pp.16251–16257.

Gong, D.W. et al., 1997. Uncoupling protein-3 is a mediator of thermogenesis regulated by thyroid hormone, beta3-adrenergic agonists, and leptin. *The Journal of biological chemistry*, 272(39), pp.24129–24132.

Grundlingh, J. et al., 2011. 2,4-dinitrophenol (DNP): a weight loss agent with significant acute toxicity and risk of death. *Journal of medical toxicology : official journal of the American College of Medical Toxicology*, 7(3), pp.205–212.

Guerra, C. et al., 1998. Abnormal nonshivering thermogenesis in mice with inherited defects of fatty acid oxidation. *Journal of Clinical Investigation*, 102(9), pp.1724–1731.

Guo, X. et al., 2012. Glycolysis in the control of blood glucose homeostasis. *Diabetes and Obesity*, 2(4), pp.358–367.

Hagen, T. & Lowell, B.B., 2000. Chimeric proteins between UCP1 and UCP3: the middle third of UCP1 is necessary and sufficient for activation by fatty acids. *Biochemical and biophysical research communications*, 276(2), pp.642–648.

Harri, M. & Hedenstam, R., 1972. Calorigenic effect of adrenaline and noradrenaline in the frog, Rana temporaria. *Comparative biochemistry and physiology. A, Comparative physiology*, 41(2), pp.409–419.

Haslam, D.W. & James, W.P.T., 2005. Obesity. *Lancet*, 366(9492), pp.1197–1209.

Heaton, J.M., 1972. The distribution of brown adipose tissue in the human., 112(Pt 1), pp.35–39.

Henriksen, E.J., 2006. Exercise training and the antioxidant alpha-lipoic acid in the treatment of insulin resistance and type 2 diabetes. *Free radical biology & medicine*, 40(1), pp.3–12.

Himms-Hagen, J. & Harper, M.E., 2001. Physiological role of UCP3 may be export of fatty acids from mitochondria when fatty acid oxidation predominates: an hypothesis. *Experimental biology and medicine (Maywood, N.J.)*, 226(2), pp.78–84.

Hissa, R., Pyörnilä, A. & Saarela, S., 1975. Effect of peripheral noradrenaline on thermoregulation in temperature-acclimated pigeon. *Comparative biochemistry and physiology. C: Comparative pharmacology*, 51(2), pp.243–247.

Houstis, N., Rosen, E.D. & Lander, E.S., 2006. Reactive oxygen species have a causal role in multiple forms of insulin resistance. *Nature*, 440(7086), pp.944–948.

Huppertz, C. et al., 2001. Uncoupling protein 3 (UCP3) stimulates glucose uptake in muscle cells through a phosphoinositide 3-kinase-dependent mechanism. *The Journal of biological chemistry*, 276(16), pp.12520–12529.

Jaburek, M. et al., 1999. Transport function and regulation of mitochondrial uncoupling proteins 2 and 3. *The Journal of biological chemistry*, 274(37), pp.26003–26007.

Janssen, U. & Stoffel, W., 2002. Disruption of mitochondrial beta -oxidation of unsaturated fatty acids in the 3,2-trans-enoyl-CoA isomerase-deficient mouse. *The Journal of biological chemistry*, 277(22), pp.19579–19584.

Jezek, P. & Freisleben, H.J., 1994. Fatty acid binding site of the mitochondrial uncoupling protein. Demonstration of its existence by EPR spectroscopy of 5-DOXYL-stearic acid. *FEBS letters*, 343(1), pp.22–26.

Jiménez-Jiménez, J. et al., 2006. Fatty acid activation of the uncoupling proteins requires the presence of the central matrix loop from UCP1. *Biochimica et biophysica acta*, 1757(9-10), pp.1292–1296.

Kelley, D. et al., 1988. Skeletal muscle glycolysis, oxidation, and storage of an oral glucose load. *Journal of Clinical Investigation*, 81(5), pp.1563–1571.

Kelley, D.E. et al., 1999. Skeletal muscle fatty acid metabolism in association with insulin resistance, obesity, and weight loss. *The American journal of physiology*, 277(6 Pt 1), pp.E1130–41.

Kellya, O.M. et al., 2012. The preservation of in vivo phosphorylated and activated uncoupling protein 3 (UCP3) in isolated skeletal muscle mitochondria following administration of 3,4-methylenedioxymethamphetamine (MDMA aka ecstasy) to rats/mice. *Mitochondrion*, 12(1), pp.110–119.

Kim, J.Y. et al., 2000. Lipid oxidation is reduced in obese human skeletal muscle. *American journal of physiology Endocrinology and metabolism*, 279(5), pp.E1039–44.

Kopec, B. & Fritz, I.B., 1971. Properties of a purified carnitine palmitoyltransferase, and evidence for the existence of other carnitine acyltransferases. *Canadian journal of*

biochemistry, 49(8), pp.941–948.

Koves, T.R. et al., 2008. Mitochondrial Overload and Incomplete Fatty Acid Oxidation Contribute to Skeletal Muscle Insulin Resistance. *Cell Metabolism*, 7(1), pp.45–56.

Kozak, L.P. & Young, M.E., 2012. news and views. *Nature Medicine*, 18(10), pp.1458–1459.

Krauss, S., Zhang, C.Y. & Lowell, B.B., 2005. The mitochondrial uncoupling-protein homologues. *Nature Reviews Molecular Cell Biology*, 6(3), pp.248–261.

Krssak, M. et al., 1998. Intramyocellular lipid concentrations are correlated with insulin sensitivity in humans: a ^{1}H NMR spectroscopy study. *Diabetologia*, pp.113–116.

Kruszynska, Y.T., Ciaraldi, T.P. & Henry, R.R., 2001. Regulation of glucose metabolism in skeletal muscle. In *Handbook of Physiology, The Endocrine System, The Endocrine Pancreas and Regulation of Metabolism*. Comprehensive Physiology 2011. Hoboken, NJ, USA: John Wiley & Sons, Inc., pp. 579–607.

Kunau, W., Dommes, V. & Schulz, H., 1995. Beta-oxidation of fatty acids in mitochondria, peroxisomes, and bacteria: A century of continued progress. *Progress in lipid research*, 34(4), pp.267–342.

Lago, C. et al., 2012. Mitochondrial respiratory uncoupling promotes keratinocyte differentiation and blocks skin carcinogenesis., 31(44), pp.4725–4731.

LaNoue, K.F. & Schoolwerth, A.C., 1979. Metabolite transport in mitochondria. *Annual review of biochemistry*, 48, pp.871–922.

LaNoue, K.F. & Tischler, M.E., 1974. Electrogenic characteristics of the mitochondrial glutamate-aspartate antiporter. *The Journal of biological chemistry*, 249(23), pp.7522–7528.

Larance, M., Ramm, G. & James, D.E., 2008. The GLUT4 code. *Molecular endocrinology (Baltimore, Md.)*, 22(2), pp.226–233.

Lee, P. et al., 2014. Irisin and FGF21 are cold-induced endocrine activators of brown fat function in humans. *Cell Metabolism*, 19(2), pp.302–309.

Liang, X. et al., 2001. Impact of the intramitochondrial enzyme organization on fatty acid oxidation. *Biochemical Society transactions*, 29(Pt 2), pp.279–282.

Lin, C.S. & Klingenberg, M., 1980. Isolation of the uncoupling protein from brown adipose tissue mitochondria. *FEBS letters*, 113(2), pp.299–303.

Liu, X. et al., 2003. Paradoxical resistance to diet-induced obesity in UCP1-deficient mice. *Journal of Clinical Investigation*, 111(3), pp.399–407.

Liu, Y.J. et al., 2005. Linkage and association analyses of the UCP3 gene with obesity phenotypes in Caucasian families. *Physiological Genomics*, 22(2), pp.197–203.

Luo, M.J. et al., 1994. Delta(3,5),Delta(2,4)-Dienoyl-Coa Isomerase From Rat-Liver Mitochondria - Purification and Characterization of a New Enzyme Involved in the Beta-Oxidation of Unsaturated Fatty-Acids. *The Journal of biological chemistry*, 269(4), pp.2384–2388.

Luthria, D.L., Baykousheva, S.P. & Sprecher, H., 1995. Double bond removal from odd-numbered carbons during peroxisomal beta-oxidation of arachidonic acid requires both 2,4-dienoyl-CoA reductase and delta 3,5,delta 2,4-dienoyl-CoA isomerase. *The Journal of biological chemistry*, 270(23), pp.13771–13776.

MacLellan, J.D., Gerrits, M.F., Gowing, A., Smith, P.J.S., Wheeler, M.B. & Harper, M.-E., 2005a. Physiological increases in uncoupling protein 3 augment fatty acid oxidation and decrease reactive oxygen species production without uncoupling respiration in muscle cells. *Diabetes*, 54(8), pp.2343–2350.

MacLellan, J.D., Gerrits, M.F., Gowing, A., Smith, P.J.S., Wheeler, M.B. & Harper, M.E., 2005b. Physiological Increases in Uncoupling Protein 3 Augment Fatty Acid Oxidation and Decrease Reactive Oxygen Species Production Without Uncoupling Respiration in Muscle Cells. *Diabetes*, 54(8), pp.2343–2350.

Mejsnar, J. & Jansky, L., 1971. Means of noradrenalin action during non-shivering thermogenesis in a single muscle. *International journal of biometeorology*, 15(2), pp.321–324.

Melnikova, I. & Wages, D., 2006. Anti-obesity therapies. *Nature reviews. Drug discovery*, 5(5), pp.369–370.

Miinalainen, I.J. et al., 2009. Mitochondrial 2,4-dienoyl-CoA Reductase Deficiency in Mice Results in Severe Hypoglycemia with Stress Intolerance and Unimpaired Ketogenesis P. A. Wood, ed. *PLoS Genetics*, 5(7), p.e1000543.

Mills, E.M. et al., 2003. Pharmacology: uncoupling the agony from ecstasy. *Nature*, 426(6965), pp.403–404.

Modis, Y. et al., 1998. The crystal structure of dienoyl-CoA isomerase at 1.5 å resolution reveals the importance of aspartate and glutamate sidechains for catalysis. *Structure*, 6(8), pp.957–970.

Morino, K., Petersen, K.F. & Shulman, G.I., 2006. Molecular mechanisms of insulin resistance in humans and their potential links with mitochondrial dysfunction. *Diabetes*, 55 Suppl 2, pp.S9–S15.

Muoio, D.M., 2014. Metabolic Inflexibility: When Mitochondrial Indecision Leads to Metabolic Gridlock. *Cell*, 159(6), pp.1253–1262.

Muoio, D.M. & Neufer, P.D., 2012. Lipid-Induced Mitochondrial Stress and Insulin Action in Muscle. *Cell Metabolism*, 15(5), pp.595–605.

Muoio, D.M. & Newgard, C.B., 2008. Mechanisms of disease: Molecular and metabolic mechanisms of insulin resistance and β-cell failure in type 2 diabetes. *Nature Reviews Molecular Cell Biology*, 9(3), pp.193–205.

Muoio, D.M. et al., 2012. Muscle-specific deletion of carnitine acetyltransferase compromises glucose tolerance and metabolic flexibility. *Cell Metabolism*, 15(5), pp.764–777.

Musa, C.V. et al., 2011. Four novel UCP3 gene variants associated with childhood obesity: effect on fatty acid oxidation and on prevention of triglyceride storage. *International Journal of Obesity*, 36(2), pp.207–217.

Musselman, M.E. & Saely, S., 2013. Diagnosis and treatment of drug-induced hyperthermia. *American journal of health-system pharmacy : AJHP : official journal of the American Society of Health-System Pharmacists*, 70(1), pp.34–42.

Nagase, I., Yoshida, T. & Saito, M., 2001. Up-regulation of uncoupling proteins by beta-adrenergic stimulation in L6 myotubes. *FEBS letters*, 494(3), pp.175–180.

Nahrendorf, M. et al., 2000. Thermogenic responses in brown fat cells are fully UCP1-dependent. UCP2 or UCP3 do not substitute for UCP1 in adrenergically or fatty scid-induced thermogenesis. *The Journal of biological chemistry*, 275(33), pp.25073–25081.

Nedergaard, J. et al., 2000. UCP1: The Original Uncoupling Protein—and Perhaps theOnly One?, pp.1–17.

Nedergaard, J., Bengtsson, T. & Cannon, B., 2007. Unexpected evidence for active brown adipose tissue in adult humans. *American journal of physiology Endocrinology and metabolism*, 293(2), pp.E444–52.

Nicholls, D.G. & Locke, R.M., 1984a. Thermogenic mechanisms in brown fat. *Physiological Reviews*, 64(1), pp.1–64.

Nicholls, D.G. & Locke, R.M., 1984b. Thermogenic mechanisms in brown fat.

Physiological Reviews, 64(1), pp.1–64.

Nielsen, B., 1998. Heat acclimation--mechanisms of adaptation to exercise in the heat., 19 Suppl 2, pp.S154–6.

Ogden, C.L. et al., 2014. Prevalence of Childhood and Adult Obesity in the United States, 2011-2012. *Jama-Journal of the American Medical Association*, 311(8), pp.806–814.

Olson, K.R. & Benowitz, N.L., 1984. Environmental and drug-induced hyperthermia. Pathophysiology, recognition, and management. *Emergency medicine clinics of North America*, 2(3), pp.459–474.

Pan, D.A. et al., 1997. Skeletal muscle triglyceride levels are inversely related to insulin action. *Diabetes*, 46(6), pp.983–988.

Petersen, K.F. et al., 2004. Impaired mitochondrial activity in the insulin-resistant offspring of patients with type 2 diabetes. *The New England journal of medicine*, 350(7), pp.664–671.

Petersen, K.F. et al., 2003. Mitochondrial dysfunction in the elderly: Possible role in insulin resistance. *Science*, 300(5622), pp.1140–1142.

Randle, P.J. et al., 1963. The glucose fatty-acid cycle. Its role in insulin sensitivity and the metabolic disturbances of diabetes mellitus. *Lancet*, 1(7285), pp.785–789.

Rea, S. & James, D.E., 1997. Moving GLUT4: the biogenesis and trafficking of GLUT4 storage vesicles. *Diabetes*, 46(11), pp.1667–1677.

Reitman, M.L., 2002. Metabolic lessons from genetically lean mice. *Annual review of nutrition*, 22(1), pp.459–482.

Ren, Y. et al., 2004. An alternative pathway of oleate beta-oxidation in Escherichia coli involving the hydrolysis of a dead-end intermediate by a thioesterase. *Faseb Journal*, 18(8), pp.C166–C166.

Roden, M. et al., 1996. Mechanism of free fatty acid-induced insulin resistance in humans. *Journal of Clinical Investigation*, 97(12), pp.2859–2865.

Rolfe, D.F. & Brown, G.C., 1997. Cellular energy utilization and molecular origin of standard metabolic rate in mammals. *Physiological Reviews*, 77(3), pp.731–758.

Rousset, S. et al., 2004. The biology of mitochondrial uncoupling proteins. *Diabetes*, 53 Suppl 1, pp.S130–5.

Rusyniak, D.E. & Sprague, J.E., 2006. Hyperthermic Syndromes Induced by Toxins. *Clinics in Laboratory Medicine*, 26(1), pp.165–184.

Safer, B., 1975. The Metabolic Significance of the Malate-Aspartate Cycle in Heart. *Circulation research*, 37(5), pp.527–533.

Samec, S., Seydoux, J. & Dullo, A.G., 1999. Post-Starvation Gene Expression of Skeletal Muscle Uncoupling Protein 2 and Uncoupling Protein 3 in Response to Dietary Fat Levels and Fatty Acid Composition A Link With Insulin Resistance. *Diabetes*, pp.436–441.

Sanchez-Alavez, M. et al., 2013. ROS and Sympathetically Mediated Mitochondria Activation in Brown Adipose Tissue Contribute to Methamphetamine-Induced Hyperthermia. *Frontiers in Endocrinology*, 4, p.44.

Schrauwen, P. et al., 1999. A novel polymorphism in the proximal UCP3 promoter region: effect on skeletal muscle UCP3 mRNA expression and obesity in male non-diabetic Pima Indians. *International Journal of Obesity*, 23(12), pp.1242–1245.

Schrauwen, P. et al., 2001. Uncoupling Protein 3 Content Is Decreased in Skeletal Muscle of Patients With Type 2 Diabetes. *Diabetes*, 50(12), pp.2870–2873.

Schulz, H., 2002. Oxidation of fatty acids in eukaryotes. *Biochemistry of Lipids, Lipoproteins, and Membranes*, 4, pp.127–150.

Schulz, H. & Kunau, W.-H., 1987. Beta-oxidation of unsaturated fatty acids: a revised pathway. *Trends in Biochemical Sciences*, 12, pp.403–406.

Seale, P. et al., 2008. PRDM16 controls a brown fat/skeletal muscle switch. *Nature*, 454(7207), pp.961–967.

Seifert, E.L. et al., 2010. Electron transport chain-dependent and -independent mechanisms of mitochondrial H2O2 emission during long-chain fatty acid oxidation. *The Journal of biological chemistry*, 285(8), pp.5748–5758.

Seifert, E.L. et al., 2008. Essential role for uncoupling protein-3 in mitochondrial adaptation to fasting but not in fatty acid oxidation or fatty acid anion export. *The Journal of biological chemistry*, 283(37), pp.25124–25131.

Sena, L.A. & Chandel, N.S., 2012. Physiological roles of mitochondrial reactive oxygen species. *Molecular Cell*, 48(2), pp.158–167.

Senese, R. et al., 2010. Uncoupling protein 3 expression levels influence insulin sensitivity, fatty acid oxidation, and related signaling pathways. *Pflügers Archiv - European Journal of Physiology*, 461(1), pp.153–164.

She, P. et al., 2007. Disruption of BCATm in mice leads to increased energy expenditure associated with the activation of a futile protein turnover cycle. *Cell Metabolism*, 6(3), pp.181–194.

Sheu, S.-S., Nauduri, D. & Anders, M.W., 2006. Targeting antioxidants to mitochondria: a new therapeutic direction. *Biochimica et biophysica acta*, 1762(2), pp.256–265.

Shoukry, K. & Schulz, H., 1998. Significance of the reductase-dependent pathway for the beta-oxidation of unsaturated fatty acids with odd-numbered double bonds. Mitochondrial metabolism of 2-trans-5-cis-octadienoyl-CoA. *The Journal of biological chemistry*, 273(12), pp.6892–6899.

Shulman, G.I. et al., 1990. Quantitation of muscle glycogen synthesis in normal subjects and subjects with non-insulin-dependent diabetes by 13C nuclear magnetic resonance spectroscopy. *The New England journal of medicine*, 322(4), pp.223–228.

Silva, J.E., 2011. Physiological importance and control of non-shivering facultative thermogenesis., 3, pp.352–371.

Silva, J.E., 2006. Thermogenic Mechanisms and Their Hormonal Regulation. *Physiological Reviews*, 86(2), pp.435–464.

Silva, J.E., 1995. Thyroid hormone control of thermogenesis and energy balance. *Thyroid : official journal of the American Thyroid Association*, 5(6), pp.481–492.

Skulachev, V.P., 1999. Anion carriers in fatty acid-mediated physiological uncoupling. *Journal of bioenergetics and biomembranes*, 31(5), pp.431–445.

Smith, R.E. & Horwitz, B.A., 1969. Brown fat and thermogenesis. *Physiological Reviews*, 49(2), pp.330–425.

Solanes, G. et al., 2000. The human uncoupling protein-3 gene promoter requires MyoD and is induced by retinoic acid in muscle cells. *Faseb Journal*, 14(14), pp.2141–2143.

Solanes, G. et al., 2005. Thyroid hormones directly activate the expression of the human and mouse uncoupling protein-3 genes through a thyroid response element in the proximal promoter region. *Biochemical Journal*, pp.1–9.

Son, C. et al., 2001. Up-regulation of uncoupling protein 3 gene expression by fatty acids and agonists for PPARs in L6 myotubes. *Endocrinology*, 142(10), pp.4189–4194.

Sprague, J.E. et al., 2005. Carvedilol reverses hyperthermia and attenuates rhabdomyolysis induced by 3,4-methylenedioxymethamphetamine (MDMA, Ecstasy) in an animal model*. *Critical Care Medicine*, 33(6), pp.1311–1316.

Sprague, J.E. et al., 2003. Hypothalamic-pituitary-thyroid axis and sympathetic nervous system involvement in hyperthermia induced by 3,4-methylenedioxymethamphetamine (Ecstasy). *The Journal of pharmacology and experimental therapeutics*, 305(1), pp.159–166.

Sprague, J.E. et al., 2007. Roles of Norepinephrine, Free Fatty Acids, Thyroid Status, and Skeletal Muscle Uncoupling Protein 3 Expression in Sympathomimetic-Induced Thermogenesis. *Journal of Pharmacology and Experimental Therapeutics*, 320(1), pp.274–280.

Sprague, J.E., Brutcher, R.E., et al., 2004. Attenuation of 3,4-methylenedioxymethamphetamine (MDMA, Ecstasy)-induced rhabdomyolysis with alpha1- plus beta3-adrenoreceptor antagonists. *British journal of pharmacology*, 142(4), pp.667–670.

Sprague, J.E., Mallett, N.M., et al., 2004. UCP3 and thyroid hormone involvement in methamphetamine-induced hyperthermia. *Biochemical Pharmacology*, 68(7), pp.1339–1343.

St-Pierre, J. et al., 2002. Topology of superoxide production from different sites in the mitochondrial electron transport chain. *The Journal of biological chemistry*, 277(47), pp.44784–44790.

Stitt, J.T., 1979. Fever versus hyperthermia. *Federation proceedings*, 38(1), pp.39–43.

Stoffel, W. & Caesar, H., 1965. [Metabolism of unsaturated fatty acids. V. On the beta-oxidation of mono- and polyene-fatty acids. Mechanism of enzymatic reactions of delta-2-cis-enoyl-CoA compounds]. *Hoppe-Seyler's Zeitschrift für physiologische Chemie*, 341(1), pp.76–83.

Sumegi, B., Porpaczy, Z. & Alkonyi, I., 1991. Kinetic advantage of the interaction between the fatty acid beta-oxidation enzymes and the complexes of the respiratory chain. *Biochimica et biophysica acta*, 1081(2), pp.121–128.

Thompson, M.P. & Kim, D., 2004. Links between fatty acids and expression of UCP2 and UCP3 mRNAs. *FEBS letters*, 568(1-3), pp.4–9.

Townsend, K.L. & Tseng, Y.-H., 2014. Brown fat fuel utilization and thermogenesis. *Trends in Endocrinology & Metabolism*, 25(4), pp.168–177.

Turner, N. et al., 2007. Excess Lipid Availability Increases Mitochondrial Fatty Acid Oxidative Capacity in Muscle: Evidence Against a Role for Reduced Fatty Acid Oxidation in Lipid-Induced Insulin Resistance in Rodents. *Diabetes*, 56(8), pp.2085–2092.

van der Vusse, G.J. et al., 2002. Critical steps in cellular fatty acid uptake and utilization. *Molecular and cellular biochemistry*, 239(1-2), pp.9–15.

van Roermund, C.W.T. et al., 2011. Differential substrate specificities of human ABCD1 and ABCD2 in peroxisomal fatty acid β-oxidation. *Biochimica et biophysica acta*, 1811(3), pp.148–152.

Vidal-Puig, A. et al., 1997. UCP3: an uncoupling protein homologue expressed preferentially and abundantly in skeletal muscle and brown adipose tissue. *Biochemical and biophysical research communications*, 235(1), pp.79–82.

Vidal-Puig, A.J. et al., 2000. Energy metabolism in uncoupling protein 3 gene knockout mice., 275(21), pp.16258–16266.

Zackova, M. et al., 2003. Activating omega-6 polyunsaturated fatty acids and inhibitory purine nucleotides are high affinity ligands for novel mitochondrial uncoupling proteins UCP2 and UCP3. *The Journal of biological chemistry*, 278(23), pp.20761–20769.

Zhang, D.Y. et al., 2001. Delta(3,5),Delta(2,4)-dienoyl-CoA isomerase is a multifunctional isomerase - A structural and mechanistic study. *The Journal of biological chemistry*, 276(17), pp.13622–13627.

Vita

Christine Ky Linh Dao was born and raised in Northridge, California. After graduating from Granada Hills Charter High School in 2004, she went on to attend Rice University in Houston, Texas. Christine attended Rice University from 2004-2009, where she was award a full student-athlete scholarship and graduated with a Bachelor of Arts degree in Kinesiology- Sports Medicine. She then joined the Division of Pharmacology and Toxiclogy, College of Pharmacy at The University of Texas at Austin in July 2009 under the mentorship of Dr. Edward M. Mills.

Email address: kylinhdao@gmail.com

This dissertation was typed by the author.